Master's thesis

NTNU
Norwegian University of Science and Technology
Faculty of Natural Sciences
Department of Biotechnology and Food Science

Jesper Evjen Pedersen

Preparation of Activated Chitosan and Synthesis of a Chitosan-Dextran Diblock

Master's thesis in Biotechnology (MBIOT5)

Supervisor: Bjørn E. Christensen

May 2020

NTNU
Norwegian University of
Science and Technology

Jesper Evjen Pedersen

Preparation of Activated Chitosan and Synthesis of a Chitosan-Dextran Diblock

Master's thesis in Biotechnology (MBIOT5)
Supervisor: Bjørn E. Christensen
May 2020

Norwegian University of Science and Technology
Faculty of Natural Sciences
Department of Biotechnology and Food Science

NTNU
Norwegian University of
Science and Technology

Preface

This master's thesis was conducted at the Department of Biotechnology and Food Science (IBT) at the Norwegian University of Science and Technology (NTNU) between January 2019 and May 2020.

Thank you to my supervisor Professor Bjørn E. Christensen for all prudent advice and insistent emphasis on always seeing the good in any situation.

Thank you to my co-supervisors PhD Candidate Ingrid Vikøren Mo and PhD Candidate Amalie Solberg for making my life so much easier. You rock!

Thank you to the people staffing the laboratories, especially Senior Engineer Olav A. Aarstad and Senior Engineer Wenche I. Strand for always being eager to help.

Last but not least, thank you to friends and family for all support and encouragement these past five years.

Trondheim, the Twenty-second of May, 2020

Jesper Evjen Pedersen

Abstract

Block copolymers (BCPs) are hybrid structures comprised of covalently bonded polymer segments. Careful selection of constituent blocks allows for the creation of novel materials with tailored properties. Of special interest are amphiphilic BCPs exhibiting self-assembly; spontaneous formation of nanoparticles has garnered much attention for its potential use in the design of targeted drug delivery systems.

Chitosan, a derivative of chitin, is a polycationic polysaccharide known for its low toxicity and antimicrobial properties. This thesis is primarily concerned with activation of chitosan by attachment of reactive bifunctional linkers to its reducing end. The thesis culminates with a demonstration of how activated chitosan can be used to synthesise a chitosan-dextran diblock.

Fully de-*N*-acetylated chitosan was depolymerised by means of nitrous acid (HNO_2) to yield chitooligosaccharides (COS) with a highly reactive 2,5-anhydro-D-mannofuranose (M-unit) at the reducing end (D_nM-type chitosan). The stability of the M-unit was studied. Importantly, it was found that when exposed to an elevated pH in combination with dehydration, the M-unit is lost due to non-enzymatic browning. The M-unit was shown to be stable as long as mild acidity was maintained.

Bifunctional linkers adipic acid dihydrazide (ADH) and *O*,*O*'-1,3-propanediylbishydroxylamine dihydrochloride (PDHA) were attached to the reducing end of chitosan via two-pot reductive amination. Both amination and reduction was found to go to completion. Reduction took considerably longer than amination but could be appreciably expedited by increasing the excess of reducing agent – in this case α-picoline borane. Attachment of ADH was considerably faster than attachment of PDHA.

The M-unit was found to be quintessential for attachment of linker. The normal D-glucosamine (D-unit) reducing end was essentially inert in comparison to the M-unit.

End-to-end conjugation of activated chitosan and dextran was performed with an excess of dextran and at 40 °C. A convenient method for removing non-conjugated dextran via size-exclusion chromatography (SEC) was demonstrated.

Sammendrag

Blokk-kopolymerer (BKPer) er hybride strukturer bestående av kovalent bundne polymer-segmenter. Et overveid valg av bestående blokker tillater laging av nye materialer med skreddersydde egenskaper. Av spesiell interesse er amfifile BKPer som utviser selvmontering: spontan formasjon av nanopartikler har mottatt mye oppmerksomhet for dets potensielle anvendelse i utvikling av systemer for målrettet leveranse av legemidler.

Kitosan, et derivat av kitin, er et polykationisk polysakkarid kjent for sin lave toksisitet og antimikrobielle egenskaper. Denne avhandlingen tar først og fremst for seg aktivering av kitosan ved påkobling av reaktive, bifunksjonelle linkere til kitosanets reduserende ende. Avhandlingen kulminerer med en demonstrasjon av hvordan aktivert kitosan kan benyttes til å syntetisere en kitosan-dekstran diblokk.

Fullstendig de-*N*-acetylert kitosan ble depolymerisert ved bruk av salpetersyrling (HNO_2) til å gi kitooligosakkarider (KOS) med en svært reaktiv 2,5-anhydro-D-mannofuranose (M-enhet) på den reduserende enden (D_nM-type kitosan). Stabiliteten til M-enheten be studert. Av spesiell viktighet ble det funnet at når eksponert for en forhøyet pH i kombinasjon med dehydrasjon ble M-enheten tapt grunnet en ikke-enzymatisk bruningsreaksjon. M-enheten var stabil så lenge mild syrlighet ble vedlikeholdt.

Bifunksjonelle linkere adipinsyre dihydrazid (ADH) og *O*,*O*'-1,3-propandiylbishydroksyl-amin dihydroklorid (PDHA) ble koblet til den reduserende enden til kitosan via two-pot reduktiv aminering. Både aminering og reduksjon gikk til fullførelse. Reduksjon tok betydelig mer tid enn aminering men kunne gjøres merkbart fortere ved å øke overskuddet av reduksjonsmiddel – i dette tilfellet α-picolin boran. Kobling av ADH var betydelig raskere enn kobling av PDHA.

M-enheten var kvintessiell når det gjaldt kobling av linkere. Den normale D-glukosamin(D-enhet)-reduserende enden var i all hovedsak inert sammenlignet med M-enheten.

Ende-mot-ende-konjugering av aktivert kitosan og dekstran ble utført med et overskudd av dekstran ved 40 °C. En nyttig metode for å fjerne ukonjugert dekstran ved hjelp av størrelses-eksklusjons-kromatografi (SEK) ble demonstrert.

Abbreviations

AcOH	acetic acid
ADH	adipic acid dihydrazide
AmAc	ammonium acetate
A-unit	*N*-acetyl-D-glucosamine
BCP	block copolymer
COS	chitooligosaccharide
Dex	dextran
D_nM	chitosan, comprised of *n* units of consecutive D-glucosamines, with a 2,5-anhydro-D-mannose reducing end
DP	degree of polymerisation
DP_n	number average degree of polymerisation
D-unit	D-glucosamine
F_A	fraction of *N*-acetyl-D-glucosamines in chitosan
GlcN	D-glucosamine
GlcNA	*N*-acetyl-D-glucosamine
HMF	5-hydroxymethylfurfural
HMWC	high molecular weight chitosan
HNO_2	nitrous acid
LMWC	low molecular weight chitosan
MP	mobile phase
M-unit	2,5-anhydro-D-mannofuranose
NaAc	sodium acetate
NaCl	sodium chloride
$NaNO_2$	sodium nitrite
PDHA	*O*,*O*'-1,3-propanediylbishydroxylamine dihydrochloride
Pic-BH_3	α-picoline borane
SEC	size-exclusion chromatography
TSP	sodium 3-(trimethylsilyl)-propionate-d_4
MWCO	molecular weight cut-off

Contents

1 Introduction

1.1 Background and motivation

Environmental concerns have motivated a global initiative to find sustainable solutions to current unsustainable practices. It is presently unclear how the Norwegian economy, largely dependent on petroleum, will adapt to an economic landscape increasingly favouring environmentally friendly alternatives. The work presented in this thesis is part of an ongoing effort to develop forward-looking technologies which attempts to make advantage of Norway's heretofore unexploited resources.

Large quantities of naturally available polysaccharides are found in Norway, notably cellulose – a major constituent of wood – and chitin – a major constituent of shrimp and crab shells. Additionally, Norway's long coastline offers good opportunity for the cultivation of algae which can be used to produce alginate, another polysaccharide of scientific interest, in part due to its gelation properties. Currently, cellulose, chitin, and alginate are considered low-value products. Novel means of refining these low-value products into high-value products could massively benefit the bioeconomic sector.

Polysaccharides can be chemically coupled to other natural or synthetic polymers in order to create hybrid materials with novel and tailored properties. End-to-end conjugation of linear polymer segments yields block copolymers (BCPs) whose self-assembly properties have generated a lot of interest. Of particular interest has been microcapsules made from BCPs in the design of targeted drug-delivery systems.[4]

Chitosan is a polycationic polysaccharide produced industrially from chitin. This thesis is primarily concerned with the synthesis of activated chitosan. Activated chitosan is chitosan modified by attachment of a linker to its reducing end, thereby enabling coupling to aldehydic species via simple reductive amination. As a proof of concept, the final part of this thesis demonstrates the synthesis of a chitosan-dextran conjugate.

Chitosan was chosen as object of study due to its promising potential in the design of drug delivery systems and gene transfection,[3] as well as its ability to form complexes with anionic species. Its promising potential is largely tied to its polycationic character.[5]

2 Theory

2.1 Polysaccharide-containing block copolymers

Block copolymers (BCPs) are composite materials made of covalently bonded polymer segments (blocks). BCPs can be linear or branched and be made of natural or synthetic polymers. Literature on BCPs has primarily been concerned with the synthesis and properties of linear diblocks and triblocks (Figure 2.1).[1, 4] Linear diblocks and triblocks are among the simplest types of BCPs and are often studied because of their emergent self-assembly behaviour.

The synthetic strategies used to construct linear diblocks and triblocks can also be used to construct BCPs of more complicated architectures, such as stars and circles (Figure 2.1). End-to-end conjugation combined with grafting onto side groups offers an even broader array of possible BCP architectures.[1, 4]

BCP technology can be used to engineer materials with novel and tailored properties. For example, thermoplastic elastomers, suitable for applications such as injection moulding and melt extrusion,[1] can be made by constructing BCPs comprised of elastic and thermoplastic (i.e. heat labile) blocks. Furthermore, BCPs made from immiscible blocks can self-assemble and form association colloids such as membranes, micelles, and polymersomes.[1, 4] Self-assembly can be controlled by various means, for instance by regulating pH,[6] temperature,[7] solvent composition,[8] and concentration of the BCP.[9]

Polymersomes made from self-assembling BCPs might be used to make microreactors,[4] for

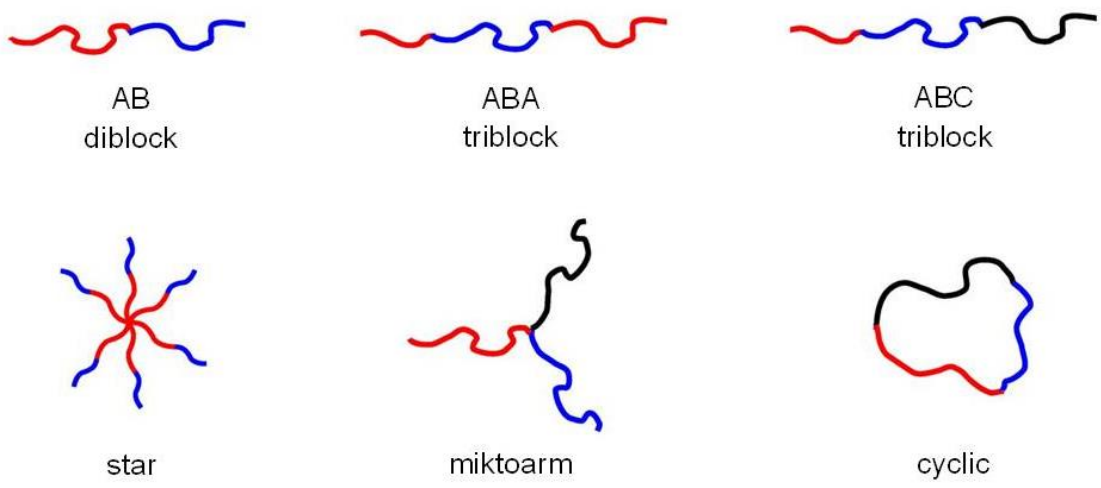

Figure 2.1. Examples of BCP architectures. Adapted from: Feng, H.; Lu, X.; Wang, W.; Kang, N.-G.; Mays, J. W. Polymers **2017**, 9, (10), 494.[1]

micellar enhanced ultrafiltration,[10] and in the design of targeted drug-delivery systems.[1, 4] As proof of concept, Upadhyay et al.[11] demonstrated that an anticancer drug-loaded polymersome made of a self-assembled BCP[1] would selectively target human cancer cells *in vitro* and rat cancer cells *in vivo*. Cell-type specificity was afforded by an overexpressed cancer-associated membrane receptor having a component of the diblock (hyaluronan) as ligand.

Although BCPs can be made from natural or synthetic polymers, incentives exists for the preferential use of natural polymers. Natural polymers grant advantages such as biodegradability[12] and biocompatibility – properties that are important for environmental and biomedical purposes.[1, 4] Use of natural polymers instead of synthetic polymers is also important from an environmental perspective as synthetic polymers are derived from petroleum. In addition, some natural polymers are by-products of established industries, such as chitin from the seafood sector.[13] Refinement of such by-products into high-value products could massively benefit the global bioeconomic sector.

Linear BCPs, as opposed to grafted copolymers, retain the native properties of their constituent blocks due to preservation of side-groups.[1, 4] Retainment of native properties is important for certain applications; the affinity between hyaluronan and the membrane receptor from Upadhyay et al.'s study[11] (above) serves as an example. End-to-end conjugation is generally more challenging to perform than grafting due to the relatively low concentration of reducing ends and the need to sometimes protect side groups.[4] Selection of solvent can also be a challenge as individual blocks may have very different solubilities.[4]

Synthesis of linear, polysaccharide-containing BCPs can broadly be categorised according to three (i-iii) main strategies.

(i) A synthetic block can be added onto a polysaccharide by 'living'/controlled polymerisation. 'Living'/controlled polymerisation requires that the polysaccharide is suitably modified at the reducing end, such as by ionisation or attachment of an initiator, and includes mechanisms such as ring-opening and radical polymerisation.[1, 4]

(ii) Enzymes can polymerise a polysaccharide onto a starting block either by the attachment of a primer to the starting block or by the starting block itself functioning as a primer.[6] For

[1]A linear poly(γ-benzyl-L-glutamate)-*b*-hyaluronan diblock (the interfix -*b*- is by convention used to distinguish between blocks).

'living'/controlled polymerisation and enzymatic polymerisation, the final degree of polymerisation (DP) is determined by the ratio of primer to monomer.[4]

(iii) 'Prefabricated' blocks (i.e. blocks that have been prepared in advance) can be connected end-to-end either by antagonistically functionalising the two ends or by using a linker. Various methods for end-to-end conjugation have been devised. Worthy of particular mention are 'click' reactions such as the copper-catalysed azid-alkyne cycloaddition reaction[4] and methods based on radical chemistry. Radical chemistry has, *inter alia*, been used to synthesise a chitosan-*b*-polyethylene glycol diblock.[14]

Another method belonging to category (iii) – and the method employed in this thesis – is end-to-end coupling by means of reductive amination (aka reductive alkylation). Reductive amination is an addition reaction between an amine and an aldehyde or ketone followed by reduction to create a stable bond.

2.2 Chitosans

2.2.1 Sources, structure and properties

Chitosans are linear polysaccharides comprised of varying proportions of *N*-acetyl-D-glucosamines (A-units) and D-glucosamines (D-units). Chitosans are naturally synthesised by some fungi but is commercially produced by alkaline de-*N*-acetylation of chitin.[15] Chitin is the second most abundant polysaccharide in the world and is found in the exoskeletons of insects and crustaceans as well as in the cell walls of certain fungi.[16]

Chitosans are non-toxic and has been approved for use in wound dressings and as a food preservative, in part due to its antimicrobial properties.[17, 18] A subject of ongoing research is chitosan as a component of drug delivery systems[19-21] and for the purpose of gene transfection.[22, 23]

Chitosans prepared by homogenous de-*N*-acetylation have randomly distributed A- and D-units.[24] Both units exist in the $^4C_1$ chair conformation and all linkages are β-(1→4) and diequatorial (Figure 2.2).[25]

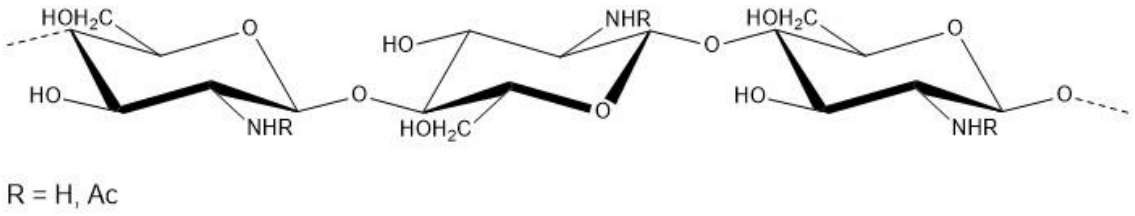

Figure 2.2. Structure of chitosan. When R = H, the residue is a D-unit; when R = Ac, the residue is an A-unit.

The properties of chitosans are highly dependent on the ratio of A- to D-units, commonly defined as fraction of A-units (F_A).

$$F_A = \frac{n_{\text{A-unit}}}{n_{\text{A-unit}} + n_{\text{D-unit}}} , \tag{2.1}$$

where $n_{\text{A-unit}}$ and $n_{\text{D-unit}}$ are relative amounts of A- and D-units per arbitrary amount of chitosan. Commercially available chitosan typically has an F_A between 0.0 and 0.3.[26]

At low pH, the D-unit's primary amine gains a positive charge by becoming protonated. The pK_a of chitosans is somewhat dependent on F_A, degree of ionisation (α), ionic strength (I) and degree of polymerisation (DP). Reported values on the pK_a of chitosans therefore vary.[3, 25]

The pK_a of a polyelectrolyte is by convention defined as the pH at 50 % degree of ionisation. A polyelectrolyte's *apparent* pK_a (pK_{app}) varies with degree of ionisation. As the degree of ionisation goes up, it becomes less and less thermodynamically favourable to further increase the charge density due to electrostatic repulsion. Consequently, the apparent pK_a becomes lower or higher as the degree of ionisation is increased, depending on whether the polymer is a polycation or a polyanion. A graph showing apparent pK_a as a function of degree of ionisation is called a Katchalsky plot. A Katchalsky plot can be constructed by employing Katchalsky's equation,[27]

$$\text{p}K_{\text{app}} = \text{pH} - \log_{10}\left(\frac{\alpha}{1-\alpha}\right) = \text{p}K_{\text{int}} - \frac{\varepsilon \Delta\Psi(\alpha)}{k_T T} , \tag{2.2}$$

where ε is the dielectric constant of the media, k_T is Boltzmann's constant, T is the temperature, $\Delta\Psi$ is the electrostatic surface potential of the polyelectrolyte, and pK_{int} is the intrinsic pK_a. The intrinsic pK_a is defined as the apparent pK_a extrapolated to 0 % degree of ionisation.[3, 25, 26, 28-30]

The apparent pK_a is positively correlated with F_A. A-units serve as spacers between charges, thereby lowering the charge density for any given degree of ionisation. The pK_a of a fully de-

N-acetylated chitosan is about 6.3 (Figure 2.3).[31-33]

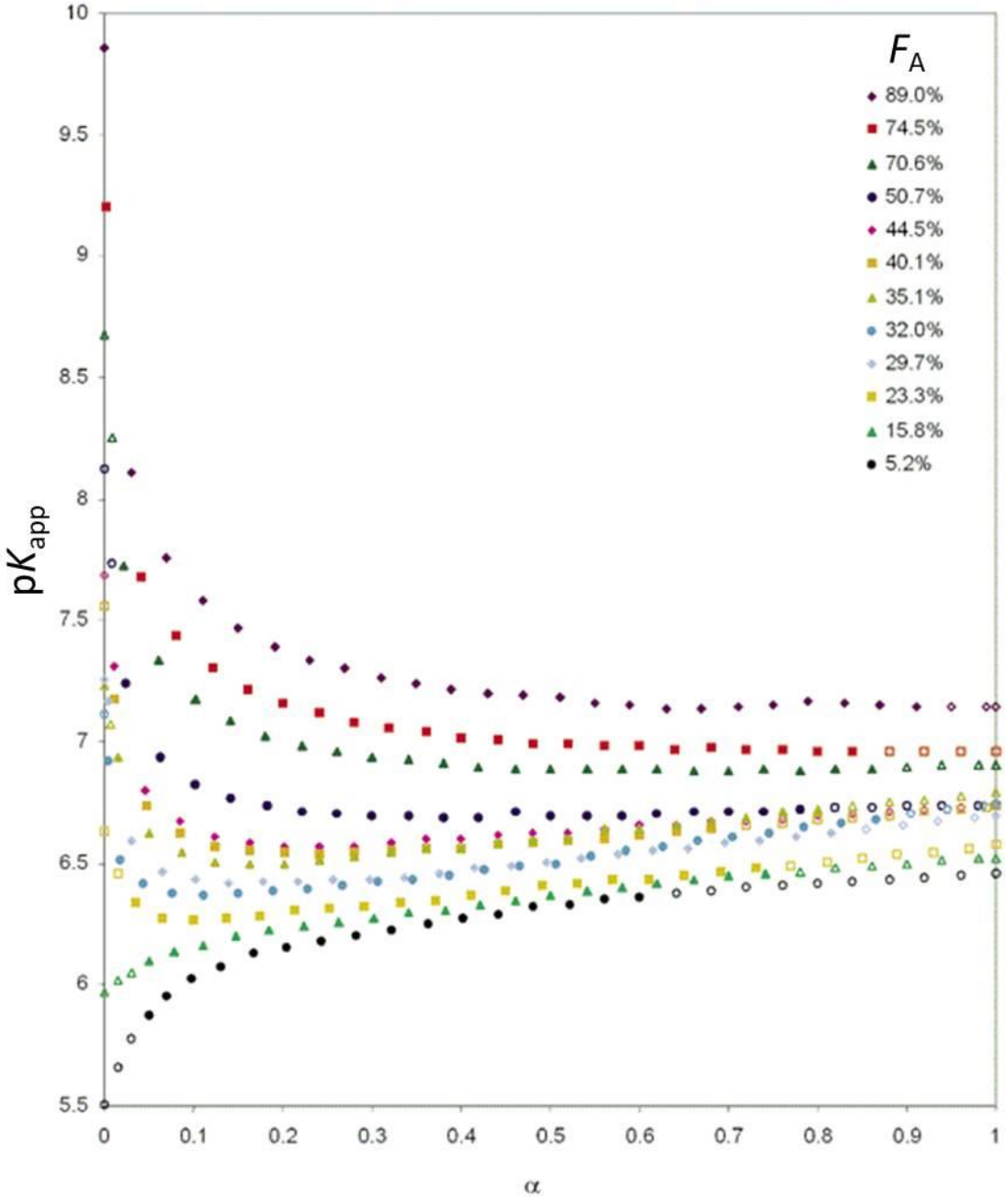

Figure 2.3. Katchalsky plot showing apparent pK_a (pK_{app}) as a function of degree of ionisation (α) for chitosans with different fractions of A-unit (F_A). Taken from: Sorlier, P.; Denuzière, A.; Viton, C.; Domard, A. *Biomacromolecules* **2001**, 2, (3), 765-772.[33]

All factors affecting the apparent pK_a's variation with degree of ionisation is dampened by ionic strength due to electrostatic screening.

Generally speaking, high molecular weight chitosan (HMWC) will only dissolve when charged. HMWC therefore exhibits limited solubility in neutral aqueous media and, importantly, at physiological pH.[26] However, HMWC with an intermediary F_A (0.4-0.6) will

dissolve even when not charged: Uninterrupted A-bocks can associate and form secondary structures which lowers solubility. The same is true of D-blocks. With an intermediary F_A and randomly distributed A- and D-units, few A- or D-blocks of sufficient length exist.[34-36]

Solubility can be improved by derivatisation such as by carboxymethylation,[37, 38] sulfation and sulfonation,[39] or, pertinently, by attachment of a lyophilic segment to the reducing end.[14]

2.2.2 Nitrous acid depolymerisation and the M-unit

Low molecular weight chitosans (LMWCs) can be obtained either by depolymerisation of chitosans or by depolymerisation and de-*N*-acetylation of chitin. Preparation of LMWCs is an area of broad scientific interest, in part due to the high viscosity and limited solubility of high molecular weight chitosans in neutral, aqueous media.[40] A wide variety of methods of depolymerisation of chitosans and chitin have been described in the literature viz. chemically (acid hydrolysis, alkaline hydrolysis, oxidative degradation), enzymatically (chitosanase, chitinase, etc.), mechanically (microfluidisation, shearing, ultransonication), and by use of high energy radiation.[41, 42] Depolymerisation by use of nitrous acid (HNO_2) is exceedingly simple to perform and generates a 2,5-anhydro-D-mannofuranose (M-unit) at the new reducing ends. Nitrous acid depolymerisation of a fully de-*N*-acetylated chitosan ($F_A = 0$) therefore yields D_nM-type chitosan.

Nitrous acid depolymerisation (Figure 2.4) begins with the protonation of HNO_2 yielding the nitrosonium ion (NO^+),

$$HNO_2 + H^+ \rightleftharpoons NO^+ + H_2O\,, \tag{2.3}$$

which attacks the C-2 primary amine of a random D-unit (step 1). The reaction, termed an *N*-nitrosation, results in an unstable diazonium ion ($–N^+{\equiv}N$).[43] The diazonium ion triggers ring contraction as the O-5–C-1 bond is broken and an O-5–C-2 bond is formed (step 2). Ring contraction is concomitant with release of N_2 and formation of a C-1 carbocation. Finally, the carbocation facilitates hydrolysis of the nearest glycosidic bond, leaving an M-unit at the new reducing end (step 3).[44, 45]

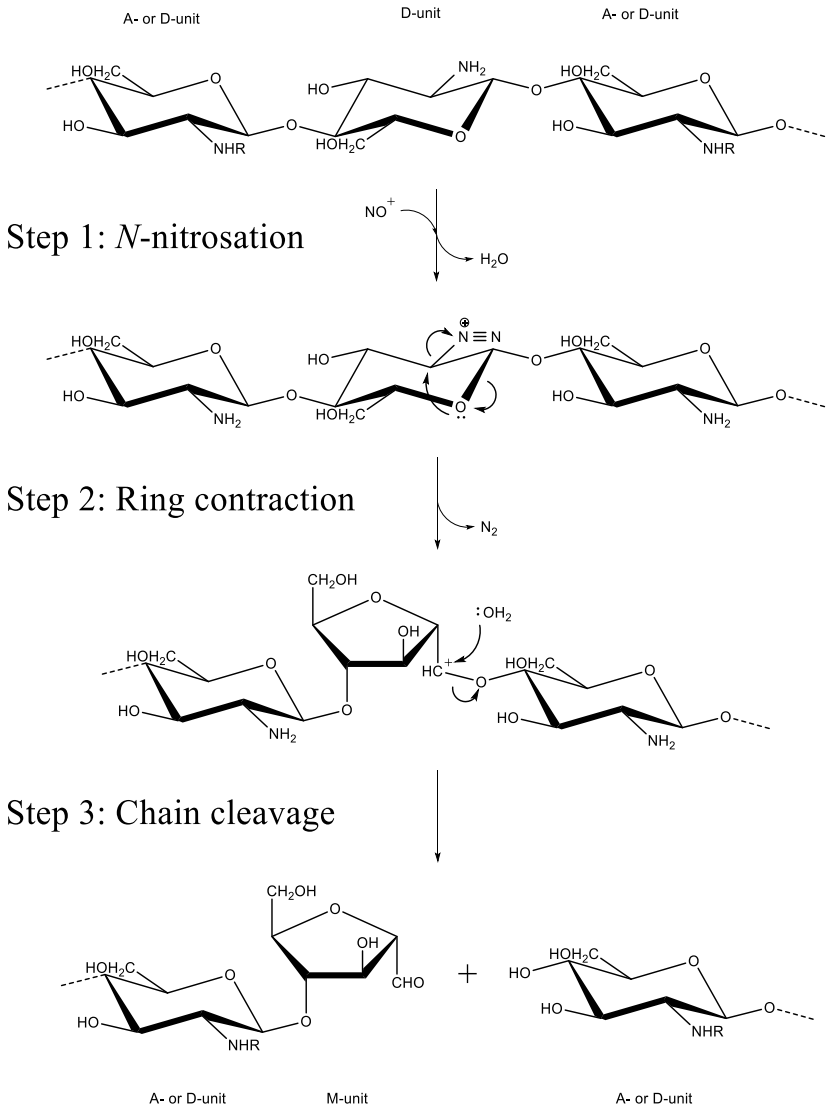

Figure 2.4. Reaction scheme of nitrous acid depolymerisation of chitosan.

The M-unit is a furanose (five-membered ring) with an externally positioned C-1 aldehyde and C-6 hydroxyl (Figure 2.5).[46] In aqueous solution, the M-unit is in a dynamic equilibrium with its aldehydic and hydrated (gem diol) forms:

$$-\mathrm{CHO} + \mathrm{H_2O} \rightleftharpoons -\mathrm{CH(OH)_2}\ . \qquad (2.4)$$

An NMR study of the D_2M-trimer (D_2O, 43 °C, pH* 5.7) found that the gem diol was the most abundant form.[47] The aldehydic form is readily reduced to 2,5-anhydro-D-mannitol.[48]

Many sugars are in a dynamic equilibrium with their aldehydic and hemiacetalic forms. Since the M-unit is permanently aldehydic, it is comparably unstable towards reactions involving the aldehyde. The high reactivity of the M-unit has been exploited to synthesise D_nM-amine conjugates.[40]

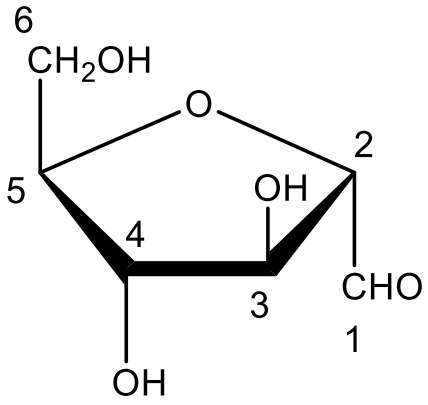

Figure 2.5. Chemical structure of 2,5-anhydro-D-mannose. Coupled via a β-(1→4)-linkage when the reducing end of chitosan.

HNO_2 selectively targets the D-unit amine as the A-unit amine is acetylated and therefore protected from chemical attack. Partially de-*N*-acetylated chitosans treated with an excess of HNO_2 therefore yields a sample of monomeric M-units and oligomeric A_nM fragments. An excess of HNO_2 combined with size-exclusion chromatography (SEC) can been used to prepare samples of purified A_nM-oligomers[47] and to determine the distribution of A-units in the source material.[49] Preparation of D_nM-oligomers requires that the source material is fully de-*N*-acetylated.[47]

Due to the simple reaction kinetics and the roughly equimolar stoichiometric relationship between HNO_2 consumed and glycosidic linkages broken, it is relatively simple to estimate the amount of HNO_2 needed to achieve a particular number average molecular weight. Assuming no side reactions and that all D-units are equally susceptible to chemical attack, Graham and Peyron[50] derived the expression

$$\frac{1}{\mathrm{DP}_1} - \frac{1}{\mathrm{DP}_0} = \frac{n}{m}\left(1 - f_\mathrm{d}\right)\left(1 - \frac{1}{\mathrm{DP}_0}\right) M_0 \,, \tag{2.5}$$

where n is initial molar amount of HNO_2, m is the total amount of chitosan, f_d is fraction of HNO_2 that is lost due to decomposition, M_0 is the mean monomer weight, and DP_0 and DP_1 are number average degree of polymerisation ($\mathrm{DP_n}$) before and after depolymerisation. Eq. (2.5) is valid for any initial molecular weight distribution but has limited predictive power upon extensive depolymerisation of partially de-*N*-acetylated chitosans as the model does not consider the distribution of A-units.[50] For fully de-*N*-acetylated chitosans, assuming extensive depolymerisation ($\mathrm{DP}_0 >> \mathrm{DP}_1$) and an insignificant contribution from side

reactions and no decomposition of HNO_2, Eq. (2.5) can be simplified to

$$\frac{1}{\mathrm{DP_n}} = \frac{n}{m} M_0 \,. \tag{2.6}$$

Since HNO_2 depolymerises chitosans in a random fashion, the final molecular weight distribution can be described by the Kuhn formula:[49]

$$W_i = \frac{i}{\mathrm{DP_n^2}} \left(1 - \frac{1}{\mathrm{DP_n^2}}\right)^{i-1} \,, \tag{2.7}$$

where W_i is the weight fraction amounted by polymers of length i.

2.2.3 Side reactions of the M-unit

The M-unit's C-1 aldehyde is susceptible to nucleophilic attack by the D-unit's C-2 primary amine. Upon nucleophilic attack, a Schiff base, i.e. an imino bond (>C=N<), is formed (Figure 2.6, step 1). Dehydration drives the reaction towards completion.[51] Schiff base formation requires that the D-unit amine is deprotonated due to the protonated amine being a poor nucleophile.[47]

Reduction of the Schiff base irreversibly creates a secondary amine (reductive amination, step 2a). Tømmeraas et al.[26] purposefully employed reductive amination to graft A_nM onto a D_nM backbone creating a brush-like structure. Irreversible branching caused by reductive amination can be avoided by: 1) preventing formation of the Schiff base by maintaining a low pH; 2) using reducing agents that do not target the imino bond;[52] 3) keeping the concentration of D_nM as low as possible.

A different side reaction (step 2b), a type of non-enzymatic browning known as the Maillard reaction, occurs when the Schiff base is subjected to acidification. Acidification causes the M-unit to be cleaved from its chain and converted to the yellow-brown compound 5-hydroxymethylfurfuraldehyde (HMF).[47] A_nM-type chitin is immune to the Maillard reaction as acetylation of the amine prevents formation of a Schiff base.[47]

The reaction cascade leading from Schiff base to HMF is not fully understood, but it has been suggested that it involves two acid-catalysed β-eliminations.[47]

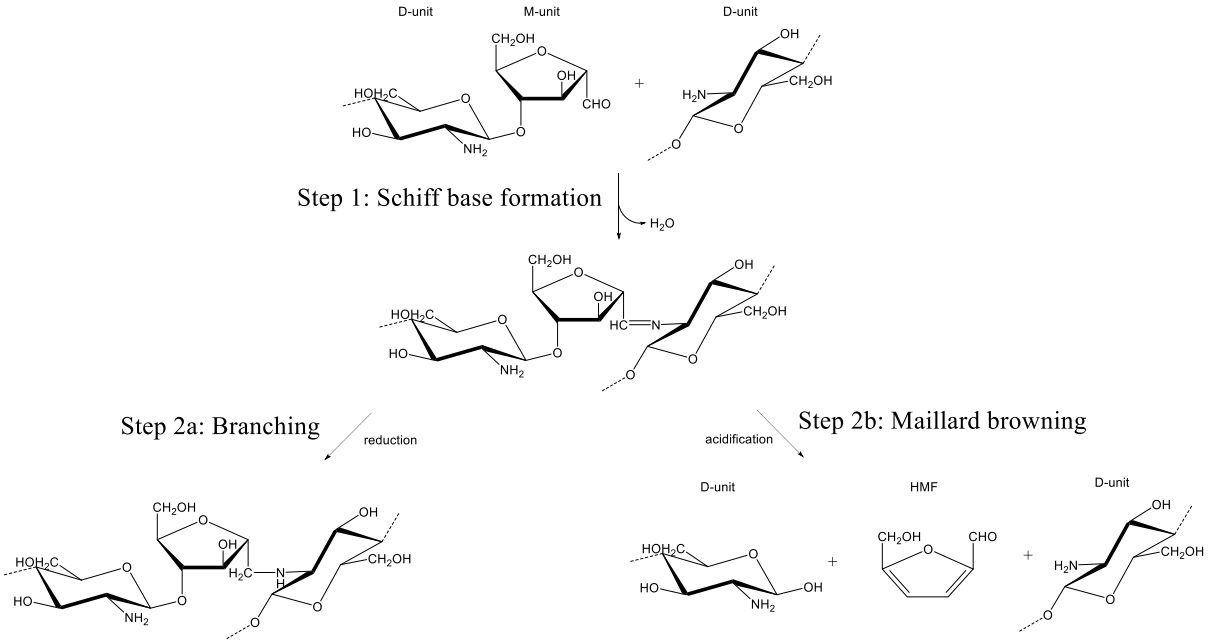

Figure 2.6. Side reactions of the M-unit. The M-unit forms a Schiff base with the D-units amine if the pH is high enough. Once the Schiff base has been formed, reduction results in permanent branching, while acidification results in loss of M-unit.

2.2.4 ^{1}H-NMR of D$_n$M-type chitosan

Chemical shifts and coupling constants for the M-unit has been determined by Tømmeraas et al.[47] (Figure 2.7).

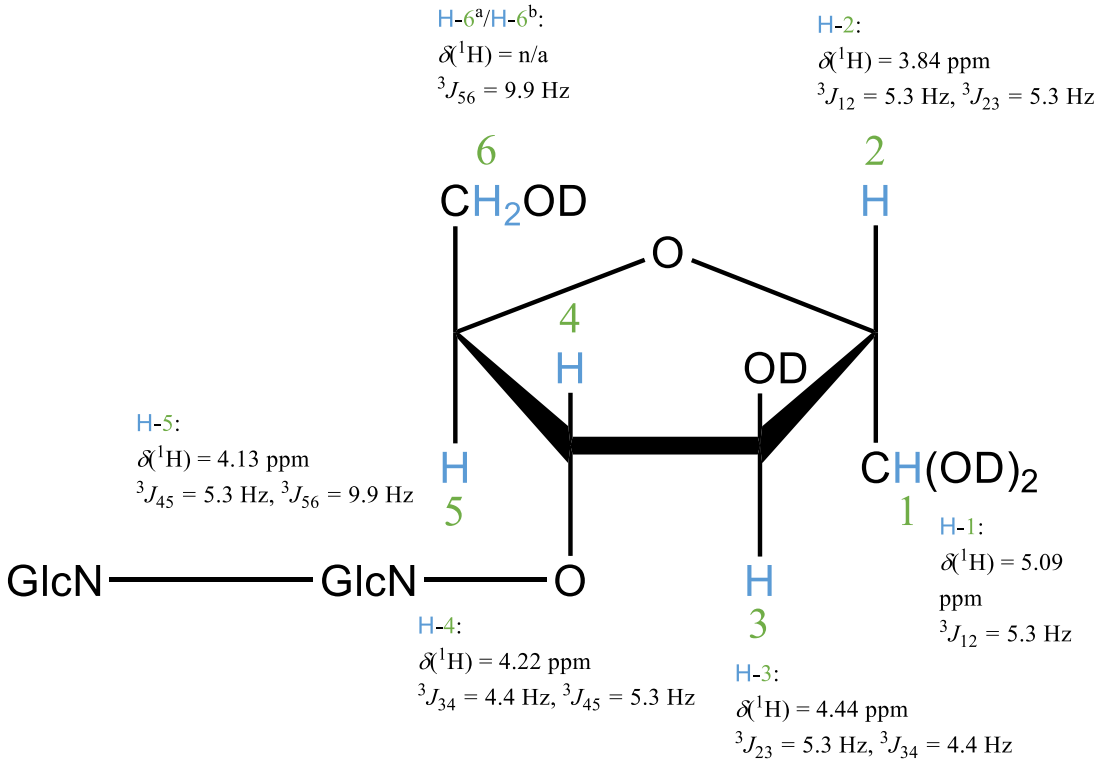

Figure 2.7. Chemical shifts (δ) and vicinal coupling constants (^3J) for the M-unit as determined by Tømmeraas, K.; Vårum, K. M.; Christensen, B. E.; Smidsrød, O. *Carbohydrate Research* **2001**, 333, (2), 137-144.[47]

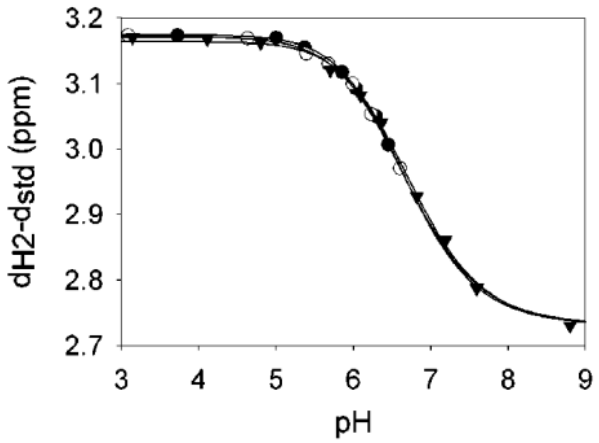

Figure 2.8. Titration curve showing how the chemical shift of the D-unit H-2 changes as a function of pH. Taken from: Strand, S. P.; Tømmeraas, K.; Vårum, K. M.; Østgaard, K. *Biomacromolecules* **2001**, 2, (4), 1310-1314.[3]

Tømmeraas et al. also determined chemical shifts and coupling constants for the D-unit reducing end. Other authors have characterised the D-units internal to the chain.[53, 54]

The chemical shift of the D-unit H-2 is sensitive to changes in pH due to the neighbouring primary amine. Protonation of the amine causes deshielding of H-2 (Figure 2.8).[3] Titration can therefore be used to shift the H-2 peak in case of overlap.

2.3 Dextrans

Dextran is a branched polysaccharide comprised entirely of D-glucose. The main chain is α-(1→6) linked while branching points are attached by α-(1→2), α-(1→3) and α-(1→4) linkages (Figure 2.9).[2] Industrial production of dextran is achieved by bacterial fermentation of sucrose; amount of branching and branching linkage type is strain dependent.[55] Dextran is FDA approved, shows low immunogenicity,[56] and has found medical use as a plasma volume expander,[57] antithrombotic agent,[58] and can reduce blood-viscosity.[59]

2.4 Reductive amination

Reductive amination is a two-step process. First, an imine is formed by a condensation reaction between an amine and a carbonyl compound. Condensation is facilitated by nucleophilic attack by the amine. Then, the imine is reduced to yield a stable secondary amine (Figure 2.10). The reduction is irreversible and so drives formation of the secondary amine to completion. Reductive amination can be performed as a two-pot or a one-pot reaction. For two-pot reductive amination, the reducing agent is added after formation of the imine.

Both formation and decomposition of the imine are acid catalysed; formation requires

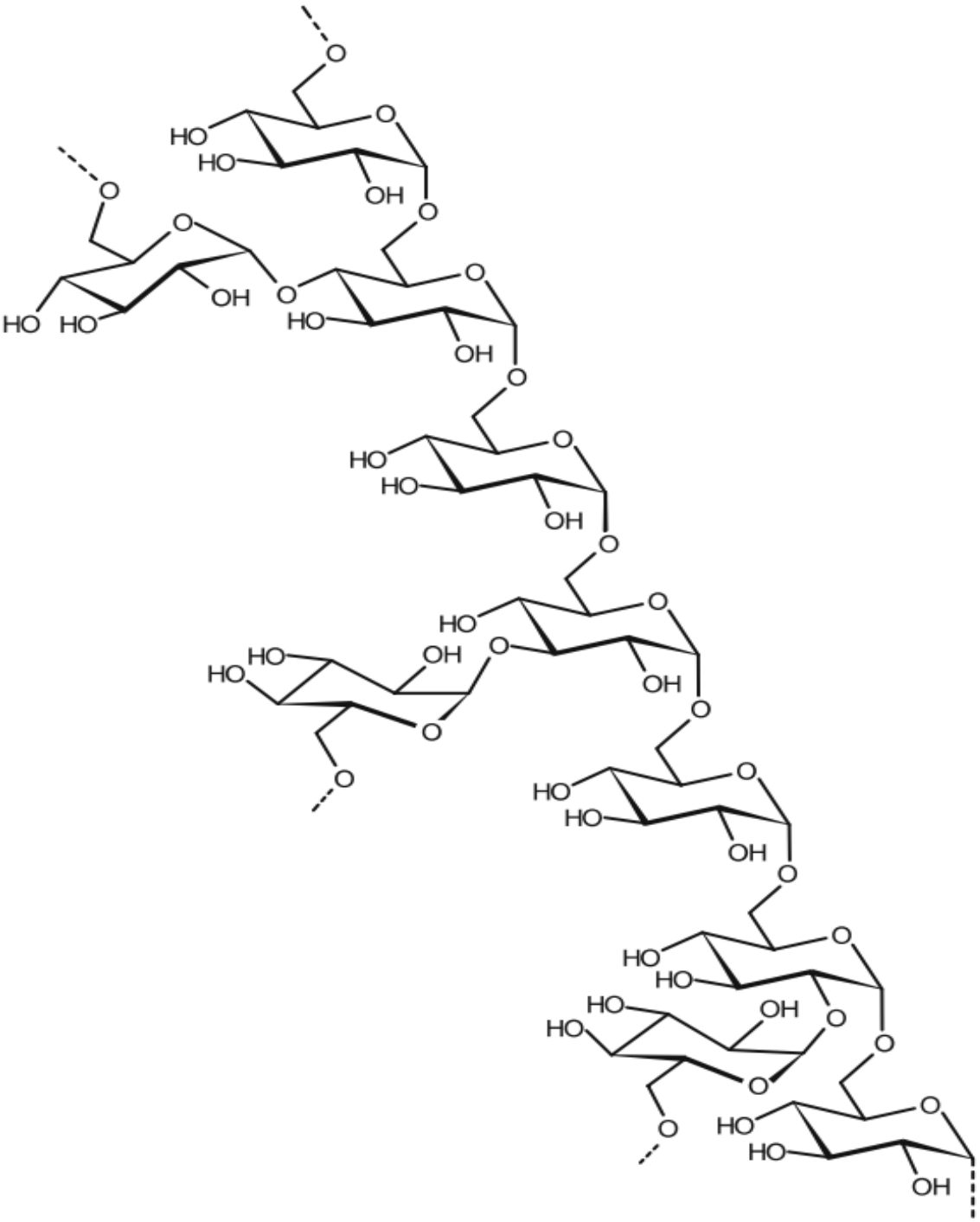

Figure 2.9. Structure of dextran. The main chain is α-(1→6) linked while while branching points are attached by α-(1→2), α-(1→3) and α-(1→4) linkages. Taken from: Heinze, T.; Liebert, T.; Heublein, B.; Hornig, S., Functional polymers based on dextran. In *Polysaccharides Ii*, Springer: **2006**; pp 199-291.[2]

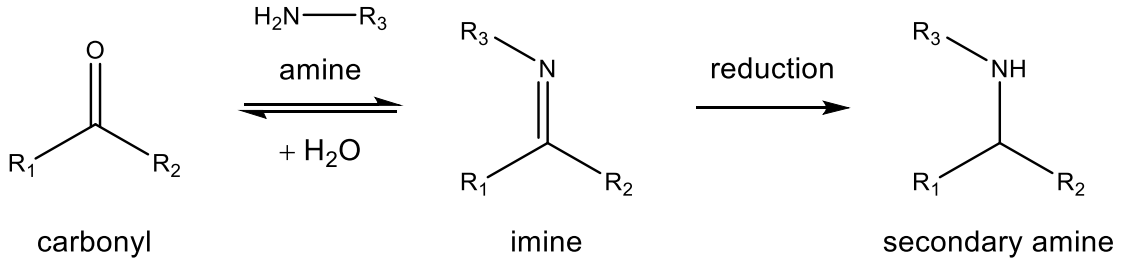

Figure 2.10. Reductive amination. A carbonyl and amine condense to form an imine. Reduction of the imine produces a stable secondary amine.

protonation of the carbonyl oxygen whereas protonation of the amine promotes decomposition. Theoretical modelling predicts that the optimal pH lies just above the pK_a of the amine.[60] Rapid condensation is therefore favoured by amines with a low pK_a. That being said, optimal pH is also influenced by choice of reducing agent, at least when performing a one-pot reaction.

2.4.1 ADH and PDHA

Adipic acid dihydrazide (ADH) and *O*,*O*'-1,3-propanediylbishydroxylamine dihydrochloride (PDHA) are symmetrical amines (Figure 2.11) commonly used to cross-link polysaccharides and proteins via reductive amination.[61] Formation of an imine using ADH and PDHA is favoured by their relatively strong nucleophilicities[62] and low pK_a. ADH as a pK_a of 3.1; PDHA has a pK_a of 4.2.[63]

When a hydrazide (i.e. ADH) or an oxyamine (i.e. PDHA) condenses with an aldehyde, the product, a Schiff base, undergoes *cis*-*trans* isomerisation (Figure 2.12).[64, 65]

2.4.2 *α*-Picoline borane

α-Picoline borane (Pic-BH_3, Figure 2.13) is a reducing agent introduced for reductive amination of polysaccharides as a less toxic alternative to the extensively used sodium

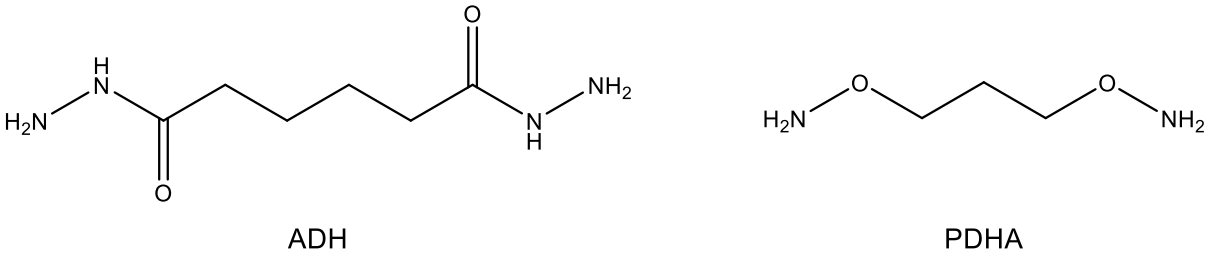

Figure 2.11. Bifunctional linkers adipic acid dihydrazide (ADH) and *O*,*O*'-1,3-propanediylbishydroxylamine dihydrochloride (PDHA).

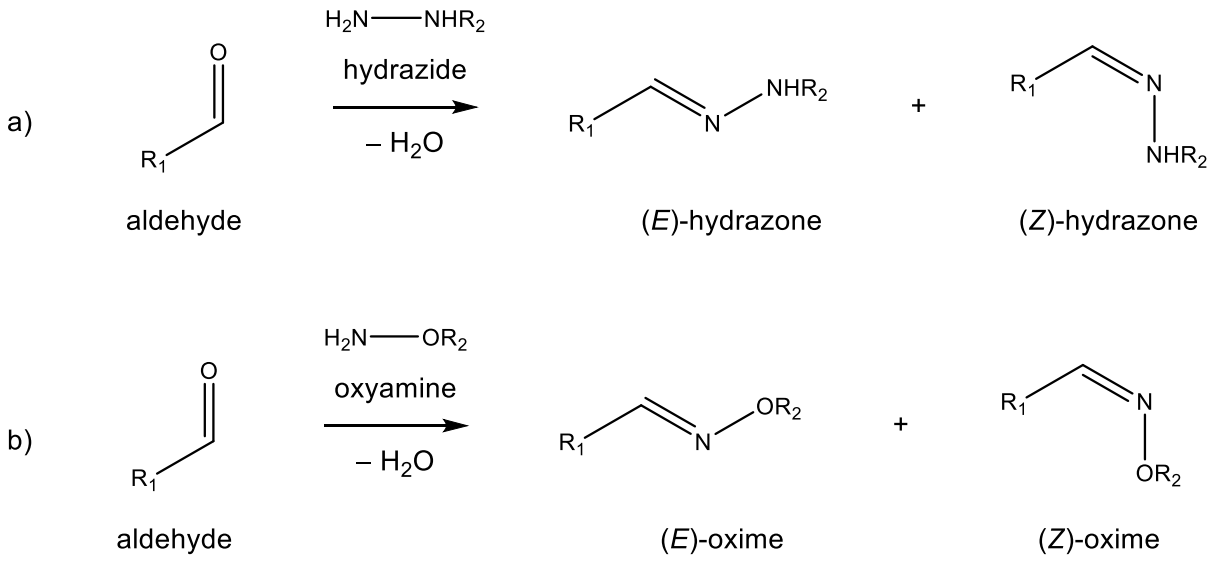

Figure 2.12. Amination reaction between aldehyde and a) hydrazide and b) oxyamine resulting in the formation of (*E*)- and (*Z*)-isomers.

cyanoborohydride ($NaBH_3CN$).[66] Pic-BH_3 is compatible with solvent-free reductive amination.[67] The rate and yield of reductive amination can be improved by making use of an excess of Pic-BH_3. However, the low solubility of Pic-BH_3 in aqueous media limits the excess that practically can be achieved.[63]

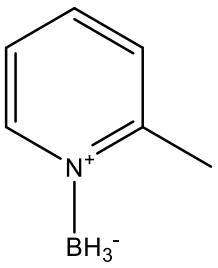

Figure 2.13. α-Picoline borane (Pic-BH_3).

2.5 Analysis methods and techniques

2.5.1 Size-exclusion chromatography[68]

Chromatography is used to identify, quantify, and purify components of complex mixtures. In essence, the chromatographic system is comprised of two or more distinct phases into which the components uniquely partition on the basis of their physicochemical properties.

Subclassifications such as ion-exchange chromatography, gas chromatography, and liquid chromatography are named by reference to the cardinal property by which the components are discriminated by – charge, volatility, and solubility for the examples just listed.

Size-exclusion chromatography (SEC) separates components based on their hydrodynamic volume. When performing SEC, a mobile phase (MP) flows through a column filled with porous beads, the pores of which are filled with a stationary phase (SP). The SP is usually just stagnant MP. Small components do not travel down the column in a straight path. Instead they take detours by randomly diffusing into the porous beads where they are retained until they randomly diffuse back out. Since the pores are tapered and not always of uniform size, smaller components can penetrate more pores and deeper compared to larger components. Consequently, the components align along a gradient from large to small as they elute (i.e. exit the column).

All components larger than the largest pore size will elute at the same time, t_0. Similarly, all components small enough to completely penetrate all pores will elute at the same time, t_i. For constant MP flow rate, components of intermediate sizes will elute at

$$t_\mathrm{e} = t_0 + Kt_\mathrm{i}\,, \tag{2.8}$$

where K is the distribution coefficient. K is a value between 0 and 1. For polymers, the distribution coefficient is a function of radius of gyration.

Upon injection, all components occupy a single, narrow band. Identical components undergo band broadening as they travel down the column. Band broadening is a consequence of how all the identical components do not travel the same exact path; all components do not enter the same pores or the exact same number of pores. Ideally, bands should be as narrow as possible when they elute as this corresponds to maximum resolution and minimal peak overlap.

The SEC system is comprised of an injector, one or multiple columns, one or multiple on-line or off-line detectors, and oftentimes a sample collector. Choice of detector depends upon the type of compound being examined. Common choices are the refractive index (RI) detector, ultraviolet (UV) detector and the flame ionisation (FI) detector.

2.5.2 Nuclear magnetic resonance spectroscopy[69, 70]

Nuclear magnetic resonance (NMR) spectroscopy is a versatile tool with applications such as the elucidation of molecular structures, identification of components in a mixture, and

quantification of equilibrium constants (e.g. pK_a and rate constants). The four main components of an NMR spectrometer are (i) a superconductive magnet, (ii) a radiofrequency (RF) emitter, (iii) a receiver, and (iv) a computer. A sample is placed in the static magnetic field generated by the superconductive magnet and exposed to electromagnetic radiation from the RF emitter. The wavelength of the electromagnetic radiation is selected so that particular nuclides in the sample (^{1}H in the case of ^{1}H-NMR) become exited. Exited nuclides reemit the radiation as they undergo spontaneous relaxation. Relaxation is detected by the receiver as a free induction decay (FID). The FID is transmitted to a computer performing a Fourier transformation. The Fourier transformation is a mathematical operation which converts the raw input (time domain) into a readable spectrum (frequency domain). The final result is a spectrum showing signal intensity as a function of chemical shift.

The signal-to-noise ratio (S/N) is proportional to the square root of the number of scans (ns, i.e. repetitions of excitation and relaxation):

$$\mathrm{S/N} \propto \sqrt{\mathrm{ns}}\,. \tag{2.9}$$

The S/N ratio is also proportional to the strength of the applied magnetic field. NMR spectrometers are designed to only operate within a narrow band of magnetic field strengths. To make use of a greater magnetic field strength therefore requires transfer of the sample to a better-grade instrument.

Spin

Nuclei possess an intrinsic angular momentum (spin). Spin is a highly quantised variable, with every possible value being described by the spin quantum number, *I*. *I* can be any integer or half-integer value in the interval [0, 6]:

$$I = 0, \frac{1}{2}, 1, \frac{3}{2}, \ldots, 6\,. \tag{2.10}$$

A particular nuclide invariably has a particular spin (Table 2.1). A nuclide with a spin quantum number of 0 does not possess spin and therefore cannot be observed by NMR. So even though ^{12}C and ^{16}O are abundantly present in polysaccharides, they will never produce an observable signal. And since nuclides with different spin quantum numbers cannot be observed simultaneously, the solvent (a potential source of much noise) can be rendered invisible by making sure it does not contain the nuclide of interest (e.g. by using deuterated solvents in the case of ^{1}H-NMR).

Table 2.1. Spin quantum number (*I*) for a few select isotopes.

Nuclide	*I*
^{12}C, ^{16}O	0
^{1}H	1/2
^{2}H, ^{14}N	1

A nucleus can occupy ($2I$ + 1) energy levels. The energy levels are denoted by the magnetic quantum number *m* which is assigned the values $m = I, I-1, \ldots, -I$. For example, ^{1}H (with I = ½) can occupy the two ($2 \cdot ½ + 1 = 2$) energy levels m = ½ and m = -½. The energy difference (ΔE) between two adjacent levels (i.e. for when $\Delta m = 1$) is given by

$$\Delta E = \frac{h\gamma}{2\pi} B_0 \,, \tag{2.11}$$

where h is Planck's constant, γ the magnetogyric ratio (a nuclide-specific constant), and B_0 the strength of the applied magnetic field. Nuclides are categorised as sensitive or insensitive, determined by the magnitude of their magnetogyric ratio; a small γ makes the nuclide hard to detect (low S/N ratio), while a large γ makes the nuclide easy to detect (high S/N ratio). ^{1}H has the greatest magnetogyric ratio of any nuclide ($\gamma_{^{1}\mathrm{H}}$ = 42.58 MHz/Tesla).

The energy, E, carried by a photon is given by the Planck-Einstein relation

$$E = h\nu \,, \tag{2.12}$$

where h is Planck's constant and ν its frequency. When a nucleus is irradiated by light matching the energy gap (ΔE, Eq. (2.11)) between two adjacent energy levels, the nucleus can absorb the light and transition into an excited, higher energy state. The exact wavelength corresponding to ΔE is known as the Larmor frequency. Note that the Larmor frequency is dependent upon the magnetic field strength applied.

Chemical shift

The nucleus is either magnetically *shielded* or *deshielded* by its local environment. Shielding causes the nucleus to resonate (i.e. become exited) at a slightly higher frequency. Deshielding has the opposite effect. Shielding is quantified as chemical shift (δ). Chemical shift is defined as a parts per million (ppm) deviation from a chosen reference. Tetramethylsilane (TMS) is the universally accepted reference for ^{1}H-NMR and ^{12}C-NMR. TMS has, by definition, a chemical shift of 0 ppm. By adding TMS to the sample, its spectrum can be easily calibrated.

Interconversion between chemical shift and resonance frequency is straightforward:

$$\delta = \frac{\nu - \nu_{\text{ref}}}{\nu_{\text{ref}}} \ , \tag{2.13}$$

where ν is the resonance frequency of the particular nucleus and ν_{ref} is the resonance frequency of the reference compound.

Coupling

The magnetic quantum number (m) of several nuclei may be interdependent due to what is known as spin-spin coupling. The most common type of coupling is indirect coupling, which is mediated by the electrons of intervening bonds. Clusters of coupled nuclei comprise spin systems. All the nuclei comprising a single spin system are not necessarily coupled; for large spin systems, nuclei at one end are not coupled to nuclei at the other end.

Nuclei that are not coupled will appear as a single, sharp peak in the NMR spectrum. Coupling results in peak splitting. The splitting pattern is determined by the number of chemically non-equivalent nuclei that the particular nucleus is coupled to. Chemically non-equivalent nuclei are nuclei in different local chemical environment. The number of peaks (referred to as multiplicity) resulting from peak splitting is given by

$$N = 2n + 1 \ , \tag{2.14}$$

where n is the number of chemically non-equivalent, coupled nuclei. The splitting pattern is symmetrical and with peak intensities described by Pascal's triangle (Table 2.2).

Table 2.2. Multiplicity and peak intensities produced by spin-spin coupling to n chemically non-equivalent nuclei.

n	Multiplicity (N)	Relative intensity (Pascal's triangle)
0	Singlet (s)	1
1	Doublet (d)	1 1
2	Triplet (t)	1 2 1
3	Quartet (q)	1 3 3 1
4	Quintet	1 4 6 4 1
5	Sextet	1 5 10 10 5 1
6	Septet	1 6 15 20 15 6 1
7	Octet	1 7 21 35 35 21 7 1

The distance between each peak is measured in Hz and is given by the coupling constant *J*. Geminal coupling is coupling across two bonds (i.e. **H**–C–**H**); vicinal coupling is coupling across three bonds (i.e. **H**–C–C–**H**); long-range coupling is coupling across four or more bonds, and only occurs under special circumstances. The coupling constant is written as J^2 and J^3 to indicate geminal and vicinal coupling, respectively.

Chemical shift, coupling constant, and splitting pattern are used corroboratively to identify chemical groups.

pH

Acids and bases do not interact identically with hydrogen (H^+) and deuterium (D^+). A distinction is therefore made between pH and pD. The empirically derived formula

$$\mathrm{pH}^* = \frac{\mathrm{pH} - 0.421}{0.9291} \tag{2.15}$$

can be used to convert between pH and pD, where pH^* is the value obtained when a standard pH-meter is used for a deuterated solution.[71] As an example, consider acetic acid (AcOH, pK_a 4.76) dissolved in D_2O. A standard pH-meter is used to find that $\mathrm{pH}^* = 4.5$. Applying Eq. (2.15), it is estimated that the solution has a pD corresponding to a pH of 4.6, which according to the Henderson-Hasselbalch equation, means that the degree of ionisation for AcOH in the deuterated solution is 41 %.

3 Materials and Methods

3.1 Materials

Two in-house samples of fully de-*N*-acetylated chitosan (F_A = 0.01) were used, one for preparation of activated chitosan (Section 3.5), the other for synthesis of a chitosan-dextran diblock (Section 3.6). The dextran is from Pharmacia Fine Chemicals. Adipic acid dihydrazide (ADH), *O*,*O*'-1,3-propanediylbishydroxylamine dihydrochloride (PDHA) and α-picoline borane (Pic-BH_3) were purchased from Sigma-Aldrich. Ultrapure water was provided by an OmniPure water system (Stakpure, Niederahr, Germany). All other chemicals used were of analytical grade.

3.2 Size-exclusion chromatography

The SEC system was comprised of three HiLoad™ 26/60 columns connected in series and packed with Superdex™ 30. The mobile phase was an AmAc buffer (0.15 M, pH 4.5) with a flow rate of 0.8 ml/min. The pump was a LC-10AD vp SHIMADZU. A Shodex RI-101 refractive index (RI) detector was connected on-line. WinDaq Data Acquisition Software was used to capture chromatograms. Fractions were collected using an LKB 2111 MultiRac collector. All material was filtered through a 0.45 μm nylon filter (Acrodisc 13 mm, Pall Corporation) before injection.

3.3 Dialysis

Dialysis was performed using Spectrum Spectra/Por Biotech Cellulose Ester (CE) dialysis membrane tubing of varying MWCO and diameter. The 500 MWCO variety was stored in an azide solution. Before use, the membranes were thoroughly soaked and rinsed with ultrapure water.

3.4 Nuclear magnetic resonance spectroscopy

All NMR-spectra were acquired using 5 mm NMR tubes, D_2O as solvent, at 25 °C, and while running a standard Bruker zg30 pulse sequence, either on a Bruker Ascend 400 MHz or on a Bruker Avance 600 MHz (Bruker BioSpin AG, Fällanden, Switzerland). Spectra processing was performed with TopSpin 4.0.8. Sometimes TSP was added as internal standard. pD adjustment was performed using DCl and NaOD. Number of scans was varied between 32 and 128. The other main parameters were: Dummy scans, ds = 2. Interscan delay, d1 = 1 s. Transmitter frequency offset, O1P = 6.175 ppm. Spectral width, sw = 20.03 ppm.

3.5 Preparation of activated chitosan

3.5.1 Nitrous acid depolymerisation and SEC fractionation

Chitosan (2197 mg, F_A = 0.01) dissolved in AcOH (*aq*, 131.8 ml, 2.5 % v/v) was cooled to 4 °C and sparged with N_2 (*g*) for 20 min. Immediately after sparging, sodium nitrite ($NaNO_2$, 207 mg) was added to give a molar ratio of 1.1 moles $NaNO_2$ per 5 moles D-unit. The reaction mixture was left in a sealed container in the dark at 4 °C for 3 days. Afterwards, the sample was dialysed (100-500 Da, volume/length = 3.1 ml/cm) for 6 h total with the dialysis buffer being changed every hour (2x 50 mM NaCl, 4x ultrapure water). 2.2 mg sample was dialysed against 6 L dialysis buffer. The dialysate was lyophilised two times and weighed. 6 mg sample was used for ^{1}H-NMR acquisition while the remaining 2169 mg were dissolved in AmAc-buffer (0.15 M, pH 4.5) and fractionated using SEC (1 run à 50 mg; 7 runs à ~300 mg).

3.5.2 Purification of SEC fractions

Fractions *h*, *l*, *m*, and *n* from the SEC fractionation of a nitrous acid depolymerisate (Section 4.1.1) were separately loaded into a 100-500 Da MWCO dialysis bag (volume/length = 3.1 ml/cm). Fractions *l* and *n* were dialysed for 4 h total and the dialysis buffer was replaced every hour. For the first two hours, the dialysis buffer was an aqueous solution containing 50 mM NaCl. For the last two hours, the dialysis buffer was a pure aqueous solution (ultrapure water).

Fractions *h* and *m* were dialysed until the conductivity of the dialysis buffer had not changed by more than 1.2 µS over two hours (took ~4 days of dialysis). About 50x the volume of sample was used as dialysis buffer. The dialysis buffer was an aqueous solution (ultrapure water) with AcOH added to give a pH of 4. The dialysis buffer was replenished regularly. After dialysis, all fractions were lyophilised twice. The fractions were resolubilised in ultrapure water after the first round of lyophilisation. Before both rounds of lyophilisation, the pH was adjusted to 3.85.

3.5.3 Activation

D_nM-type chitosan (7.0 mg; Appendix B) produced by nitrous acid depolymerisation of a fully de-*N*-acetylated chitosan (Section 3.5.1) was dissolved in a deuterated NaAc buffer (500 µl) with added TSP. The NaAc buffer was prepared by mixing AcOD (99.5 % D_4), D_2O, TSP and exactly enough NaOD to give a final pH of 4.0, a final acetate concentration of 500 mM, and a final TSP concentration of 2 mM. ADH (3.5 mg) was added to the buffer solution which

was thereafter tracked by ^{1}H-NMR. After equilibrium had been reached, Pic-BH_3 (3.2 mg) was added. The reaction was performed at RT and with constant stirring.

Following the protocol just outlined, two experiments with PDHA instead of ADH was performed. For the first experiment: 7.0 mg D_nM-type chitosan (fraction *m*), 3.6 mg PDHA, 500 µl deuterated NaAc buffer and 3.2 mg Pic-BH_3. For the second experiment: 10.8 mg D_nM-type chitosan (fraction *m*), 5.1 mg PDHA, 700 µl deuterated NaAc-buffer and 30.1 mg Pic-BH_3.

3.5.4 Background reduction

D_nM-type chitosan (7.7 mg; Appendix B) produced by nitrous acid depolymerisation of a fully de-*N*-acetylated chitosan (Section 3.5.1) was dissolved in a deuterated NaAc-buffer (500 µl). Makin of the NaAc buffer was detailed in the previous section. Pic-BH_3 (3.2 mg) was added and the reaction was followed by ^{1}H-NMR. The reaction was performed at room temperature and with constant stirring.

3.6 Desalting

3.6.1 Dialysis: escape rates of salts

Three solutions were made: NaCl (*aq*, 0.15 M), AmAc (*aq*, 0.15 M), and NaAc (*aq*, 0.15 M). 9 dialysis bags (volume/length = 6.4 ml/cm) with MWCO 12-14 kDa were loaded with 32 ml solution (3 bags à 32 ml for each solution). The 3 bags containing the same solution were together immersed in 8 L dialysis buffer (ultrapure water). An aliquot (4 ml) from inside each bag was taken every hour and its conductivity was measured. The dialysis buffer was replenished every hour. The dialysis buffer was not stirred.

3.6.2 Desalting by means of size-exclusion chromatography

Two samples were prepared: 1) AmAc (*aq*, 0.15 M, 2.5 ml) and 2) AmAc (*aq*, 0.15 M, 2.5 ml) with added chitosan (7.5 mg of fraction *a* (Figure 4.2)). The MP was made by dissolving 56 µM AcOH in ultrapure water to give a solution of pH 4.5. A PD-10 Desalting Column prepacked with Sephadex™ G-25 Medium was prepared by allowing 5 ml of MP to completely enter the packed bed five times in a row. After the column had been prepared by equilibrating it with MP, one of the samples was applied to the column and allowed to completely enter the packed bed. Immediately after, 3.5 ml of MP was applied on top of the sample and fraction collection was begun. 10 drops were counted for each fraction until 22 fractions had been collected. When the 3.5 ml of MP had completely entered the packed bed,

a new 3.5 ml was immediately applied. This was repeated until all 22 fractions had been collected. Each fraction was diluted with 2.5 ml of MP. A conductivity meter zeroed against ultrapure water was used to measure the conductivity of each fraction. The protocol was repeated twice, once for each sample.

3.7 Synthesis of a chitosan-dextran diblock

3.7.1 Preparation of activated chitosan

Two aliquots of D$_n$M-type chitosan (200 mg per aliquot, DP$_n$ 22, Appendix C), prepared by Marianne Øksnes Dalheim (Department of Biotechnology and Food science, NTNU) by nitrous acid depolymerisation of a fully de-*N*-acetylated chitosan, was dissolved in a NaAc buffer (500 µl per aliquot, pH 4.5). The NaAc buffer was prepared as described in Section 3.5.3 but with non-deuterated chemicals and without addition of TSP. ADH (108 mg) was added to one of the aliquots while PDHA (111 mg) was added to the other. The mixtures were left to react for 4 h, at room temperature, without stirring. Pic-BH$_3$ (132 mg) was then added to both aliquots. The aliquot containing ADH was left for 72 h, at room temperature, with stirring. The aliquot containing PDHA was left for 260 h, at room temperature, with stirring. Both aliquots were then fractionated by SEC using a AmAc buffer (0.15 M, pH 4.5) as mobile phase (Section 3.2). Individual fractions were purified by dialysis and lyophilisation.

3.7.2 Preparation of dextran

Low molecular weight dextran (600 mg) was prepared by acid hydrolysis (performed by Odin Weberg Haarberg, Department of Biotechnology and Food science, NTNU). The dextran was fractionated over several runs by SEC using an AmAc buffer (0.15 M, pH 4.5) as mobile phase (Section 3.2). Injection volume and concentration was 4 ml and 50 mg/ml. Individual fraction were lyophilised five times in order to remove AmAc introduced by the SEC buffer. The fractions were resolubilised in ultrapure water between each round of lyophilisation.

3.7.3 Conjugation of activated chitosan and dextran

D$_n$M-ADH + Dex

D$_n$M-ADH (DP$_n$ 41, 26 mg) was completely dissolved in a NaAc buffer (500 µl, pH 4.5). First, Pic-BH$_3$ (10 mg) was added. Then, dextran (DP$_n$ 15, 45 mg) was added. The reaction mixture was left in a 40 °C water bath for 6 days. Afterwards, the sample was dialysed against ultrapure water for 2 days (3.5 kDa MWCO) and then lyophilised. After lyophilisation, the sample was run on SEC and lyophilised another 5 times to remove AmAc introduced by the SEC buffer.

D_nM-PDHA + Dex

D_nM-PDHA (DP_n 300, 15 mg) was completely dissolved in a NaAc buffer (500 µl, pH 4.5). First, Pic-BH_3 (2.6 mg) was added. Then, dextran (DP_n 15, 6.7 mg) was added. The reaction mixture was left in a 40 °C water bath for 4 days. Afterwards, the sample was dialysed against ultrapure water for 2 days (3.5 kDa MWCO) and then lyophilised. After lyophilisation, the sample was run on SEC and lyophilised another 5 times to remove AmAc introduced by the SEC buffer.

4 Results

4.1 Preparation of activated chitosan

4.1.1 Nitrous acid depolymerisation and SEC fractionation

Fully de-*N*-acetylated chitosan (F_A = 0.01) was depolymerised by means of nitrous acid and a ^{1}H-NMR spectrum of the nonfractionated depolymerisate was aquired (Figure 4.1). Peak assignment was performed based on data published by Tømmeraas et al.[47]

Appearing at 5.10 ppm was a strong doublet indicative of the M-unit gem diol H-1. The less abundant aldehydic form of the M-unit was not observed. A broad signal of medium intensity at 8.00 ppm matched what would be expected for an M-unit Schiff base.[47] Comparing the 5.10 and 8.00 ppm signal intensities, a ratio of 73:27 was determined.

Both M- and D-unit reducing ends were present in the depolymerisate. By adding the signal intensities for the M-unit gem diol and the M-unit Schiff base and making a comparison to the α-D-unit H-1 signal (5.44 ppm), it was found that 98 % of the material had the M-unit reducing end. No signal for the β-D-unit was observed, although not surprisingly considering

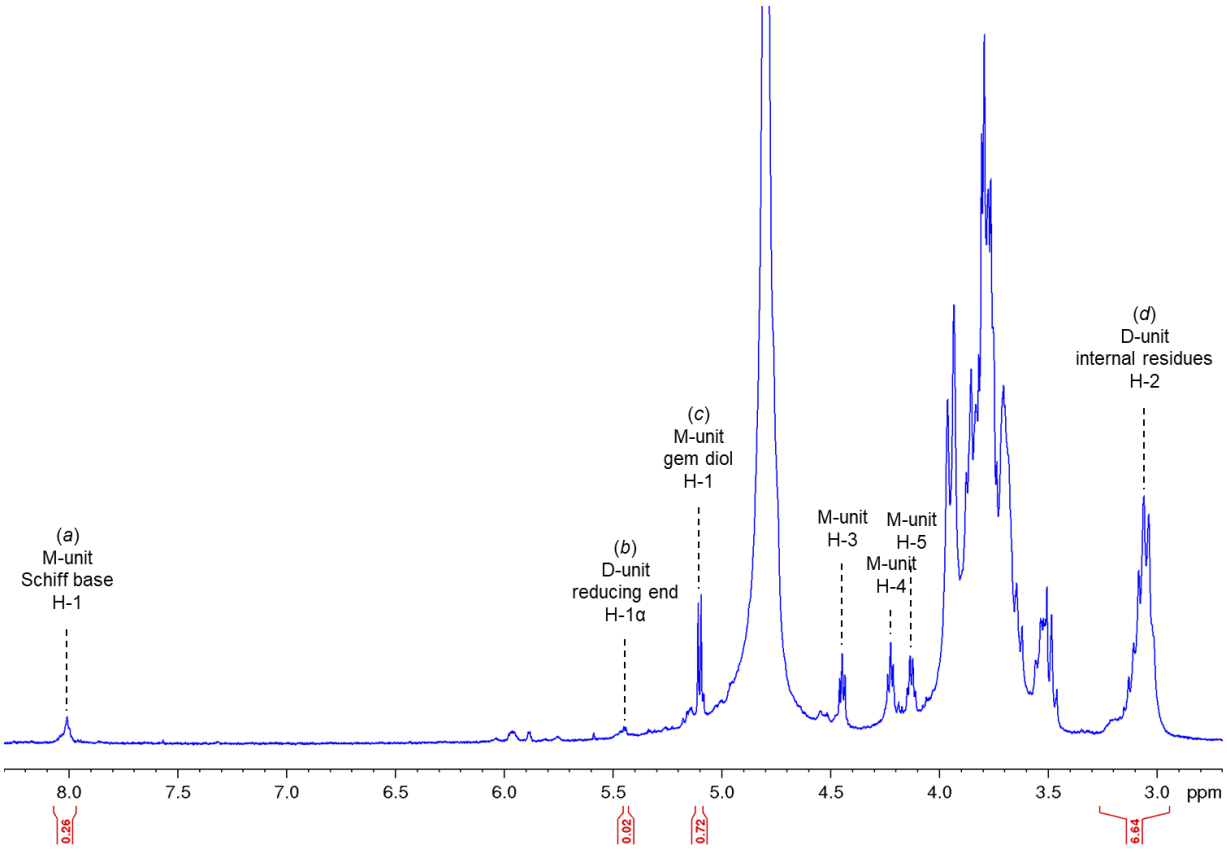

Figure 4.1. ^{1}H-NMR spectrum of a nitrous acid depolymerised, fully de-*N*-acetylated chitosan (F_A = 0.01). Recorded at 400.13 MHz, 25 °C, and with D_2O as solvent.

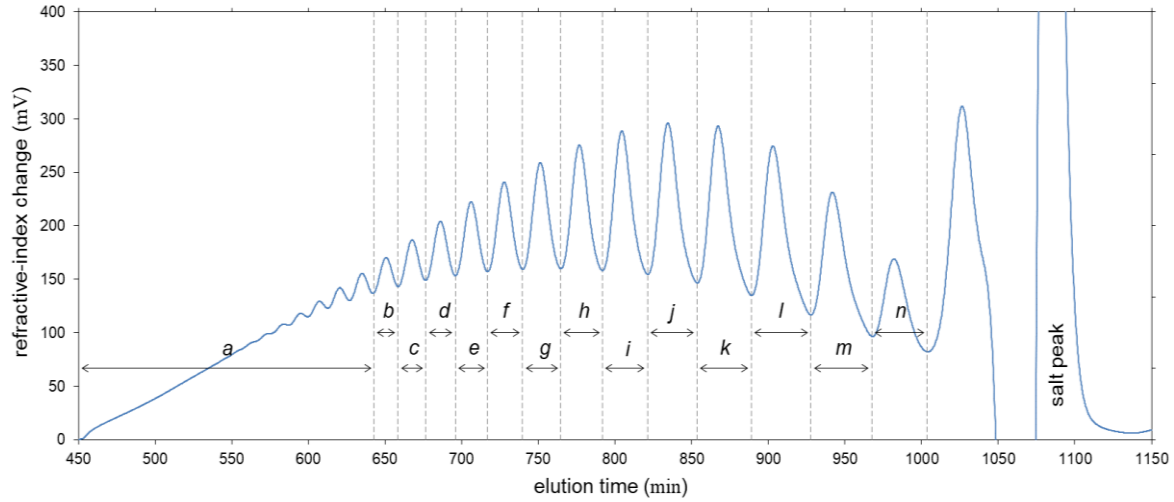

Figure 4.2. Size-exclusion chromatogram of a nitrous acid depolymerised, fully de-*N*-acetylated chitosan (17 mg/ml upon injection). Comprising the SEC-system was three serially connected HiLoad™ 26/60 columns packed with Superdex™ 30 feeding an on-line refractive index detector. Mobile phase = AmAc (0.15 mM, pH 4.5). Injection volume = 4 ml. Flow rate = 0.8 ml/min.

the faint appearance of the α-D-unit H-1 and that the β anomer is less abundant than the α anomer.[53]

The D-unit H-2 produced a broad signal in the 3.26–2.94 ppm region.[53] By considering the M-unit gem diol, α-D-unit and M-unit Schiff base as reducing ends, a DP_n of 7.6 was estimated:

$$DP_n = \frac{I_{(d)}}{I_{(a)} + I_{(b)} + I_{(c)}} + 1 = \frac{6.6}{0.26 + 0.02 + 0.72} + 1 = 7.6\,. \qquad (4.1)$$

A SEC chromatogram of the depolymerisate (Figure 4.2) showed that the longest chains eluted 450 min after injection while the shortest chains eluted within 1050 min. Discernible peaks started to elute after about 550 min. Peaks belonging to progressively shorter chains eluted with progressively better resolution. Although the peaks eluting later are clearly discernible, they are not baseline separated.

4.1.2 Purification of SEC fractions

Fractions *l* & *n* and *h* & *m* were from the same batch of SEC fractionated, nitrous acid depolymerised, fully de-*N*-acetylated chitosan (Section 4.1.1). Fractions *l* and *n* were dialysed for 4 hours, lyophilised twice and then redissolved in pH* 3.85 D_2O. Fractions *h* and *m* were treated identically, except for that they were dialysed for ~4 days instead of 4 hours (Section 3.5.2).

The ^{1}H-NMR spectra of fractions *l* and *n* (4 h of dialysis) showed almost complete loss of M-

unit (Figure 4.3a). Several peaks characteristic of HMF, a product of non-enzymatic browning (Section 2.2.3**),** were identified. A broad triplet produced by ammonium[(72)] was also clearly visible in both spectra. In contrast, the ^{1}H-NMR spectra of fractions *h* and *m* (4 days of dialysis) showed presence of M-unit and absence of ammonium and HMF (Figure 4.3b).

4.1.3 Stability of the M-unit during long-term storage

A nitrous acid depolymerisate of a fully de-*N*-acetylated chitosan (Section 4.1.1) was stored in the dark, at room temperature, and dissolved in pH* 5 D_2O. After 9 months, every M-unit had disappeared while HMF had appeared (Figure 4.4).

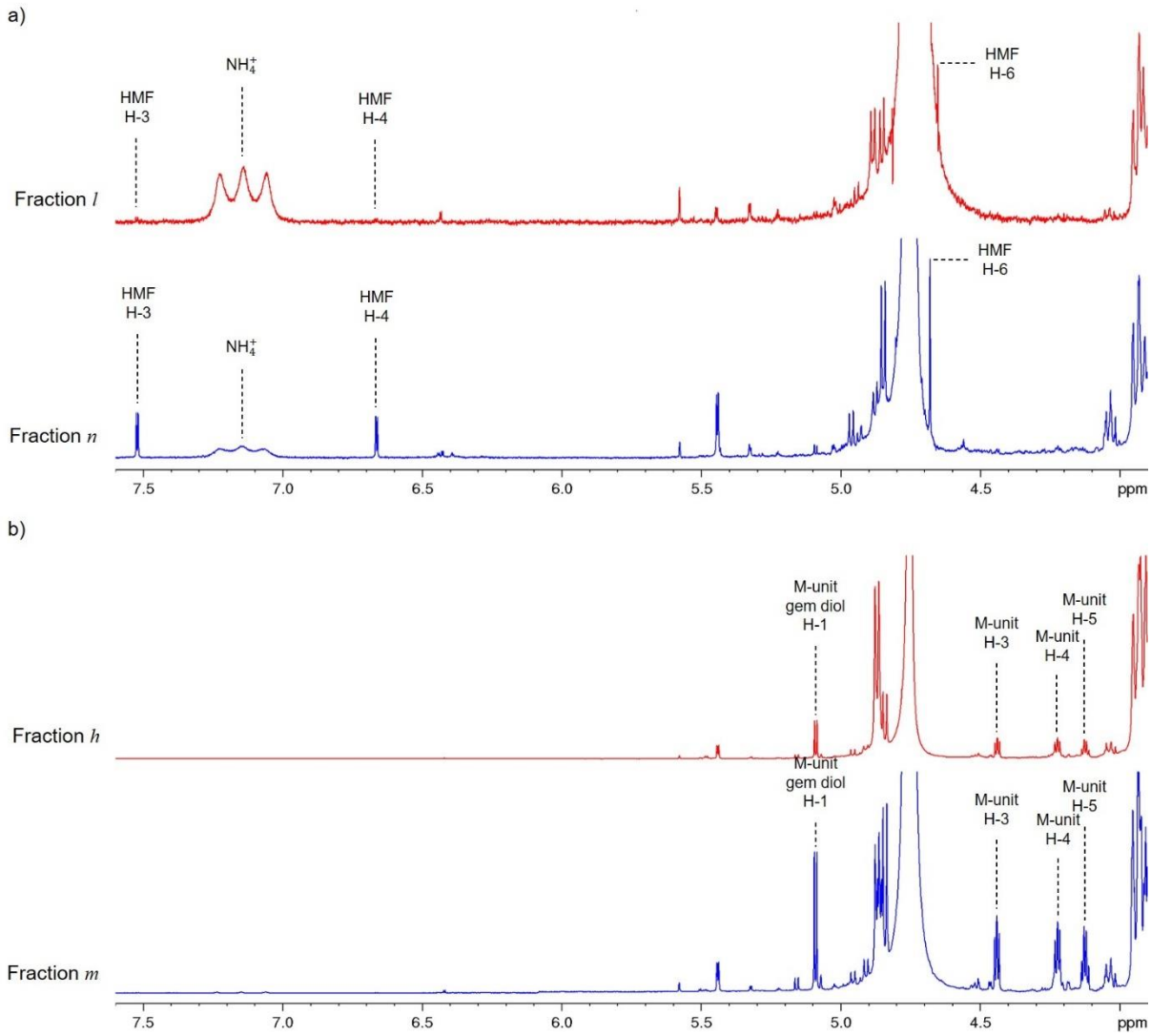

Figure 4.3. ^{1}H-NMR spectra of four fractions from the same batch of nitrous acid depolymerised, fully de-*N*-acetylated chitosan. Recorded at 600.18 MHz, 25 °C, and with a pH* 3.85 D_2O as solvent. **a)** Fractions dialysed for 4 hours, and **b)** fractions dialysed for 4 days.

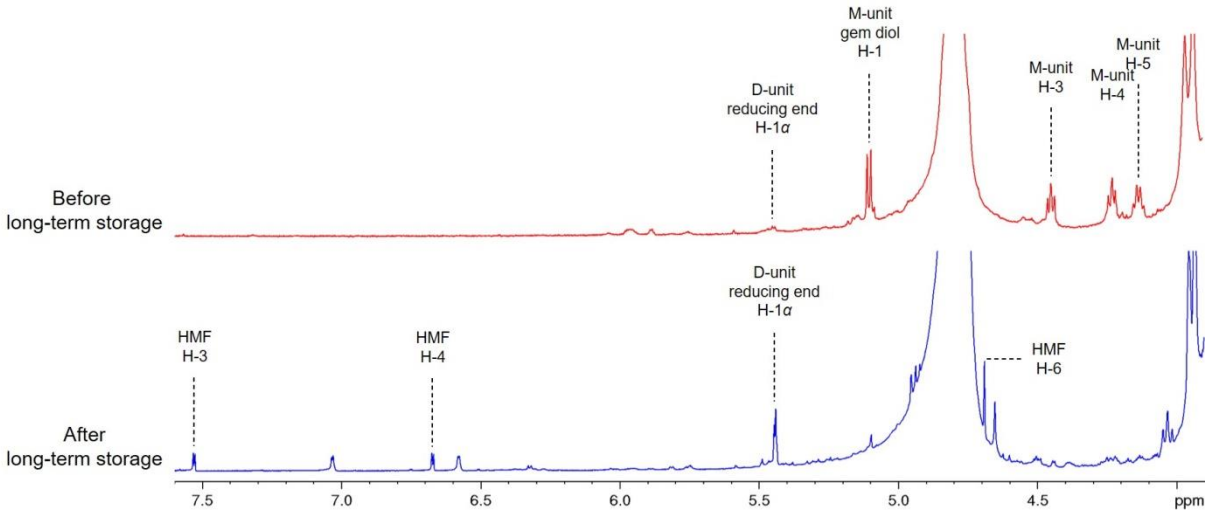

Figure 4.4. ^{1}H-NMR spectra showing the same sample 9 months apart. For 9 months, the sample was stored in the dark, at room temperature and dissolved in D_2O (pH* 5). Upper spectrum was recorded at 400.13 MHz and 25 °C; bottom spectrum was recorded at 600.18 MHz and 25 °C. Sample concentration = 13 mg/ml.

4.1.4 Activation

4.1.4.1 Amination

D_nM-type chitosan (5.0 DP_n; Appendix B) produced by nitrous acid depolymerisation of a fully de-*N*-acetylated chitosan (Section 3.5.1) was separately mixed with ADH and PDHA (Section 3.5.3). Amination was tracked by ^{1}H-NMR. The intensity of the M-unit H-1 signal before addition of ADH and PDHA (at t = 0 h) was used as a basis for estimation of yield; 100 % yield corresponds to a signal intensity equal to that of the M-unit H-1 at t = 0 h. All spectra were calibrated using TSP as internal standard. Peak assignment for the D_nM=PDHA oximes was performed according to Coudurier et al.;[73] peak assignment for the D_nM=ADH hydrazones were deduced by comparison to peak assignment for D_nM=PDHA[73] and other D_nM Schiff bases.[40]

Based on a characterisation of the D_nM-sample (Appendix B), it was estimated that the concentration of D_nM was 12 mM. The D_nM-sample contained some amount of $(GlcN)_n$, i.e. strands without the M-unit reducing end; this material was accounted for to find the true amount of D_nM in the sample. A 3.4x molar excess of ADH and PDHA was used. The D_nM and amines react 1:1.

Although some $(GlcN)_n$ was present in the mix, it did not react appreciably with either ADH or PDHA over the course of the experiment; no measurable decrease in signal intensities for $(GlcN)_n$ reducing ends was observed (Figure 4.5a and Figure 4.6a).

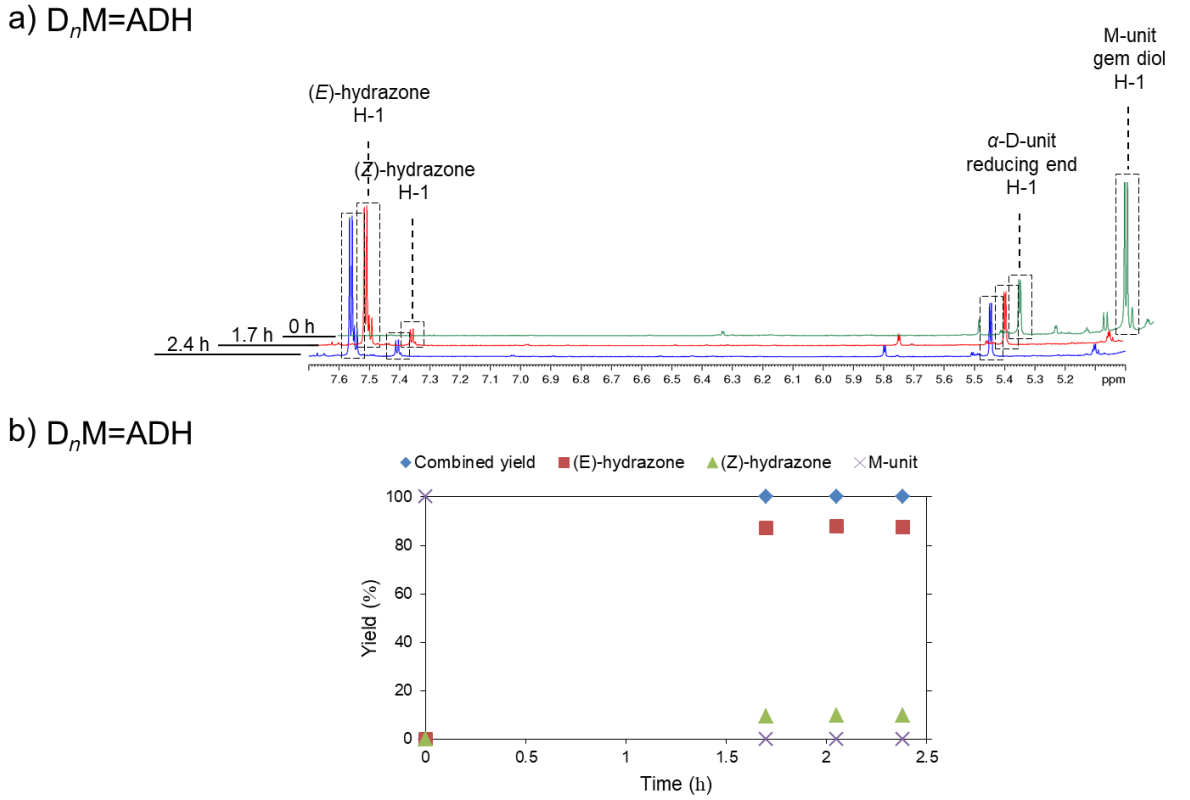

Figure 4.5. D_nM (12 mM) was dissolved in a NaAc-buffer (500mM, pH 4.5) and mixed with a 3.4x molar excess of ADH (40 mM). Performed at RT. **a)** ^{1}H-NMR tracking of the amination reaction. **b)** Yield of (*E*)-hydrazone, (*Z*)-hydrazone and unreacted D_nM (M-unit) as a function of time. Combined yield is the sum of the yield for the (*E*)- and (*Z*)-hydrazones.

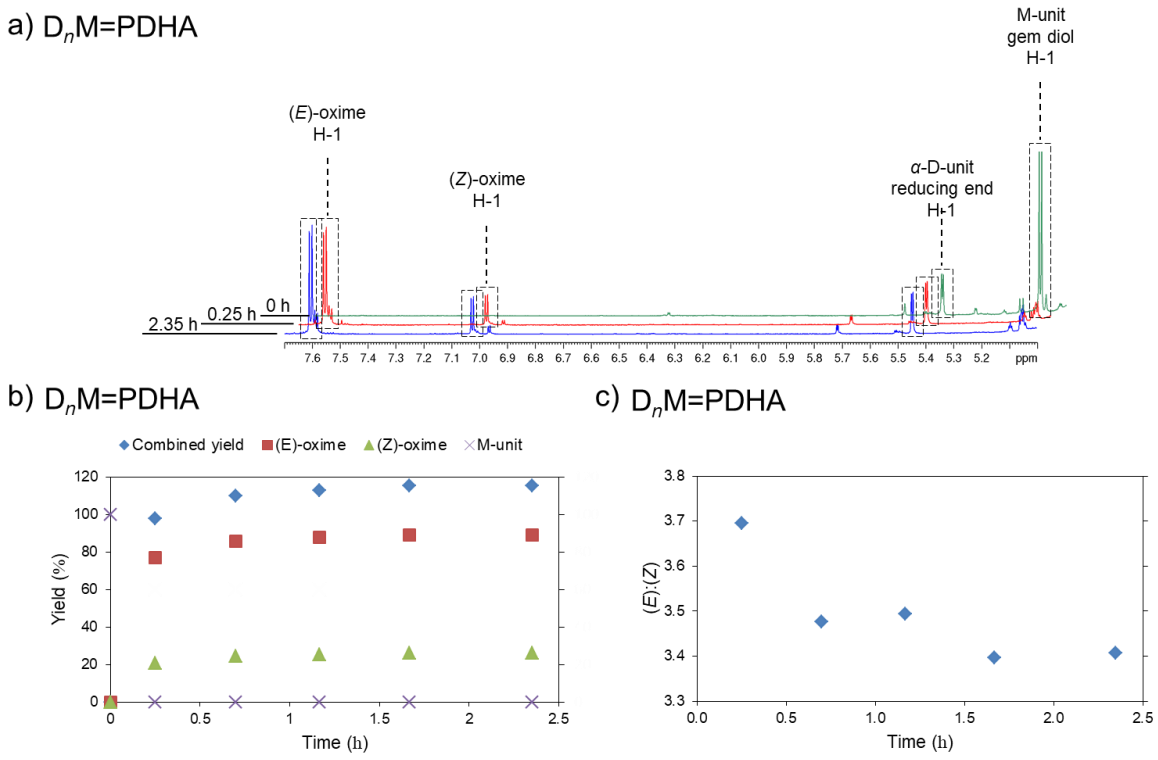

Figure 4.6. D_nM (12 mM) was dissolved in a NaAc-buffer (500mM, pH 4.5) and mixed with a 3.4x molar excess of PDHA (40 mM). Performed at RT. **a)** ^{1}H-NMR tracking of the amination reaction. **b)** Yield of (*E*)-oxime, (*Z*)-oxime and unreacted D_nM (M-unit) as a function of time. Combined yield is the sum of the yield for the (*E*)- and (*Z*)-oximes.

Within 1.7 h, ADH gave a 100 % equilibrium yield of hydrazones (D_nM=ADH). The (*E*):(*Z*)-hydrazone ratio was determined as 90:10 (Figure 4.5)

PDHA gave an oxime (D_nM=PDHA) equilibrium yield of 115 % after 2.5 h. After 0.25 h, no unreacted D_nM remained. Yield of oxime after 0.25 h was 98 %. The (*E*):(*Z*)-oxime ratio decreased somewhat as the yield increased, from 79:21 at 0.25 h to 77:23 at 2.5 h (Figure 4.6).

4.1.4.2 Reduction

D_nM=ADH and D_nM=PDHA was prepared by amination of D_nM (5.0 DP_n; Appendix B) by the dihydrazide ADH and the dioxyamine PDHA (Section 3.5.3). An excess of the reducing agent Pic-BH_3 was then added in order to create the stable secondary amines D_nM-ADH and D_nM-PDHA (Figure 4.7a and Figure 4.8a). Kinetics of reduction was studied by ^{1}H-NMR.

A 5.2x molar excess of Pic-BH_3 (62 mM) was used for the reduction of D_nM=ADH (12 mM). Peak assignment for the ^{1}H-NMR spectra showing the reduction of D_nM=ADH was deduced by comparison to peak assignment for D_nM=PDHA[73] and other D_nM Schiff bases.[40] Within 20 h (Figure 4.9a), the (*E*)- and (*Z*)-hydrazone signals (Figure 4.7b) fully disappeared. A broad signal indicative of the secondary amine (position 1' – conjugate 2; Figure 4.7a) appeared at about 3.04 ppm.

Reduction of D_nM=PDHA was performed using two different excesses of Pic-BH_3: In one case, a 5.2x molar excess, in the other, a 32x (410 mM) molar excess. With a 5.2x molar excess, 80 % conversion had been achieved after 170 h (Figure 4.10a). The same conversion was achieved after 70 h with a 32x molar excess. An M-unit H-1 signal indicative of the secondary amine (position 1' – conjugate 2; Figure 4.8a) appeared at 3.23 ppm (Figure 4.8b). Peak assignment was performed according to Coudurier et al.[73]

By modelling reduction as a first-order reaction, a 0.44 h^{-1} rate constant was determined for D_nM=ADH treated with a 5.2x molar excess of Pic-BH_3 (Figure 4.9b). Conversely, the same excess of Pic-BH_3 yielded a 0.012 h^{-1} rate constant for D_nM=PDHA (Figure 4.10b). When the excess was increased to 32x (a 6-fold difference), the reduction rate of D_nM=PDHA was doubled (Figure 4.10d).

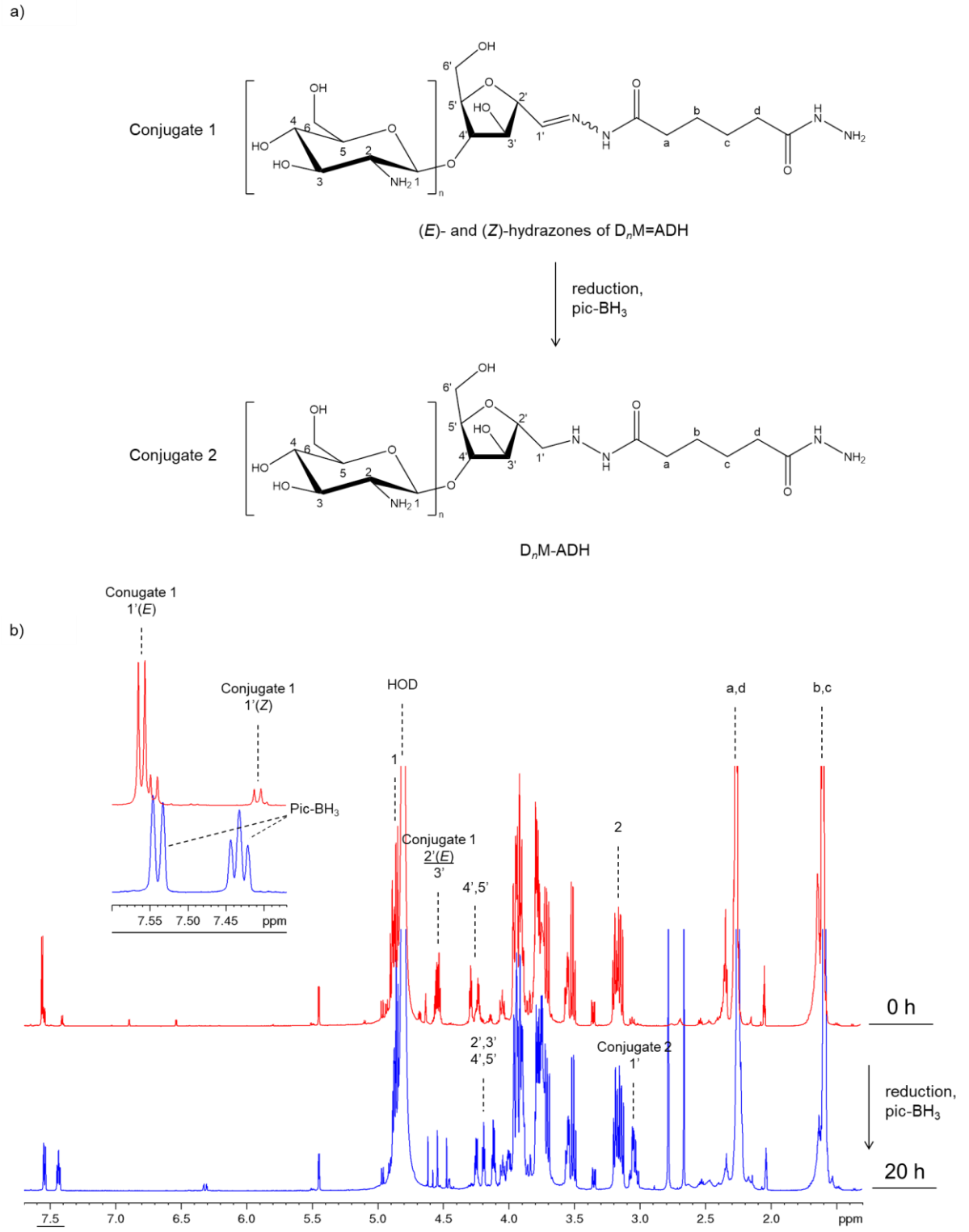

Figure 4.7. A 5.2x molar excess of Pic-BH_3 was added to a NaAc-buffer (500mM, pH 4.5) containing fully dissolved D_nM=ADH (12 mM). **a)** Reductive conversion of the D_nM=ADH Schiff base to the D_nM-ADH secondary amine. **b)** ^{1}H-NMR spectra showing reaction mixture before and 20 h after addition of Pic-BH_3. The reaction was performed at RT and with constant stirring.

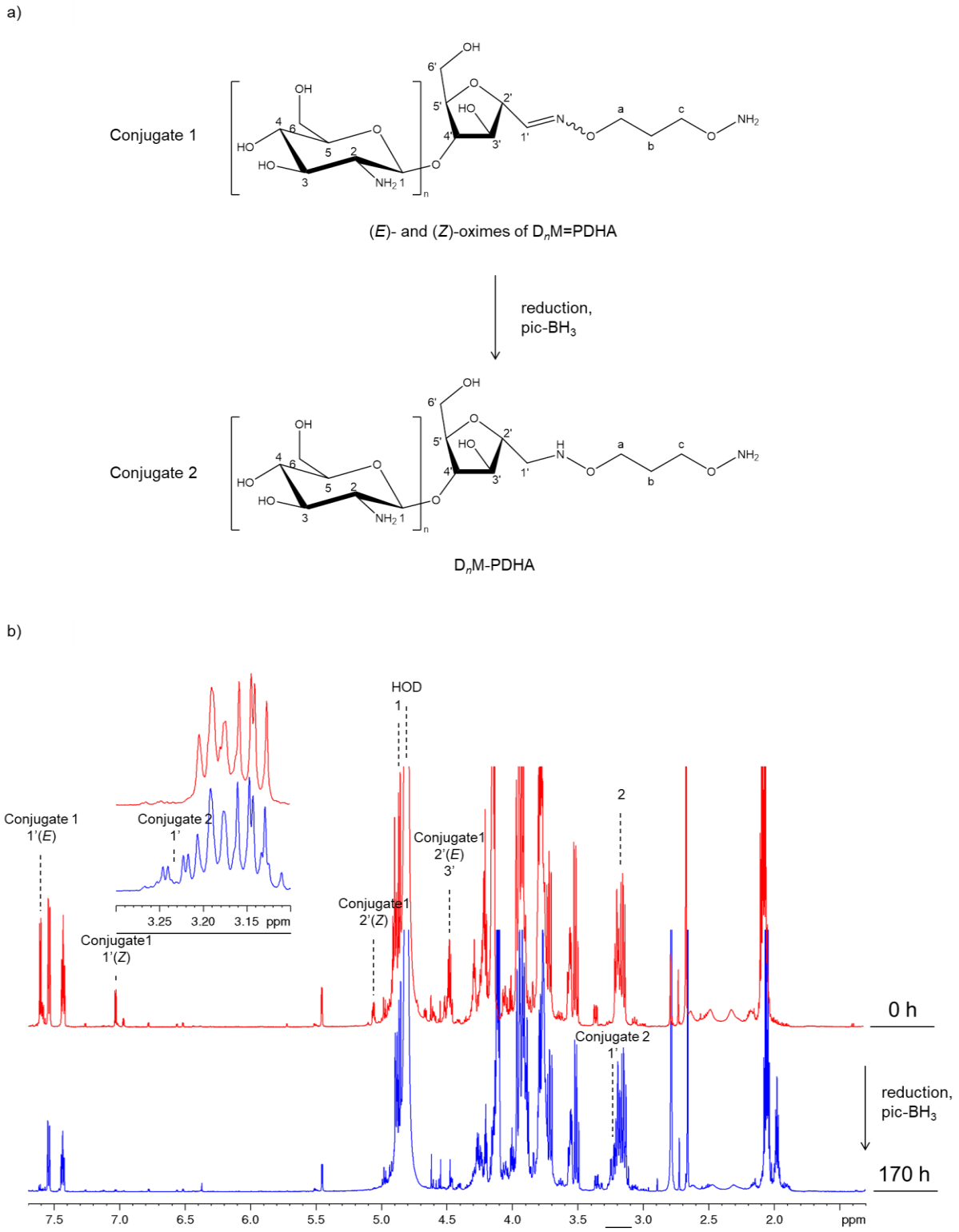

Figure 4.8. A 5.2x molar excess of Pic-BH_3 was added to a NaAc-buffer (500mM, pH 4.5) containing fully dissolved D_nM=PDHA (12 mM). **a)** Reductive conversion of the D_nM=PDHA Schiff base to the D_nM-PDHA secondary amine. **b)** ^{1}H-NMR spectra showing reaction mixture immediately and 170 h after addition of Pic-BH_3. The reaction was performed at RT and with constant stirring.

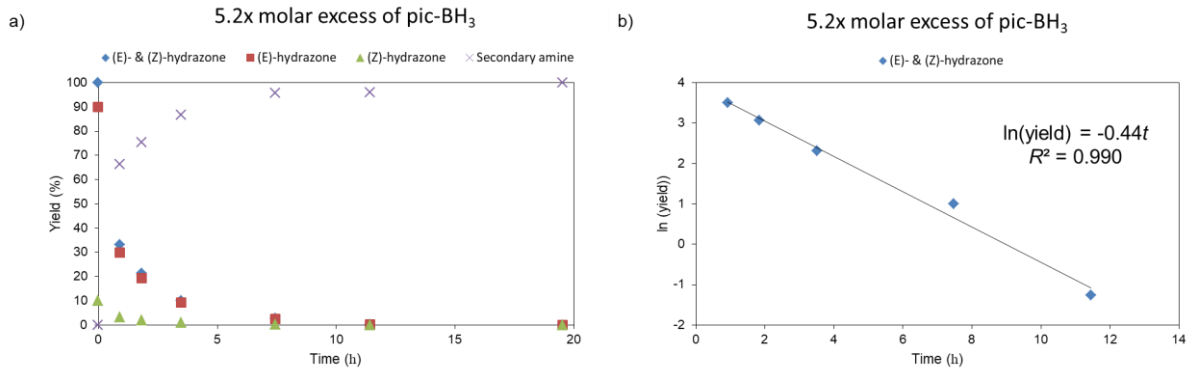

Figure 4.9. A 5.2x molar excess of Pic-BH_3 was added to a NaAc-buffer (500mM, pH 4.5) containing fully dissolved D_nM=ADH (12 mM). **a)** Yield of (*E*)-hydrazone, (*Z*)-hydrazone and D_nM-ADH secondary amine as a function of time after addition of Pic-BH_3. The reaction was performed at RT and with constant stirring. **b)** Semi-log plot showing yield of (*E*)- and (*Z*)-hydrazones. The data points have been fitted by linear regression.

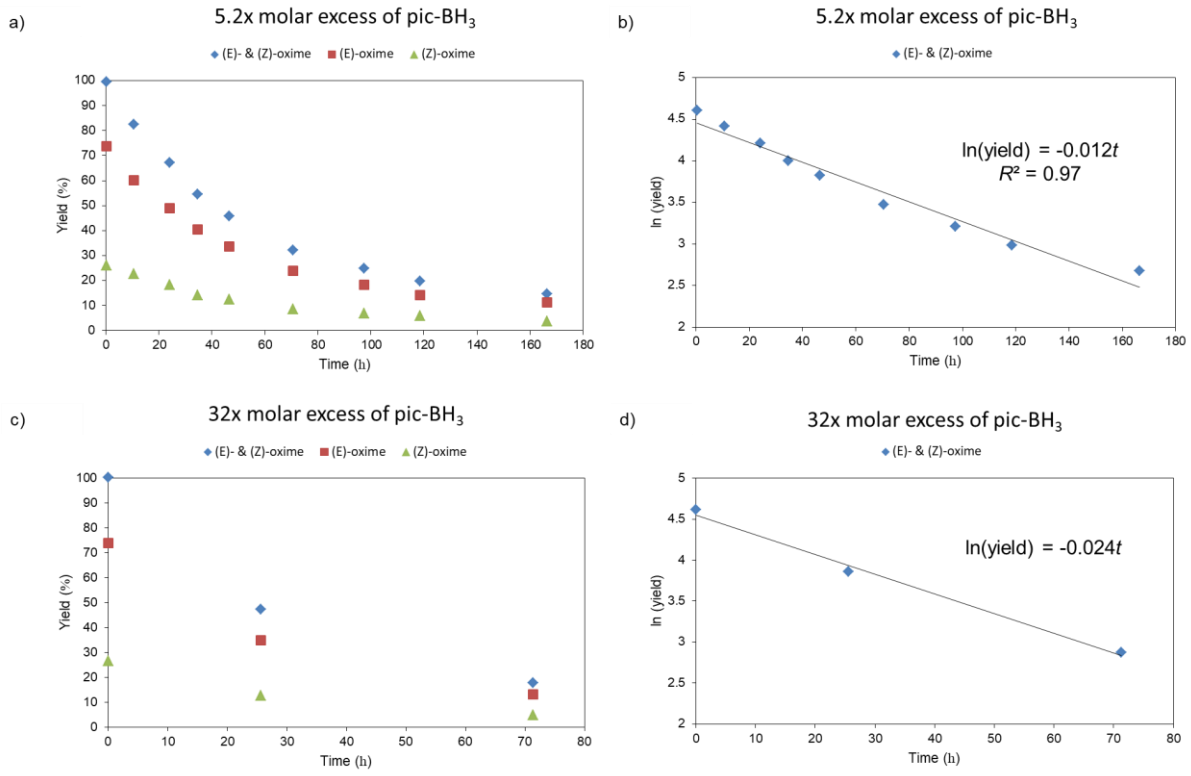

Figure 4.10. Pic-BH_3 was added to a NaAc-buffer (500mM, pH 4.5) containing fully dissolved D_nM=PDHA (12 mM). **a)** Yield of (*E*)-oxime, (*Z*)-oxime and D_nM-PDHA secondary amine as a function of time after addition of a 5.2x molar excess of Pic-BH_3. **c)** Yield of (*E*)-oxime, (*Z*)-oxime and D_nM-PDHA secondary amine as a function of time after addition of a 32x molar excess of Pic-BH_3. **b)** & **c)** Semi-log plot showing yield of (*E*)- and (*Z*)-oximes. The data points have been fitted by linear regression. The reaction was performed at RT and with constant stirring.

4.1.4.3 Background reduction

4.7 molar equivalents of Pic-BH_3 (62 mM) was added to a sample of D_nM-type chitosan (13 mM) dissolved in a NaAc buffer (500 mM, pH 4.5). The reaction was followed by ^{1}H-NMR (Section 3.5.4).

It took about 20 h for the signal produced by the M-unit H-1 to fully disappear (Figure 4.11a and b). A plot showing the inverse of the signal intensity as a function of time (Figure 4.11c), revealed that it could be described as a second-order reaction with a 0.029 M^{-1} h^{-1} rate constant.

The sample contained some amount of $(GlcN)_n$, as evidenced by the signal produced by the α-D-unit H-1. No appreciable reduction of the D-unit reducing end was observed.

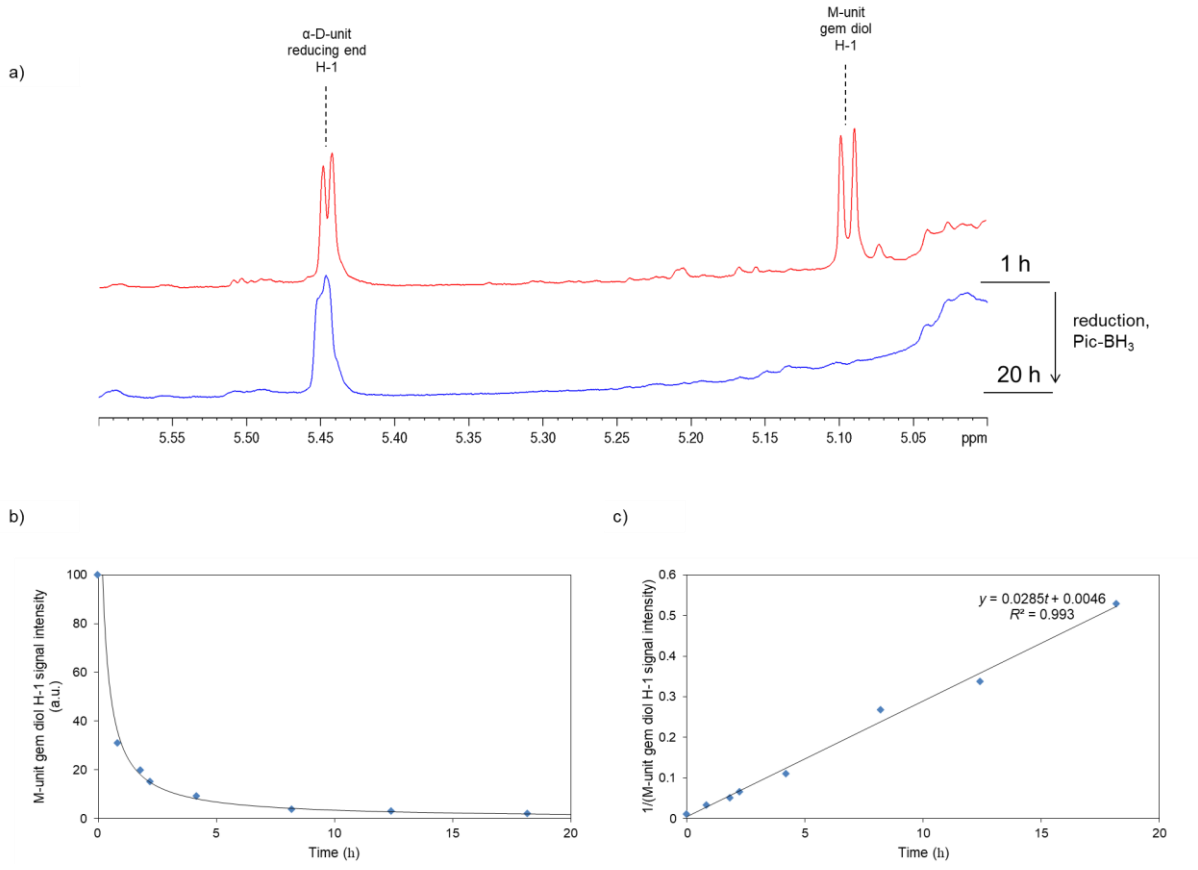

Figure 4.11. 4.7 molar equivalents of Pic-BH_3 (62 mM) was mixed with D_nM-type chitosan (13 mM) dissolved in a NaAc buffer (500 mM, pH 4.5). The reaction was performed at room temperature and with constant stirring. **a)** ^{1}H-NMR spectrum showing the disappearance of the M-unit gem diol H-1 signal. **b)** Intensity of the M-unit H-1 signal as a function of time after addition of Pic-BH_3. The solid line depicts modelling of the data as a second-order reaction. **c)** Inverse of the M-unit H-1 signal intensity as a function of time after addition of Pic-BH_3. Linear regression was performed in order to find the second-order rate constant.

4.2 Desalting

4.2.1 Dialysis: escape rates of salts

Escape rates of the three salts NaAc, AmAc and NaCl were measured for a 12-14 kDa MWCO dialysis bag (volume/length = 6.4 mL/cm). The dialysis buffer was not stirred, but replenished every hour. Measurements of conductivity inside the dialysis bags was converted to salt concentration using standard curves (Appendix D). Escape plots showing the natural logarithm of the salt concentration over time were produced (Figure 4.12). Linear regression was performed. The first data point (at t = 0 h) was omitted from the regression. First-order rate constants were determined based on the regression results.

Based on a first-order regression model, rate constants (k) and the time it took for half of the salt to escape ($t_{1/2}$) were calculated (Table 4.1).

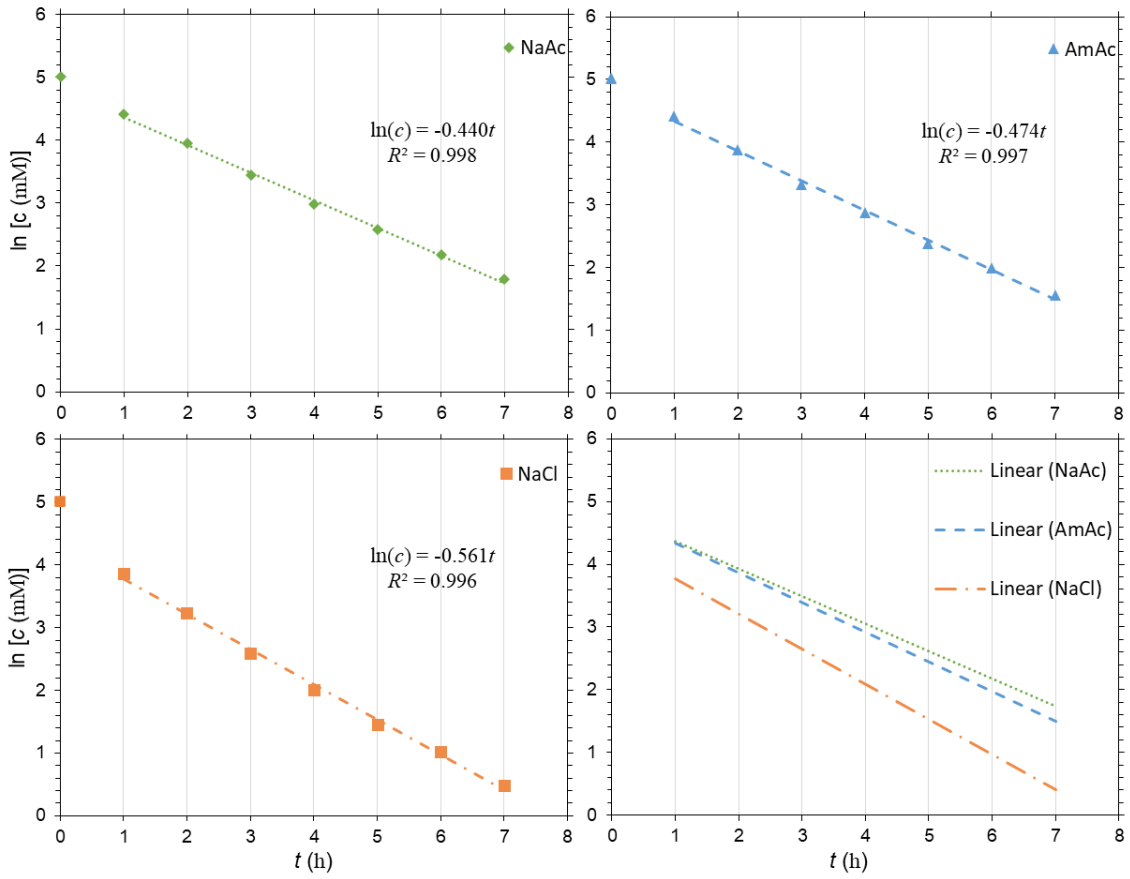

Figure 4.12. Escape plots for the three salts NaAc, AmAc, and NaCl for a 12-14 kDa dialysis bag (volume/length = 6.4 mL/cm). The dialysis buffer was not stirred, but replenished every hour. The lower right-hand plot shows all linear regression results side-by-side.

Table 4.1. Parameters of kinetic modelling of salt escape rates. Rate constants (k) and time it took for half of the salt to escape ($t_{1/2}$) from the dialysis bag.

Salt	k (h^{-1})	$t_{1/2}$ (h)
NaAc	-0.440	1.5
AmAc	-0.474	1.4
NaCl	-0.561	1.1

4.2.2 Desalination by means of size-exclusion chromatography

The chromatogram shown in (Figure 4.13) is the combined result of two separate SEC-runs. The first run was of a sample containing only AmAc, producing the AmAc-peak. The second run was of a sample containing AmAc *and* COS. Subtracting the first run from the second, gave the COS-peak. A Gaussian function was fitted to the two peaks based on the least squares method.

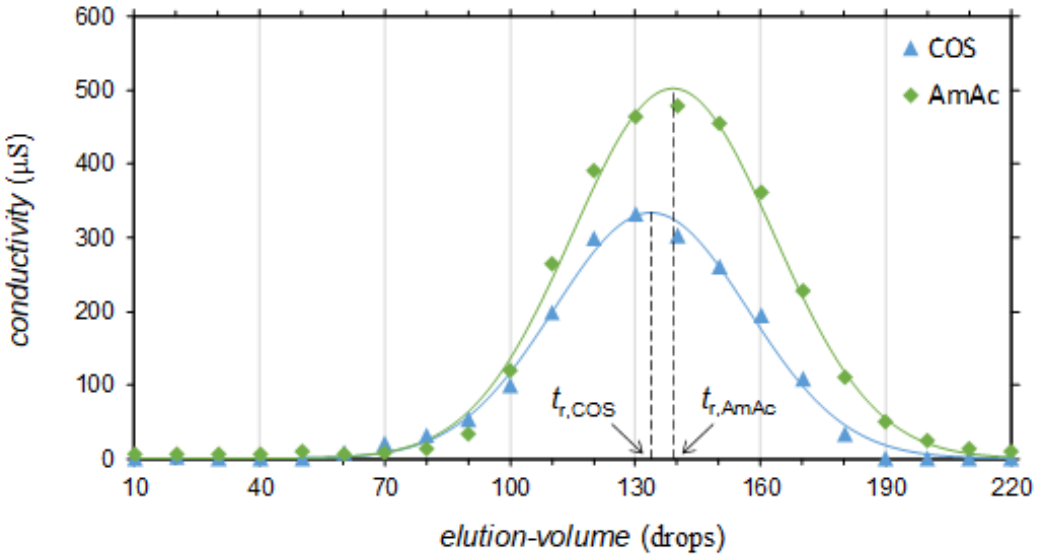

Figure 4.13. Size-exclusion chromatogram of a sample containing AmAc and COS. The green markers (◆) identify the AmAc; the blue markers (▲) identify the COS. Gaussian functions, drawn as smooth lines, was fitted to the two elution profiles using the least squares method. $t_{r,AmAc}$ is the retention time for the AmAc-peak; $t_{r,COS}$ is the retention time for the COS-peak.

4.3 Synthesis of a chitosan-dextran diblock

4.3.1 Preparation of activated chitosan

Activated chitosan (D_nM-ADH and D_nM-PDHA) was prepared by two-pot reductive amination (Section 3.7.1) and fractionated using SEC (Figure 4.14). Fraction i_{ADH} and i_{PDHA} (see figure) were dialysed and lyophilised.

A ^{1}H-NMR spectrum of fraction i_{ADH} (Figure 4.15) revealed that attachment of linker (ADH) was successful. This conclusion can be drawn based on several telltale signs. The characteristic pattern of peaks in the 4.3-4.1 ppm region and the broad peak at 3.05 ppm directly indicate attachment of linker (see Figure 4.7). Lack of M-unit gem diol H-1 peak at 5.1 ppm means that no unreacted D_nM remains in the sample (see Figure 4.5). The spectrum also shows that all activated chitosan was completely reduced since no (*E*)- and (*Z*)-hydrazone are present (see Figure 4.7). By evaluation of peak integrals, a DP_n of 41 was estimated:

$$DP_n \approx \frac{40.44}{0.18 + 1.64/2} = 41\,. \tag{4.2}$$

The ^{1}H-NMR spectrum acquired of fraction i_{PDHA} (Figure 4.16), although of a poorer resolution due to a comparably high DP_n, also clearly show that the linker (PDHA) was successfully attached. Attachment of linker should produce a peak at 3.23 ppm. The appearance of this peak could not be definitely verified due to the spectrums poor resolution. However, it can still be concluded that the linker was successfully attached due to the lack of M-unit gem diol H-1 peak at 5.1 ppm (see Figure 4.6). Additionally, no (*E*)- and (*Z*)-oximes are present which means that all activated chitosan must have been reduced. More evidence in support of successful attachment of linker is provided in Section 4.3.3 where the same sample is used to synthesise a chitosan-dextran diblock.

Accurate estimation of DPn could not be performed due to the lacking quality of the spectrum. But, assuming 18 % normal D-unit reducing ends as found for fraction i_{ADH} (ignoring the β-D-unit which could not be identified), a ballpark DP_n of 330 was estimated:

$$DP_n \approx \frac{330.84}{0.18 + 1.64/2} = 330\,. \tag{4.3}$$

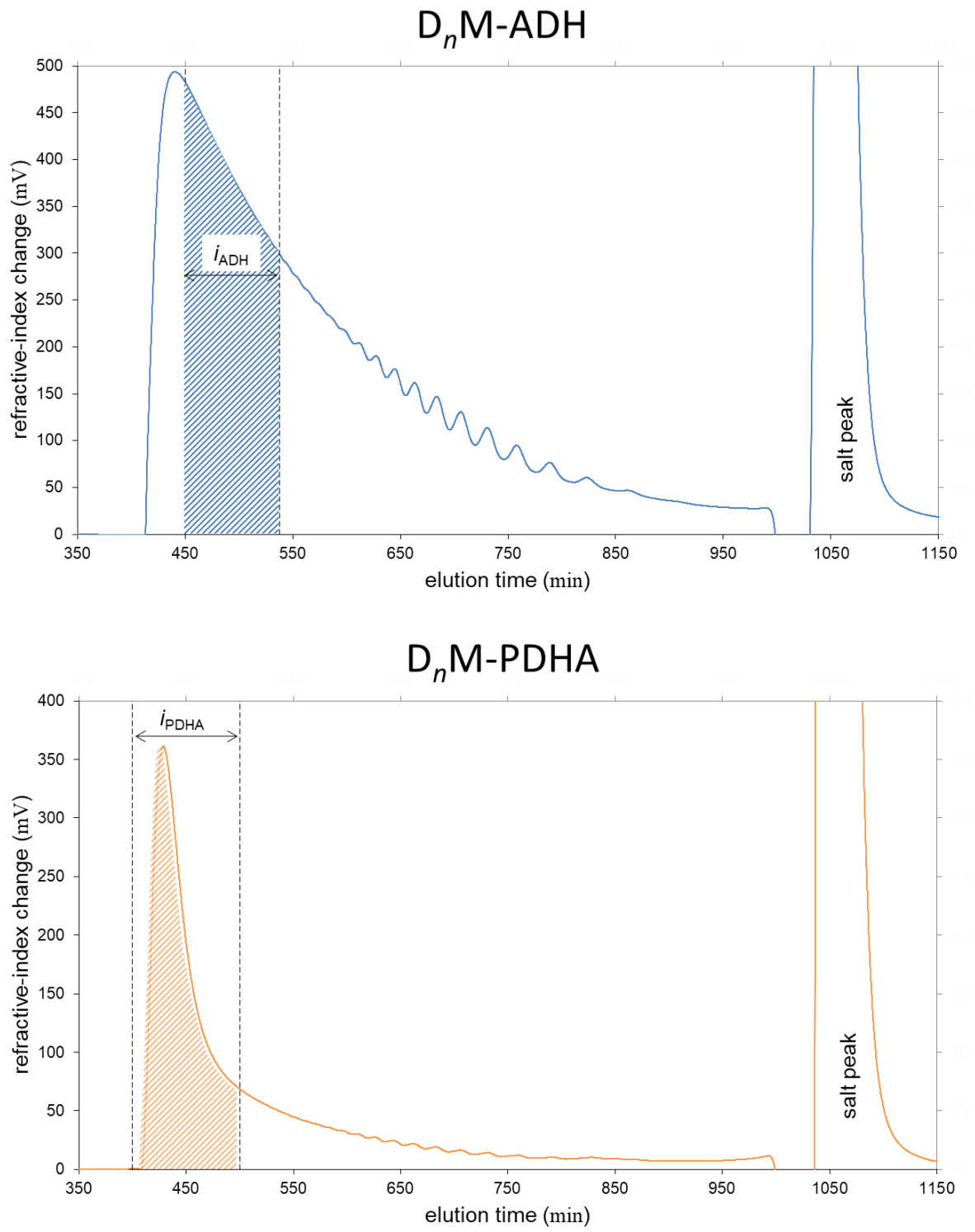

Figure 4.14. Size-exclusion chromatograms of a nitrous acid depolymerised, fully de-*N*-acetylated chitosan (DnM-type chitosan) attached to bifunctional linkers ADH and PDHA via reductive amination. Comprising the SEC-system was three serially connected HiLoad™ 26/60 columns packed with Superdex™ 30 feeding into an on-line refractive index detector. Mobile phase = AmAc (0.15 mM, pH 4.5). Flow rate = 0.8 ml/min.

a)

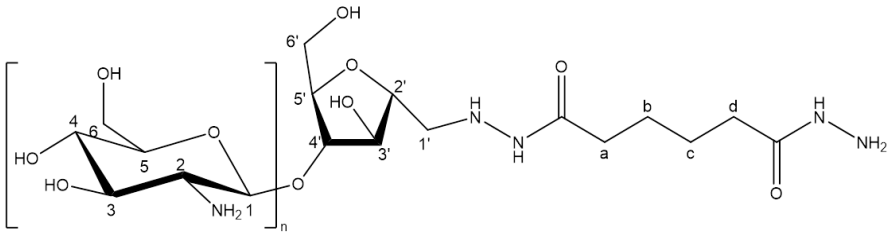

D$_n$M-ADH

b)

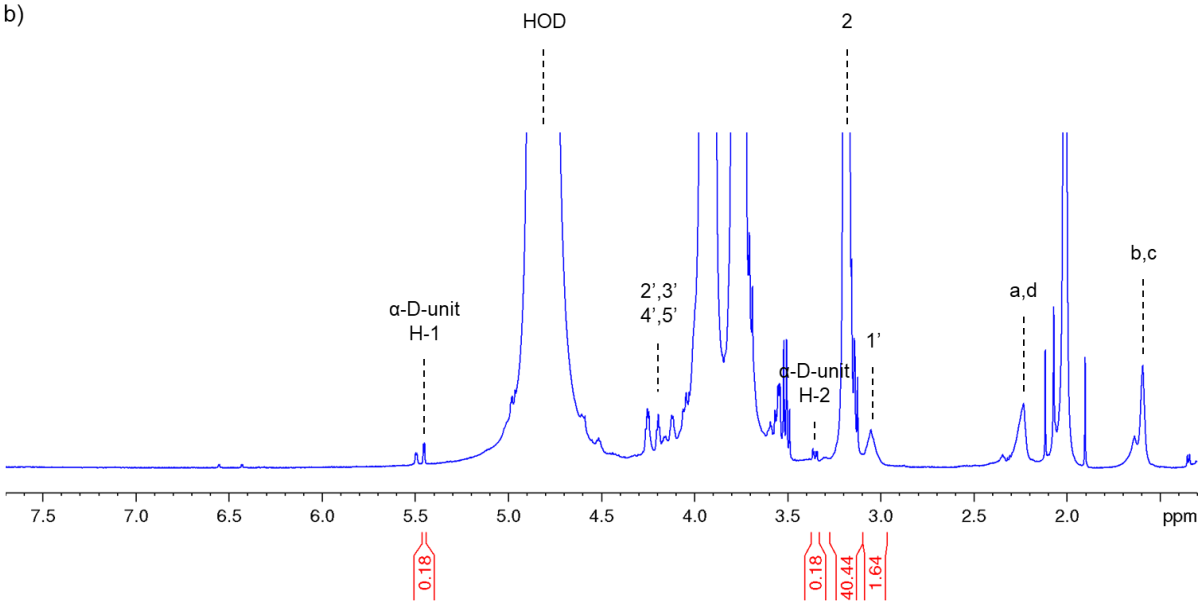

Figure 4.15. ^{1}H-NMR spectrum of a nitrous acid depolymerised, fully de-*N*-acetylated chitosan (DnM-type chitosan) attached to bifunctional linker ADH via reductive amination. Recorded at 600.18 MHz, 25 °C, and with D_2O as solvent.

a)

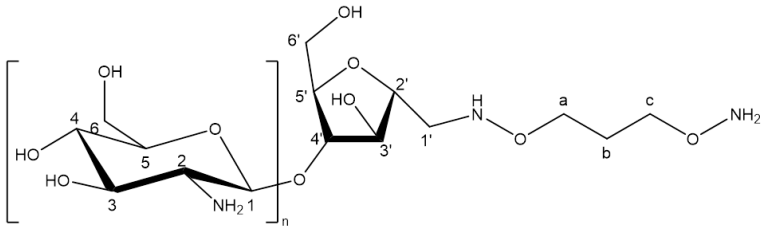

D_nM-PDHA

b)

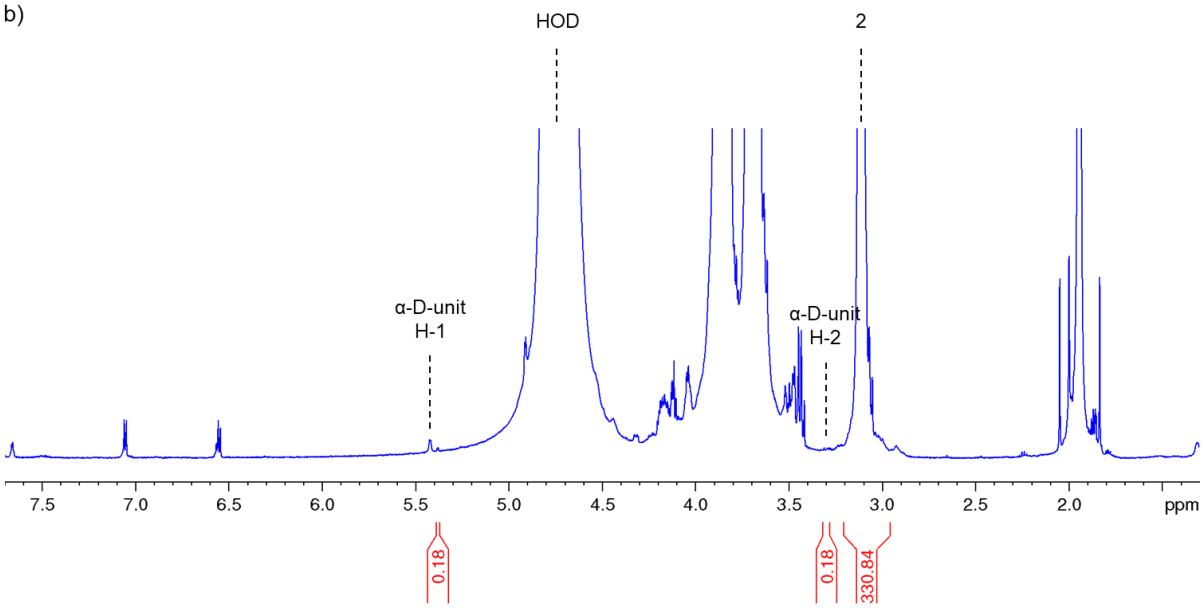

Figure 4.16. ^{1}H-NMR spectrum of a nitrous acid depolymerised, fully de-*N*-acetylated chitosan (DnM-type chitosan) attached to bifunctional linker PDHA via reductive amination. Recorded at 600.18 MHz, 25 °C, and with D_2O as solvent.

4.3.2 Preparation of dextran

A sample of low molecular weight dextran (DP_n 34), prepared by acid hydrolysis, was fractionated by SEC (Section 3.5.2, Figure 4.17). Fraction ε (see figure) was lyophilised five times in order to remove AmAc introduced by the SEC buffer.

Fraction ε was characterised based on an acquired ^{1}H-NMR spectrum (Figure 4.18). The fraction was found to have a DP_n of 15,

$$DP_n = \frac{15.31}{0.44 + 0.56} = 15\,, \tag{4.4}$$

and a degree of branching (DB) of 2.2 %,

$$DB = \frac{0.37}{0.37 + 0.44 + 0.56 + 15.31} \times 100\,\% = 2.2\,\%\,. \tag{4.5}$$

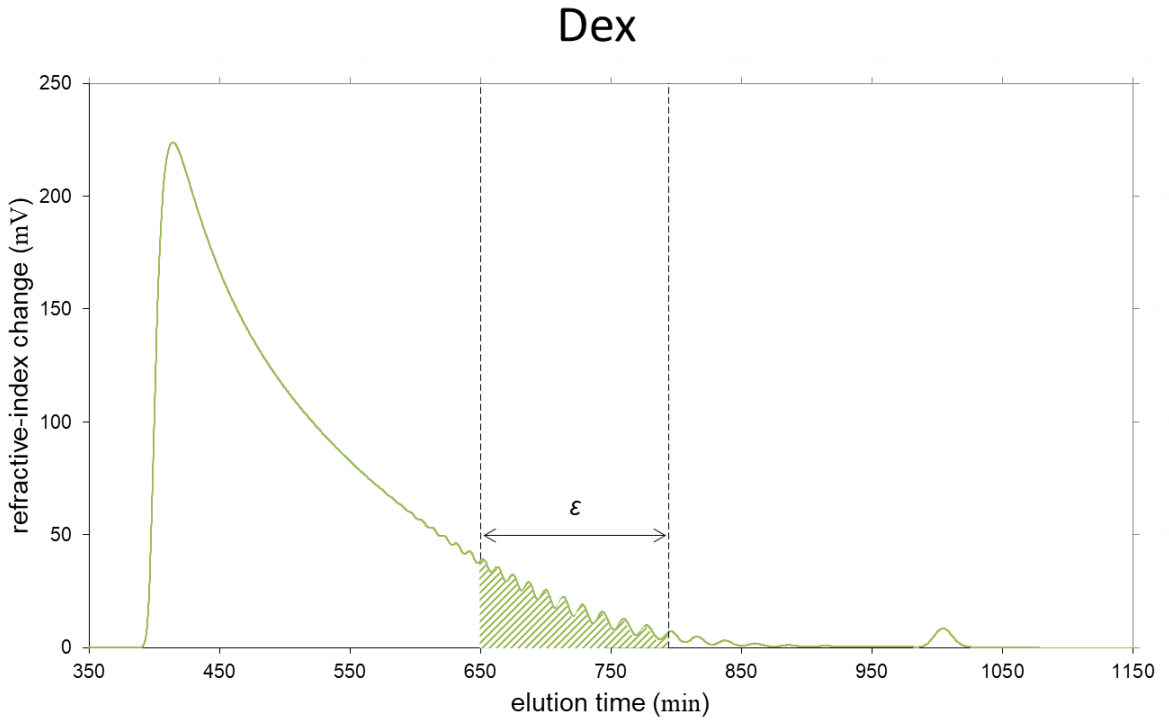

Figure 4.17. Size-exclusion chromatogram of an acid hydrolysed dextran (DP_n 34). Comprising the SEC-system was three serially connected HiLoad™ 26/60 columns packed with Superdex™ 30 feeding into an on-line refractive index detector. Mobile phase = AmAc (0.15 mM, pH 4.5). Flow rate = 0.8 ml/min.

a)

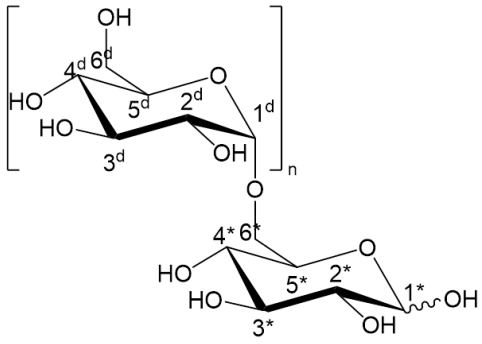

Dex

b)

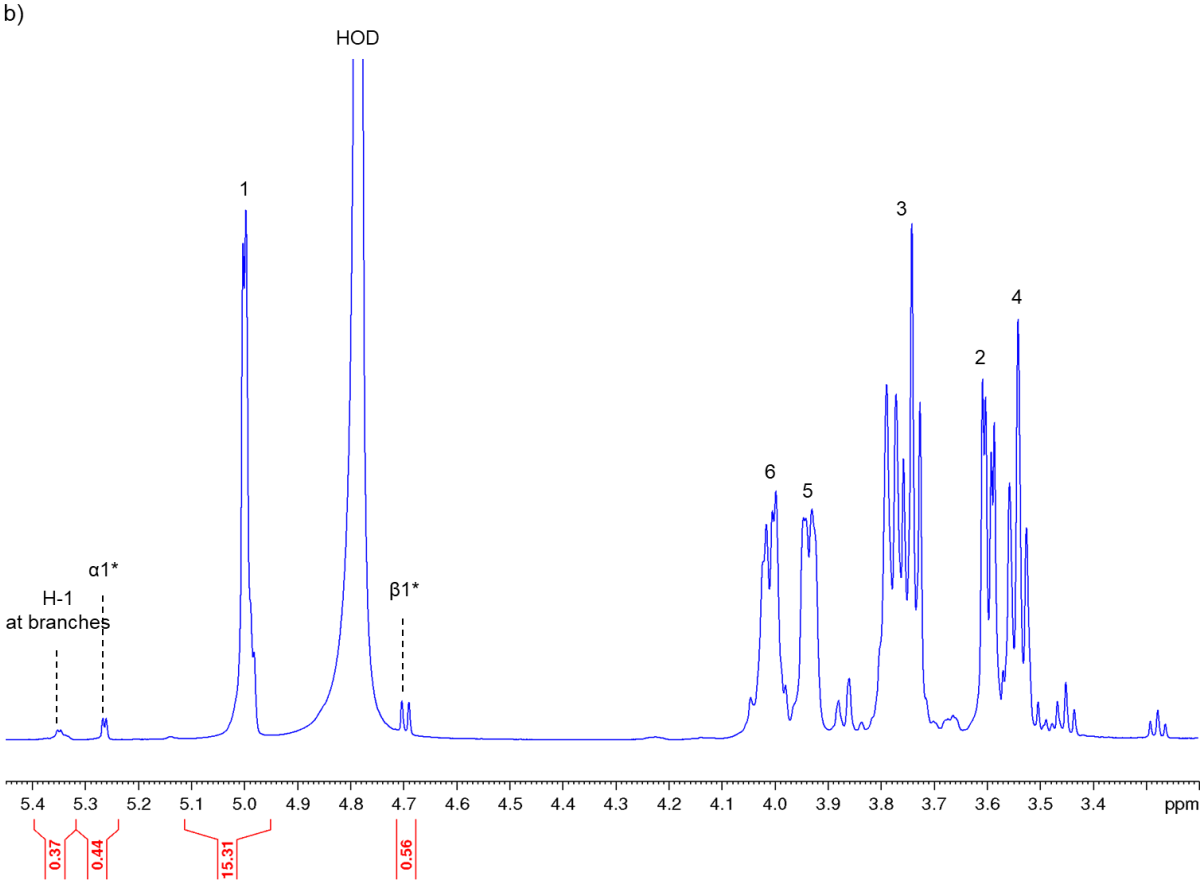

Figure 4.18. ^{1}H-NMR spectrum of an acid hydrolysed dextran (fraction *ε* from Section 4.3.2). Recorded at 600.18 MHz, 25 °C, and with D_2O as solvent.

4.3.3 Conjugation of activated chitosan and dextran

D_nM-ADH + Dex

Pic-BH_3 (30x excess) and dextran (DP_n 15, 4x excess) was added to D_nM-ADH (DP_n 41, 8 mM) completely dissolved in a NaAc buffer (500 µl, pH 4.5). Reductive amination was allowed to proceed for 6 days at 40 °C. Non-conjugated dextran was removed by SEC. A ^{1}H-NMR spectrum was acquired of fraction γ_{ADH} (Figure 4.20).

Comparing the ^{1}H-NMR spectra (Figure 4.21) for the two reagents (D_nM-ADH and dextran) and fraction γ_{ADH}, two signs indicative of successful formation of D_nM-ADH-Dex was found. The first sign is the unmistakable presence of dextran in fraction γ_{ADH}. Dextran makes its presence obvious by virtue of the intense and sharp peak at 5.0 ppm. The mere presence of dextran is arguably enough to conclude that conjugation (at least some) has occurred; all non-conjugated dextran would have been removed during SEC and should not be present in fraction γ_{ADH}.

The second indication of successful conjugation is the appearance of a new signal at 4.2 ppm. The *β-N*-pyranoside of dextran coupled to ADH produces a peak at this chemical shift value (Odin W. Haarberg, *Towards Dextran-Based Block Polysaccharides*, Master's Thesis, 2018).

D_nM-PDHA + Dex

Pic-BH_3 (80x excess) and dextran (DP_n 15, 8x excess) was added to D_nM-PDHA (DP_n 330, 1 mM) completely dissolved in a NaAc buffer (250 µl, pH 4.5). Reductive amination was allowed to proceed for 4 days at 40 °C. Non-conjugated dextran was removed by SEC. A ^{1}H-NMR spectrum was acquired of fraction γ_{PDHA} (Figure 4.22).

As for D_nM-ADH + Dex, conjugation was confirmed by the simple observation that dextran was present in fraction γ_{PDHA} (Figure 4.23). Other than that, there was no way to tell that conjugation had occurred.

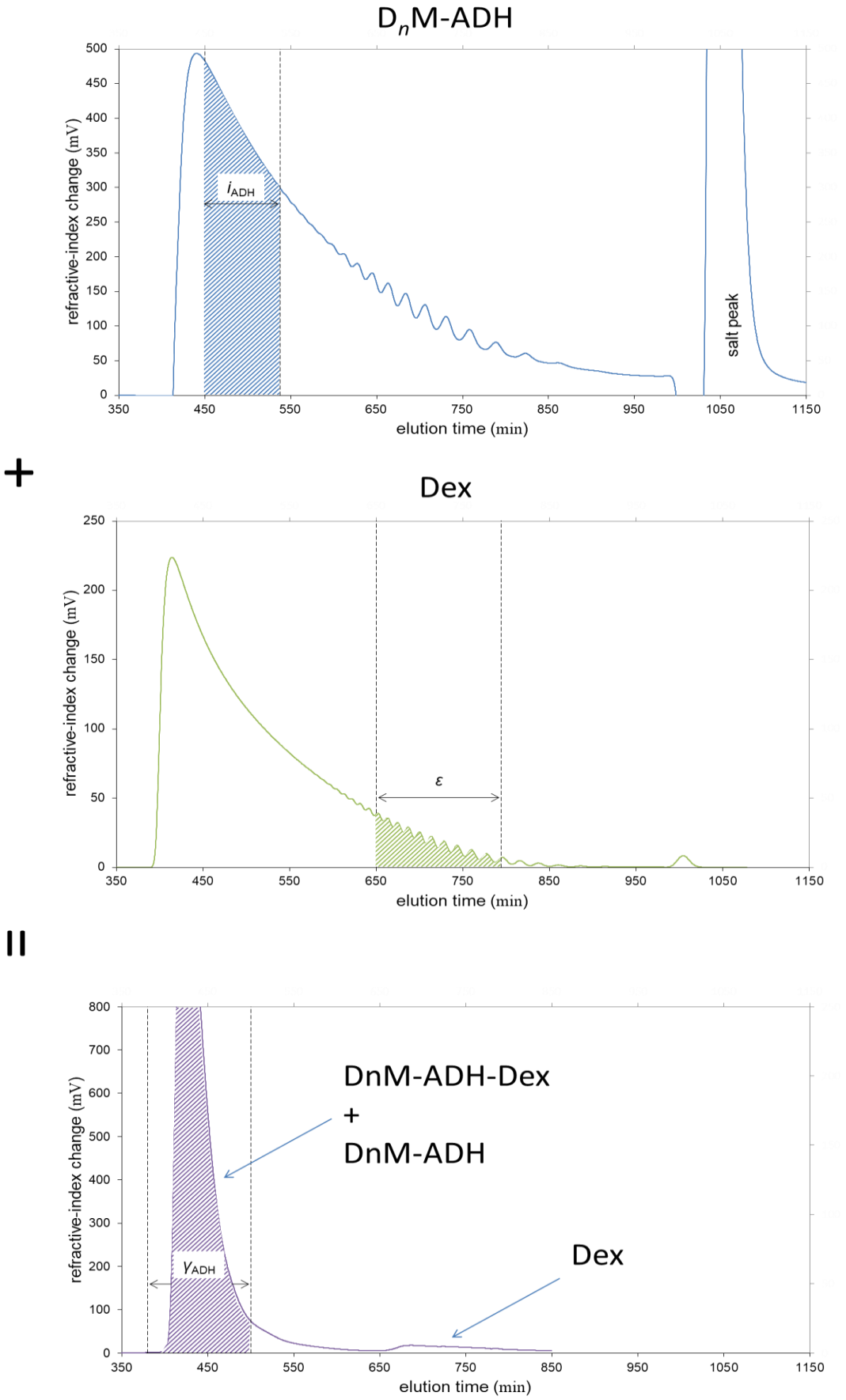

Figure 4.20. The two upper size-exclusion chromatograms shows D$_n$M-ADH and dextran. Fraction i_{ADH} and ε were conjugated by reductive amination. The bottom chromatogram shows the product after reductive amination. All three samples were run on the same SEC system. The SEC system was comprised of three serially connected HiLoad™ 26/60 columns packed with Superdex™ 30 feeding into an on-line refractive index detector. Mobile phase = AmAc (0.15 mM, pH 4.5). Flow rate = 0.8 ml/min.

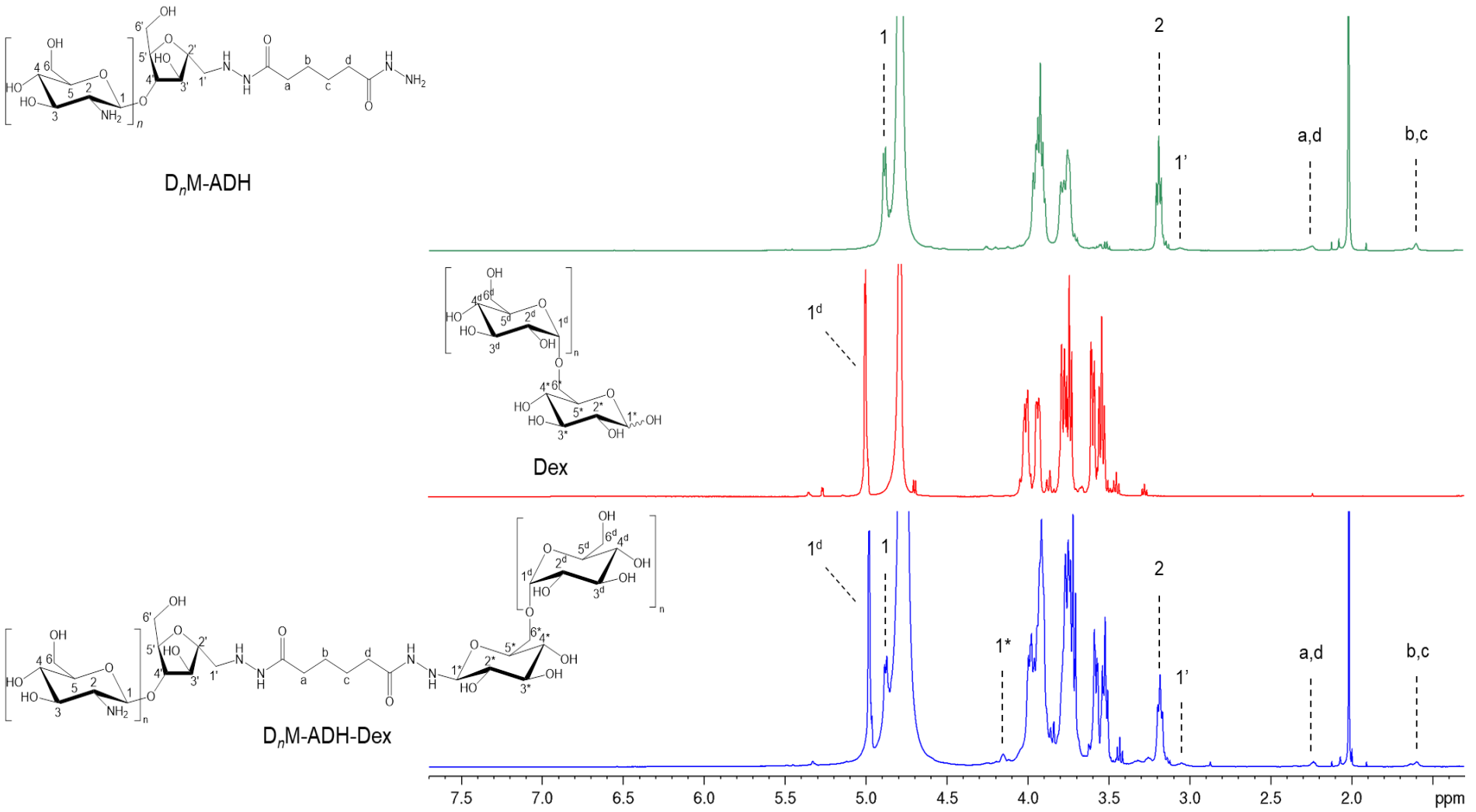

Figure 4.21. The two upper ^{1}H-NMR spectra shows D$_n$M-ADH and dextran. The two samples were conjugated by reductive amination. The bottom spectrum shows the product after reductive amination after non-conjugated dextran had been removed.

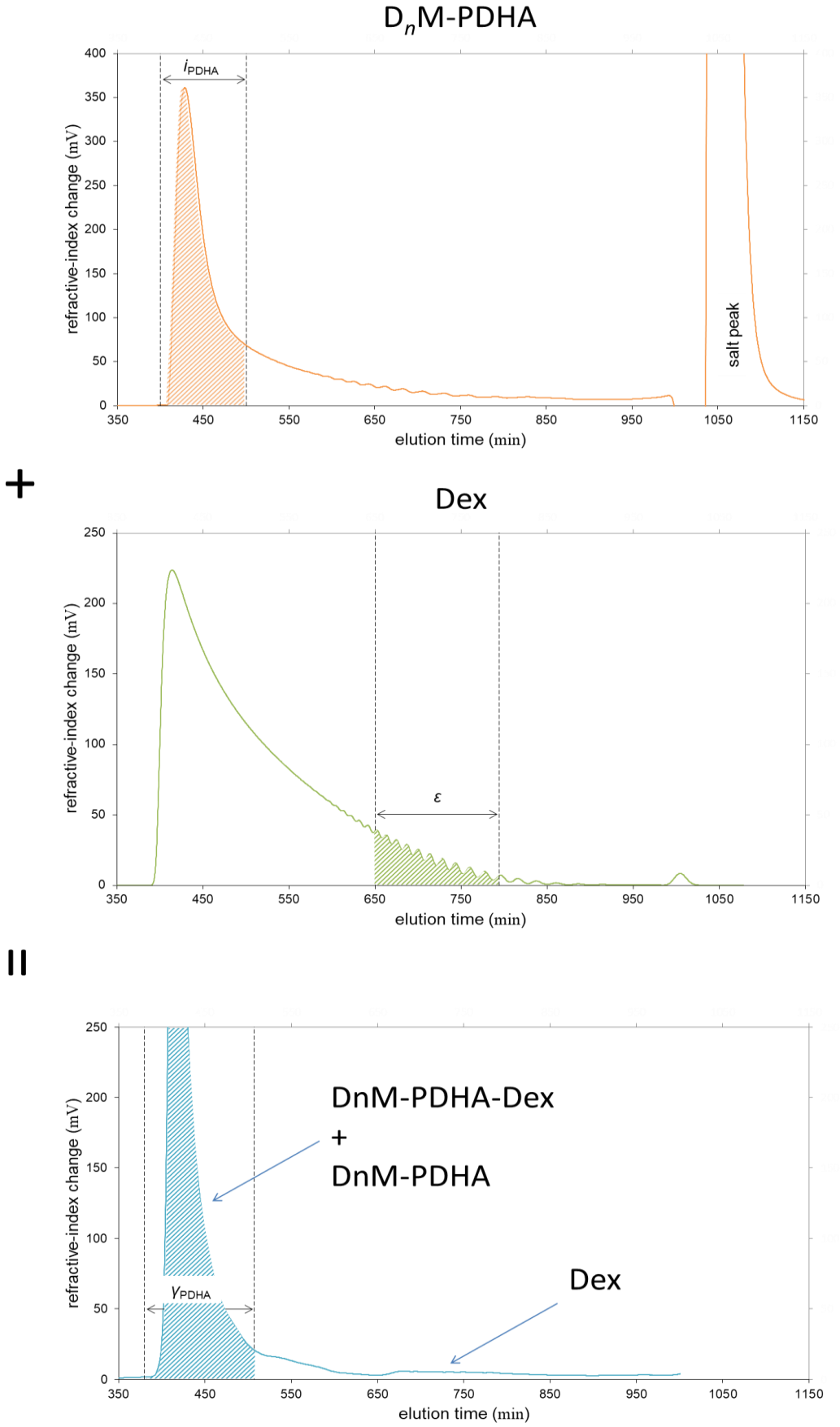

Figure 4.22. The two upper size-exclusion chromatograms shows D$_n$M-PDHA and dextran. Fraction i_{PDHA} and ε were conjugated by reductive amination. The bottom chromatogram shows the product after reductive amination. All three samples were run on the same SEC system. The SEC system was comprised of three serially connected HiLoad™ 26/60 columns packed with Superdex™ 30 feeding into an on-line refractive index detector. Mobile phase = AmAc (0.15 mM, pH 4.5). Flow rate = 0.8 ml/min.

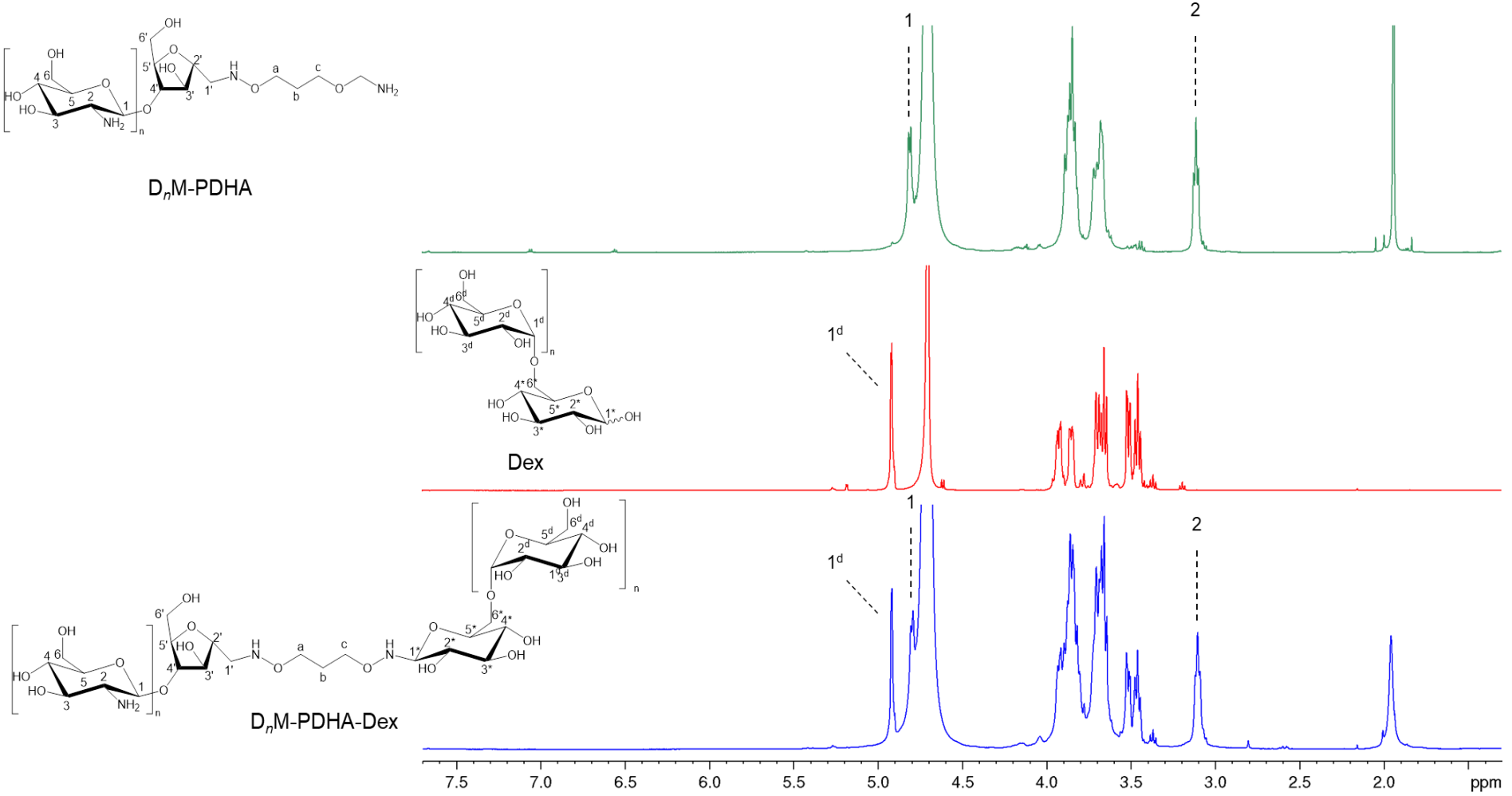

Figure 4.23. The two upper ^{1}H-NMR spectra shows D$_n$M-PDHA and dextran. The two samples were conjugated by reductive amination. The bottom spectrum shows the product after reductive amination after non-conjugated dextran had been removed.

5 Discussion

5.1 Preparation of activated chitosan

5.1.1 Nitrous acid depolymerisation of fully de-*N*-acetylated chitosan

The very first step towards preparation of activated chitosan is nitrous acid depolymerisation. Nitrous acid depolymerisation of a fully de-*N*-acetylated chitosan (F_A = 0) results in D_nM-type chitosan, i.e. chitosan modified at the reducing end by a 2,5-anhydro-D-mannofuranose (M-unit). As will be discussed later, the M-unit is critical in that it enables rapid and efficient attachment of a linker.

For depolymerisation, 1.0 moles of nitrous acid was used per 4.5 moles of D-unit. A DP_n of about 4.5 would therefore be expected. ^{1}H-NMR integration provided an estimated DP_n of 7.6 (Figure 4.1). The discrepancy may be explained by decomposition of nitrous acid or by a significantly lower initial DP_n (not determined) than assumed. In this particular case, the exact extent of depolymerisation was not of special importance. That being said, if initial DP_n is known and appropriate measures are taken to minimise decomposition, nitrous acid depolymerisation can be used to precisely modify the molecular weight of chitosan.(50)

27 % of the M-unit reducing ends appeared as a Schiff base (Figure 4.1). It is here argued that the Schiff base was formed between the M-unit aldehyde and the D-unit amine due a significant rise in pH. The pH was at no point measured or intentionally adjusted. An explanation accounting for the rise in pH, and a possible preventative measure, is given in the next section.

Schiff base formation between the M- and D-unit should be avoided at all costs as it cannot be reversed: Normally, Schiff bases formation can be reversed by simple acid treatment. Acid treatment would in this case result in loss of M-unit due to non-enzymatic browning (Section 2.2.3).

5.1.2 Stability of the M-unit and lyophilisation of volatile acids

After nitrous acid depolymerisation, the D_nM oligomers were fractionated by SEC (Section 3.5.1). Individual fractions were then purified by removal of AmAc introduced by the SEC buffer (Section 3.5.2). AmAc is volatile and can as such be removed by lyophilisation. Only a small amount of AmAc is however removed per round of lyophilisation. Dialysis was therefore implemented prior to lyophilisation in order to expedite removal of AmAc.

An experiment was performed where duration of dialysis was varied. Short duration (4 h) caused the M-unit to be cleaved from the chain and converted to HMF. In contrast, the M-unit was preserved and no HMF was formed when the duration was extended to 4 days (Figure 4.3).

The results can be explained by an observation made by Tømmeraas et al.[47] They observed a rise in pH during lyophilisation and attributed this phenomenon to the presence of AmAc: Acetate is removed at a faster rate compared to ammonium due to its greater volatility. When the acid:base ratio is changed, so is the pH.

When the D-unit amine becomes deprotonated, it will nucleophilically attack the M-unit aldehyde, thereby forming a Schiff base. Subsequent lowering of the pH, to which point the D-unit amine becomes protonated, facilitates cleavage of the M-unit and its conversion to HMF in a process of non-enzymatic browning (Section 2.2.3). The pH* was manually lowered to 3.85 before the ^{1}H-NMR spectra were acquired. This was likely when – as it was for Tømmeraas et al. – the Schiff base decomposed to yield HMF.

If the hypothesis put forward by Tømmeraas et al. is correct, that AmAc is at blame for Schiff base formation, then more complete removal of AmAc prior to lyophilisation should prevent its occurrence. This is exactly what the results presented here demonstrate.

In addition to providing evidence for Tømmeraas et al.'s hypothesis, another experiment was performed that provides insight into the conditions required for Schiff base formation. The experiment was identical to the long-duration dialysis-experiment already discussed, expect for that AcOH not was added to the dialysis buffer. Over the course of the experiment, the pH was routinely measured as it reached a maximum value of 6.4. Although not shown here, a pH of 6.4 was not enough to cause Schiff base formation even though pH 6.4 is slightly above the ~6.3 pK_a of fully de-*N*-acetylated chitosan (Section 2.2.1). This observation provides evidence for dehydration as driving factor; Schiff base formation is a condensation reaction and as such will pull the reaction towards completion as water is removed.

A rise in pH caused by the lyophilisation of a volatile acid is also likely why the presence of a Schiff base was identified for the depolymerisate (previous section). AcOH (*aq*, 2.5 % v/v), used for nitrous acid depolymerisation, would have evaporated during lyophilisation thereby causing the pH to rise. The depolymerisate was dialysed for 6 h prior to lyophilisation. Apparently, 6 h of dialysis was not enough to remove a sufficient amount of AcOH. In order to avoid Schiff base formation, it can therefore be recommended that a less volatile acid, such

as HCl, is used for nitrous acid depolymerisation of fully de-*N*-acetylated chitosan. Either that, or the volatile acid must be removed by some other means prior to lyophilisation.

After purification, the material used for the long duration dialysis, fractions of the depolymerisate discussed in the previous section, only had about 60 % M-unit reducing ends with the remaining 40 % being of the normal D-unit type. The low percentage of M-unit reducing ends is not due to loss of M-unit during purification. If that was the case, HMF should have been observed in their ^{1}H-NMR spectra. Instead, the missing M-units are accounted for by the Schiff bases observed for the depolymerisate (previous section). The Schiff bases were subjected to acidification as the depolymerisate was injected onto the SEC column. The SEC buffer has a pH of 4.5. The low pH must have caused non-enzymatic browning for the Schiff bases that were present. The HMF must have eluted in the last peak before the salt peak (Figure 4.2).

5.1.3 Stability of the M-unit during long-term storage

D_nM-type chitosan (13 mg/ml**)** was stored in the dark, at room temperature and dissolved in D_2O (pH* 5). After 9 months, every M-unit had undergone non-enzymatic browning (Figure 4.4).

As was discussed in the previous section, non-enzymatic browning occurs if the pH transiently rises above the pK_a of the D-unit amine (Section 2.2.3). A transient rise in pH is however unlikely to have occurred during storage. Instead the results suggest that non-enzymatic browning of D_nM-type chitosan can occur even at a constant and relatively low pH. Even pH 6.4 is not enough to cause browning over a short period of time, at least not without the aid of dehydration (previous section). However, the result show that even a relatively low pH is not enough to prevent decomposition over a long period of time.

Glycosyl Schiff bases are known to undergo non-enzymatic browning on standing in a moist atmosphere.[51] Rate of browning can be lowered by decreasing the temperature or pH,[74] or by decreasing the sample concentration.[75] Decomposition during storage can also be prevented by blocking the M-unit's carbonyl function; a carbonyl group is a prerequisite for Schiff base formation. This particular approach to deal with the instability of the M-unit is employed later in this thesis as part of an alternative protocol for the synthesis of activated chitosan (Section 5.3).

5.1.4 Activation

Activated chitosan here refers to D_nM-type chitosan coupled to one of two linker molecules: either ADH (D_nM-ADH) or PDHA (D_nM-PDHA). The following sections (Section 5.1.4.1 and Section 5.1.4.2) deal with the two-step process of preparation of activated chitosan. The first step is amination to yield a Schiff base of the activated chitosan (D_nM=ADH/PDHA). The second step is reduction of the Schiff base to yield the activated chitosan as a stable secondary amine (D_nM-ADH/PDHA).

5.1.4.1 Amination

D_nM (12 mM) mixed with a 3.4x molar excess of ADH resulted in a 100 % equilibrium yield of D_nM=ADH within 1.7 h (Figure 4.5). The (*E*):(*Z*)-hydrazone ratio was determined as 90:10.

When D_nM (12 mM) was mixed with a 3.4x molar excess of PDHA, the M-unit gem diol H-1 signal (representing unreacted D_nM) disappeared within 15 min (Figure 4.6ab). Appearing within the same 15 min were (*E*)- and (*Z*)-oximes accounting for 98 % of the disappeared M-unit. Over the next 2 h, the yield of (*E*)- and (*Z*)-oxime increased from 98 % to 115 %. It therefore seems that the amination reaction between D_nM and PDHA had reached completion after 15 min, but that unaccounted for side reactions caused the oxime-yield to further increase. Further support for complete D_nM=PDHA formation by 15 min is provided by the (*E*)-oxime:(*Z*)-oxime ratio (Figure 4.6c). The (*E*):(*Z*) ratio declines from 3.7 after 15 min to 3.4 within 2 h. A shift in (*E*):(*Z*) ratio would be expected if a different chemical species were to react with PDHA.

Coudurier et al.[73] also reacted PDHA with D_nM. Employing a D_nM concentration of 0.15 mM, a 10x molar excess of PDHA and a pH 5 aqueous solution as solvent (pH held constant), they observed complete yield after 30 min. They also report that the reaction rate was slower at pH 4. The experiment discussed here was performed at a D_nM concentration of 12 mM, a 3.4x excess of PDHA and with a pH 4.5 NaAc-buffer as solvent. By direct comparison it seems that a higher concentration of D_nM matters more to the reaction rate than pH and excess of PDHA.

Coudurier et al. noted that when the amination was performed at pH 4 (vs pH 5), new signals appeared in the 8.2-5.5 ppm region. They speculated that these signals may be the result of side reactions or the instability of D_nM=PDHA at such acidic conditions. Although not shown, it is noted that such signals, some with the exact same chemical shift values to the ones found by Coudurier et al., also appeared in this case where the amination was performed

at pH 4.5.

For both D_nM=ADH and D_nM=PDHA, the abundance of the (*E*)-isomer was greater than than that of the (*Z*)-isomer. Their relative abundance reflects their relative stability; the (*E*)-isomer is more stable due to less steric strain imposed by the geometry around the imino double bond.

5.1.4.2 Reduction

D_nM=PDHA (12 mM) mixed with a 5.2x molar excess of Pic-BH_3 resulted in 80 % conversion to the D_nM-PDHA secondary amine within 170 h (Figure 4.8 and Figure 4.10). A 0.024 h^{-1} rate constant was found when the reduction was modelled as a first-order reaction. When the molar excess of Pic-BH_3 was increased 6-fold to 32x, the rate was doubled.

D_nM=ADH (12 mM) mixed with a 5.2x molar excess of Pic-BH_3 resulted in total conversion to the DnM-ADH secondary amine within 20 h (Figure 4.7 and Figure 4.9). A 0.44 h^{-1} rate constant was found when the reduction was modelled as a first-order reaction.

With a 5.2x molar excess of Pic-BH_3, the rate constant for the reduction of the D_nM=ADH Schiff base is 18 times greater than that for the D_nM=PDHA Schiff base. In this regard, ADH seems preferable to PDHA as a linker. However, when deciding what linker to use, one must also take into consideration what will be attached to the other end of the bifunctional linker. Reductive amination of ADH is not always faster than for PDHA. The opposite is true of reductive amination of N-acetyl-D-glucosamines[63] and for dextran (unpublished work by Ingrid Vikøren Mo and Amalie Solberg, Department of Biotechnology and Food science, NTNU).

5.1.4.3 Background reduction

An experiment was performed where reduction of the M-unit reducing end by Pic-BH_3 (background reduction) was kinetically modelled (Section 3.5.4). For two-pot reductive amination, background reduction is of no concern since amination runs to completion (Section 5.1.4.1). However, for one-pot reductive amination, background reduction and amination

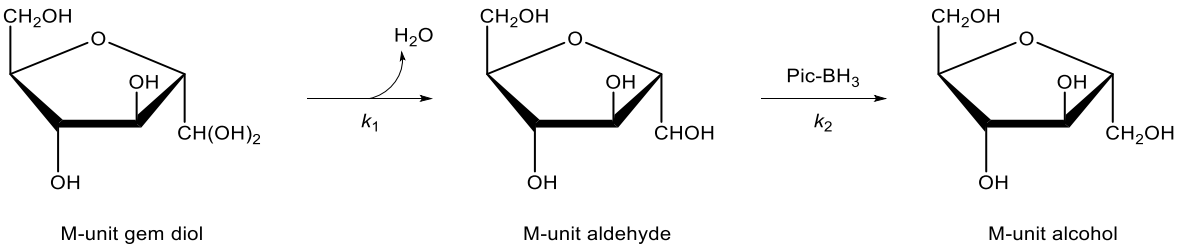

Figure 5.1. Presumed scheme of reduction of the 2,5-anhydro-D-mannofuranose (M-unit) reducing end.

become competing reactions. Modelling of background reduction and amination is therefore needed to make an informed decision about optimal amount of reducing agent and amine.

The rate of disappearance of the M-unit gem diol was found to follow that of a second-order reaction (Section 4.1.4.3). Presumably, background reduction of the M-unit gem diol is a two-step reaction. The gem diol must first be converted to an aldehyde. The aldehyde is then reduced to an alcohol. The M-unit aldehyde produces a ^{1}H-NMR signal at 9.49 ppm.[47] At no point was a signal observed at 9.49 ppm. If it is therefore assumed that $k_2 \gg k_1$ (Figure 5.1), then the rate limiting step becomes the formation of an aldehyde. Since the rate limiting step decides the rate of the overall reaction, it can be concluded that the overall rate of background reduction is described by k_2, found to be 0.029 M^{-1} h^{-1}.

Background reduction was performed with a 4.7x molar excess of Pic-BH_3. Amination, performed with a 3.4x molar excess of ADH and PDHA, progressed at a comparably much faster rate (Section 5.1.4.1). It therefore seems that one-pot reductive amination at these excesses would greatly favour amination over background reduction. That being said, when deciding on excess of Pic-BH_3, rate of reduction of the amination product must also be considered. Reduction of D_nM=PDHA is especially slow unless a very large excess of Pic-BH_3 is used (Section 5.1.4.2). Anyway, the time-savings that could be expected of a one-pot vs two-pot reductive amination are minor considering that reduction is very slow compared to amination.

5.1.5 M-unit isomerism

The M-unit exists as two isomers (unpublished work by Ingrid Vikøren Mo, Department of Biotechnology and Food science, NTNU). All discussion so far has been concerned with the most abundant (major) isomer, namely 2,5-anhydro-D-mannofuranose. The less abundant (minor) isomer is 3,5-anhydro-D-mannofuranose (Figure 5.2).

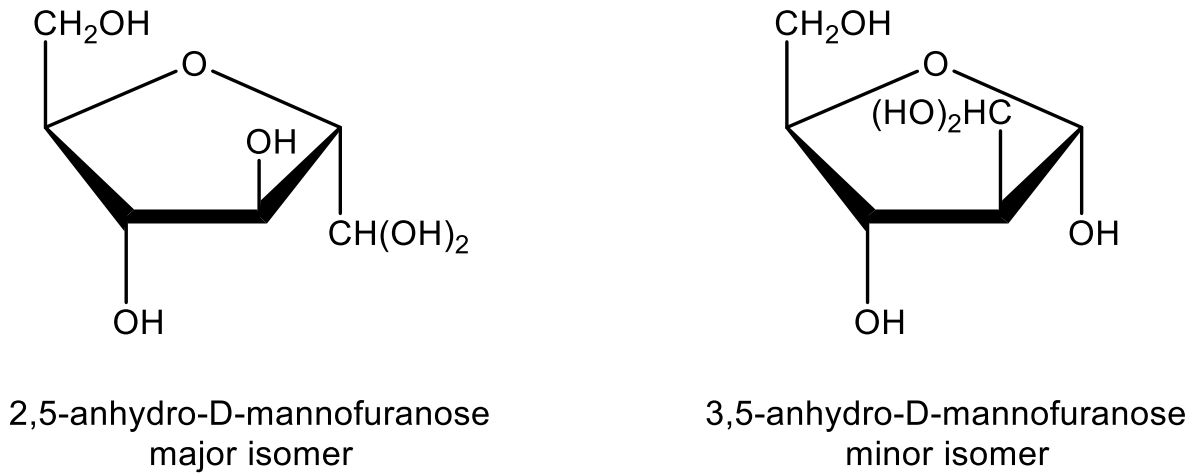

Figure 5.2. The two M-unit isomers.

In the ^{1}H-NMR spectrum (temp. = 25 °C, solvent = D2O. pH* = 4.0), the gem diol form of the minor isomer appears at 5.16 ppm (using TSP as internal standard) and with a 7.15 Hz coupling constant (Appendix B, Figure B.1).

The mechanism responsible for generation of the minor isomer is unknown. However, the minor isomer was identified as early as in the ^{1}H-NMR spectrum of the nitrous acid depolymerisate discussed in Section 5.1.1. It must therefore have been generated either during nitrous acid depolymerisation or during purification prior to ^{1}H-NMR acquisition (Section 3.5.1).

Interestingly, the minor isomer is not always generated. For example, the depolymerisate prepared by Moussa et al.[40] and the depolymerisate prepared by Marianne Øksnes Dalheim (Appendix C) do not appear to contain the minor isomer. A noteworthy differences that may account for the lack of minor isomer is that Moussa et al. and Dalheim used HCl instead of AcOH to perform the depolymerisation.

The sample used to prepare activated chitosan (Section 4.1.4) contained the major and minor isomer in the ratio 91:9 (Appendix B). The isomers behaved identically with respect to amination by ADH and PDHA and subsequent reduction. The two isomers are expected to produce different bond angles when conjugated. This may affect the properties of the conjugate.

5.2 Desalting

5.2.1 Dialysis: escape rates of salts

Although simple to perform, dialysis can be time-consuming and a cause of loss of material; the MWCO of a dialysis membrane is not a hard threshold, but instead represents the rate at which material, salt or otherwise, moves across it.

It would be useful to know how quickly salt escapes from a dialysis bag given its MWCO and diameter. That way one could more easily determine the minimum amount of dialysis required to remove a specified amount of salt. Keeping dialysis to a minimum is important as to avoid unnecessary loss of valuable material.

In an effort to shed some light on the kinetics of dialysis, escape rates for three salts – NaAc, AmAc and NaCl – for a 12-14 kDa membrane with a 6.4 mL/cm volume-to-length ratio were determined (Section 4.2.1).

The results show that the escape rates follow a first-order description when the dialysis buffer is replenished every hour. When the first data point (at t = 0 h) was omitted from the regression, the coefficient of determination (R^2) improved for all three salts. The improvement can be explained physically by a large initial influx of buffer into the bag: Due to the solute concentration being higher on the inside compared to on the outside of the bag, buffer will tend to enter the bag in an attempt to neutralise the concentration difference. When this happens, the salt becomes diluted, thereby making the measured concentration 'artificially' low. The dilution effect diminishes over time as the inward flow of buffer eventually is halted when the dialysis bag is no longer able to expand.

Comparing the salts, their escape rates from highest to lowest were: NaCl > AmAc > NaAc. The ranking can in part be explained by the relatively large size of acetate. Given that the MWCO is much larger than the hydrodynamic volume of the solutes, the escape rates can be assumed to be exclusively dependent on their respective diffusion coefficients.

It is important to note that the escape rates were determined in absence of any other material. The escape rates may be significantly affected by the presence of charged species trapped inside the bag. For instance, chitosan may retain a significant amount of negatively charged species as part of its ionic atmosphere.

5.2.2 Desalting by means of size-exclusion chromatography

Given some of the disadvantages of dialysis discussed above, it was decided to investigate SEC as an alternative approach to desalting. SEC has the advantage of being quick to perform, potentially less loss of material, and that amount of salt that has been removed can be easily quantified by analysis of the chromatogram.

Martosuyono et al.[76] desalted a COS-sample using both dialysis and SEC. They found that SEC, performed with a HiPrep 26/10 Desalting column packed with G-25 Superfine Sephadex™, resulted in less loss of material compared to dialysis, performed with a 10 kDa MWCO membrane.

Our lab was not equipped with a desalting column of similar quality to the one Martosuyono et al. had used. Instead, desalting was attempted using a PD-10 Desalting Column packed with G-25 Medium Sephadex™, i.e. a comparably shorter (5 cm vs 10 cm) and narrower (15 mm vs 26 mm i.d.) column, packed with larger beads (50-150 μm vs 20-50 μm diameter). PD-10 columns are intended to be used for desalting of protein samples, but it was hypothesised that the column would provide good enough resolution to also work for partial desalting of COS-samples.

Figure 4.13 conclusively show that the resolution afforded by the PD-10 column was too low to permit desalting of the COS-sample; the overlap between the salt-peak and the COS-peak was complete. The COS sample used had a DP_n of about 50 (determined by ^{1}H-NMR).

Despite failing to achieve desalting, the experiment demonstrated that the COS was readily detectable by conductivity even at a very low concentration. The sample had to be diluted prior to measure of conductivity to give a COS-concentration of about 0.3 mg/mL.

For very low molecular weight chitosan, the solubility does not need to be improved by making the MP acidic. Martosuyono et al. used a pure aqueous MP. However, for chitosan of higher molecular weight, acidification will be required. Fortunately, the experiment showcased here demonstrated that the AcOH added to the MP to make it acidic did not noticeably reduce the signal-to-noise ratio, even at such a low COS-concentration.

In conclusion, the experiment demonstrated the viability of desalting of COS-samples by means of SEC using an acidified MP and a conductivity meter as detector. All that is required is a column of high enough quality.

5.3 Synthesis of a chitosan-dextran diblock

Activated chitosan (DnM-ADH and DnM-PDHA) was successfully conjugated to dextran by one-pot reductive amination (Section 4.3). In order to improve reaction rate, an excess of dextran and reducing agent was used. Additionally, the temperature was brought from RT to 40 °C. The temperature was not increased any further in case reagents or product were unexpectedly heat-labile.

A relatively high molecular weight fraction of D_nM-ADH and a relatively low molecular weight fraction of dextran was chosen so that non-conjugated dextran could be removed by SEC. Any dextran that remained could therefore be assumed to be conjugated. In this manner, SEC serves a dual purpose, to help with verifying conjugation and by purifying the product. The technique is scalable, both with respect to quantity and size of the conjugate. But to maximally exploit the benefit offered by SEC, two principles must be kept in mind.

In this particular case, only non-conjugated dextran was removed. Non-conjugated chitosan remained in the sample. This was a consequence of how the DP_n of the chitosan was much greater than that of the dextran. There was a relatively small difference between the DP_n of the conjugated vs. non-conjugated chitosan. Consequently, the SEC system, operating at the limits of its capability, could not afford the required resolution to separate conjugated from non-conjugated chitosan.

A solution to this problem would be to employ such a large excess of dextran so that 100 % of the chitosan would become conjugated. Alternatively, if reagents of approximately equal DP_n were to be conjugated, it would be much more feasible to find a SEC system that would be able to separate reagents form product.

In the first part of this thesis dealing with preparation of activated chitosan (Section 5.1), depolymerised chitosan was first fractionated, then activated. Here, the protocol was reversed. The depolymerisate was first activated, then fractionated. By performing activation sooner rather than later, the instability of the M-unit becomes less of a restriction. The free M-unit (non-activated chitosan) is lost to non-enzymatic browning unless mild acidity is maintained. Maintaining permanent acidity complicates handling, especially if the protocol involves use of volatile acids (Section 5.1.2). When activated, the M-unit is protected from non-enzymatic browning. It therefore no longer becomes an absolute requirement to maintain mild acidity. Early activation is consequently recommended.

5.4 Future work

The results presented in this thesis has laid the groundworks for the preparation of block copolymers based on chitosan. Ultimately, the goal is to develop a simple, cost effective and time effective protocol for the synthesis of activated chitosan.

Several small and rudimentary studies could be performed which likely would significantly improve the protocol for synthesis of activated chitosan.

A lot could potentially be gained from finding ways to increase rates of reduction. It was shown here that increasing the excess of Pic-BH_3 significantly increased rates of reduction. It would be useful to known how much Pic-BH_3 should be used in order to achieve a maximum rate of reduction. The upper limit of the excess that can be achieved is ultimately determined by the limited solubility of Pic-BH_3. A study could also be performed to see how temperature affects rate of reduction. Dependence on chitosan concentration could also be investigated. By comparing the results presented here with published literature, it seems that rate of reduction is highly dependent on the concentration of chitosan.

At the moment, reductive amination itself only constitutes a small fraction of the work involved in preparing activated chitosan. A majority of time and effort is spent purifying reagents and products via SEC, dialysis and lyophilisation. Finding more efficient ways of purification could dramatically increase preparation time. Experimentation with solvent precipitation and centrifugation would be a good place to start.

Before going to great lengths in order to optimise the protocol for synthesis of activated protocol, potential applications should be investigated. The solubility of chitosan is a big deal. Solubility studies can be performed to show how the solubility of chitosan can be improved by conjugating to a lyophilic block. Another suggestion is to synthesise chitosan-alginate blocks and to perform gelation experiments.

It could also be of interest to investigate the compatibility of activated chitosan with common derivatisation techniques such as carboxymethylation and sulfatation.

6 Conclusion

Nitrous acid depolymerisation of fully de-*N*-acetylated chitosan yields chitooligosaccharides with a 2,5-anhydro-D-mannofuranose (M-unit) reducing end (D_nM-type chitosan). Bifunctional linkers adipic acid dihydrazide (ADH) and *O*,*O*'-1,3-propanediylbishydroxylamine dihydrochloride (PDHA) were attached to the M-unit via two-pot reductive amination. Reduction was performed using the reducing agent α-picoline borane (Pic-BH_3).

Amination of D_nM by ADH (3.4x molar excess) gave complete yield of amination product within 100 min but possibly significantly sooner. It took 20 h to fully reduce the amination product using a 5.2x molar excess of Pic-BH_3. The reduction was a first-order reaction with a 0.44 h^{-1} rate constant. Both amination and reduction was performed in a pH 4.5 NaAc buffer (500 mM) at RT.

The amination reaction between D_nM and PDHA (3.4x molar excess) resulted in complete yield in 15 min. Using a 5.2x molar excess of Pic-BH_3, the reduction had reached 80 % completion (not yet at equilibrium) by the 170 h mark. The reduction was a first-order reaction with a 0.012 h^{-1} rate constant. When the molar excess of Pic-BH_3 was increased 6-fold (to 32x), the rate was doubled. By comparison, with 32x Pic-BH_3, 80 % yield was reached in 70 h. Both amination and reduction was performed in a pH 4.5 NaAc buffer (500 mM) at RT.

An experiment was performed in order to compare the rate of background reduction, i.e. reduction of the non-aminated M-unit, and rate of amination. The rate of background reduction was found to be a second-order reaction much slower than the rate of amination. Reductive amination can therefore potentially be performed as a one-pot reaction without significant loss of material due to background reduction.

It is quintessential for activation that the chitosan is modified at the reducing end with something more reactive than a normal glucosamine (D-unit). The D-unit was found to be essentially inert with respect to amination.

The M-unit was found to be highly unstable when subjected to an elevated pH in combination with dehydration. If mild acidity was not constantly maintained, the M-unit was cleaved from the chain and converted to 5-hydroxymethylfurfural (HMF) due to a process of non-enzymatic browning. Special care is advised when volatile acids are used in combination with lyophilisation. The M-unit was lost unless a majority of the volatile acid was removed prior to

lyophilisation. The M-unit was also found to be unstable when stored in a pH 5 aqueous solution over a longer period of time.

Amination of the M-unit prevents loss due to non-enzymatic browning. It is therefore recommended that amination is performed as early as possible in order to eliminate the possibility of loss.

A brief investigation into desalting was performed. It was attempted to desalt a sample of chitooligosaccharide used a PD-10 column. The column did not provide sufficient resolution. But the experiment did serve to demonstrate the feasibility of using an acidified aqueous solution as mobile phase and of using a conductivity detector for even a very dilute sample of of chitosan.

To shed some light on the kinetics of dialysis, the escape rates of three salts (NaAc, AmAc and NaCl) was determined for a 12-14 kDa membrane. The escape rates of all three salts were first order and they had a $t_{1/2}$ of about 60-90 min.

A chitosan-dextran diblock was synthesised via one-pot reductive amination between activated chitosan and dextran. The reaction was performed with an excess of dextran and at 40 °C. More time was given to reductive amination of the ADH activated chitosan (6 days) compared to that of the PDHA activated chitosan (4 days). This was done as it is known that reductive amination between ADH and dextran is slower than reductive amination between PDHA and dextran. A protocol was demonstrated that allowed for easy removal of non-conjugated dextran via SEC.

References

1. Feng H, Lu X, Wang W, Kang N-G, Mays JW. Block copolymers: Synthesis, self-assembly, and applications. Polymers. 2017;9(10):494.
2. Heinze T, Liebert T, Heublein B, Hornig S. Functional polymers based on dextran. Polysaccharides Ii: Springer; 2006. p. 199-291.
3. Strand SP, Tømmeraas K, Vårum KM, Østgaard K. Electrophoretic light scattering studies of chitosans with different degrees of N-acetylation. Biomacromolecules. 2001;2(4):1310-4.
4. Schatz C, Lecommandoux S. Polysaccharide-containing block copolymers: synthesis, properties and applications of an emerging family of glycoconjugates. Macromolecular rapid communications. 2010;31(19):1664-84.
5. Kim K, Chen WC, Heo Y, Wang Y. Polycations and their biomedical applications. Progress in Polymer Science. 2016;60:18-50.
6. Nakauchida T, Takata Y, Yamamoto K, Kadokawa J-i. Chemoenzymatic synthesis and pH-responsive properties of amphoteric block polysaccharides. Organic & biomolecular chemistry. 2016;14(27):6449-56.
7. Xiao Y, Chinoy ZS, Pecastaings G, Bathany K, Garanger E, Lecommandoux S. Design of Polysaccharide-b-Elastin-Like Polypeptide Bioconjugates and Their Thermoresponsive Self-Assembly. Biomacromolecules. 2019.
8. Cooksey TJ, Singh A, Le KM, Wang S, Kelley EG, He L, et al. Tuning Biocompatible Block Copolymer Micelles by Varying Solvent Composition: Core/Corona Structure and Solvent Uptake. Macromolecules. 2017;50(11):4322-34.
9. Karayianni M, Pispas S. Self-assembly of amphiphilic block copolymers in selective solvents. Fluorescence Studies of Polymer Containing Systems: Springer; 2016. p. 27-63.
10. Choi Y-k, Lee S-B, Lee D-J, Ishigami Y, Kajiuchi T. Micellar enhanced ultrafiltration using PEO–PPO–PEO block copolymers. Journal of membrane science. 1998;148(2):185-94.
11. Upadhyay KK, Bhatt AN, Mishra AK, Dwarakanath BS, Jain S, Schatz C, et al. The intracellular drug delivery and anti tumor activity of doxorubicin loaded poly (γ-benzyl l-glutamate)-b-hyaluronan polymersomes. Biomaterials. 2010;31(10):2882-92.
12. Kim S, Stannett V, Gilbert R. Biodegradable cellulose block copolymers. Journal of Macromolecular Science—Chemistry. 1976;10(4):671-9.
13. Yadav M, Goswami P, Paritosh K, Kumar M, Pareek N, Vivekanand V. Seafood waste: A source for preparation of commercially employable chitin/chitosan materials. Bioresources and Bioprocessing. 2019;6(1):8.
14. Ganji F, Abdekhodaie M. Synthesis and characterization of a new thermosensitive chitosan–PEG diblock copolymer. Carbohydrate Polymers. 2008;74(3):435-41.
15. Ahmed S, Ahmad M, Ikram S. Chitosan: a natural antimicrobial agent-a review. Journal of Applicable Chemistry. 2014;3(2):493-503.
16. Roberts GA. Structure of chitin and chitosan. Chitin chemistry: Springer; 1992. p. 1-53.
17. Kean T, Thanou M. Biodegradation, biodistribution and toxicity of chitosan. Advanced drug delivery reviews. 2010;62(1):3-11.
18. Goy RC, Britto Dd, Assis OB. A review of the antimicrobial activity of chitosan. Polímeros. 2009;19(3):241-7.
19. Schipper NG, Vårum KM, Artursson P. Chitosans as absorption enhancers for poorly absorbable drugs. 1: Influence of molecular weight and degree of acetylation on drug transport across human intestinal epithelial (Caco-2) cells. Pharmaceutical research. 1996;13(11):1686-92.
20. Davis S. Drug delivery systems. Interdisciplinary Science Reviews. 2000;25(3):175-83.

21. Dufes C, Schätzlein AG, Tetley L, Gray AI, Watson DG, Olivier J-C, et al. Niosomes and polymeric chitosan based vesicles bearing transferrin and glucose ligands for drug targeting. Pharmaceutical research. 2000;17(10):1250-8.
22. Mao H-Q, Roy K, Troung-Le VL, Janes KA, Lin KY, Wang Y, et al. Chitosan-DNA nanoparticles as gene carriers: synthesis, characterization and transfection efficiency. Journal of controlled release. 2001;70(3):399-421.
23. Köping-Höggård M, Tubulekas I, Guan H, Edwards K, Nilsson M, Vårum KM, et al. Chitosan as a nonviral gene delivery system. Structure–property relationships and characteristics compared with polyethylenimine in vitro and after lung administration in vivo. Gene therapy. 2001;8(14):1108-21.
24. Vårum KM, Antohonsen MW, Grasdalen H, Smidsrød O. Determination of the degree of N-acetylation and the distribution of N-acetyl groups in partially N-deacetylated chitins (chitosans) by high-field nmr spectroscopy. Carbohydrate Research. 1991;211(1):17-23.
25. Varum KM, Smidsrød O. 14 Chitosans. Food Polysaccharides and Their Applications. 2006:497.
26. Tømmeraas K, Köping-Höggård M, Vårum KM, Christensen BE, Artursson P, Smidsrød O. Preparation and characterisation of chitosans with oligosaccharide branches. Carbohydrate research. 2002;337(24):2455-62.
27. Katchalsky A, Shavit N, Eisenberg H. Dissociation of weak polymeric acids and bases. Journal of Polymer Science. 1954;13(68):69-84.
28. Wang QZ, Chen XG, Liu N, Wang SX, Liu CS, Meng XH, et al. Protonation constants of chitosan with different molecular weight and degree of deacetylation. Carbohydrate polymers. 2006;65(2):194-201.
29. Wani MY, Hasan N, Malik MA. Chitosan and Aloe vera: Two gifts of nature. Journal of Dispersion Science and Technology. 2010;31(6):799-811.
30. Barbosa M, Gonçalves I, Moreno P, Goncalves R, Santos S, Pego A, et al. 2.13 Chitosan. 2017.
31. Domard A. pH and cd measurements on a fully deacetylated chitosan: application to CuII—polymer interactions. International Journal of Biological Macromolecules. 1987;9(2):98-104.
32. Anthonsen MW, Smidsrød O. Hydrogen ion titration of chitosans with varying degrees of N-acetylation by monitoring induced 1H-NMR chemical shifts. Carbohydrate Polymers. 1995;26(4):303-5.
33. Sorlier P, Denuzière A, Viton C, Domard A. Relation between the degree of acetylation and the electrostatic properties of chitin and chitosan. Biomacromolecules. 2001;2(3):765-72.
34. Vårum KM, Ottøy MH, Smidsrød O. Water-solubility of partially N-acetylated chitosans as a function of pH: effect of chemical composition and depolymerisation. Carbohydrate Polymers. 1994;25(2):65-70.
35. Lu S, Song X, Cao D, Chen Y, Yao K. Preparation of water-soluble chitosan. Journal of Applied Polymer Science. 2004;91(6):3497-503.
36. Sannan T, Kurita K, Iwakura Y. Studies on chitin, 2. Effect of deacetylation on solubility. Die Makromolekulare Chemie: Macromolecular Chemistry and Physics. 1976;177(12):3589-600.
37. Upadhyaya L, Singh J, Agarwal V, Tewari RP. Biomedical applications of carboxymethyl chitosans. Carbohydrate polymers. 2013;91(1):452-66.
38. Mourya V, Inamdar NN, Tiwari A. Carboxymethyl chitosan and its applications. Advanced Materials Letters. 2010;1(1):11-33.
39. Dimassi S, Tabary N, Chai F, Blanchemain N, Martel B. Sulfonated and sulfated chitosan derivatives for biomedical applications: A review. Carbohydrate polymers.

2018;202:382-96.
40. Moussa A, Crépet A, Ladavière C, Trombotto S. Reducing-end "clickable" functionalizations of chitosan oligomers for the synthesis of chitosan-based diblock copolymers. Carbohydrate polymers. 2019;219:387-94.
41. Mourya V, Inamdar N, Choudhari YM. Chitooligosaccharides: synthesis, characterization and applications. Polymer Science Series A. 2011;53(7):583-612.
42. Tsai M-L, Chen R. Modifying the molecular weight of chitosan. Chitosan Based Biomaterials Volume 1: Elsevier; 2017. p. 135-58.
43. Solomons G, Fryhle C, Snyder S. Organic Chemistry Internation Student Version. 11 ed: Wiley; 2013.
44. Peat S. The chemistry of anhydro sugars. Advances in carbohydrate chemistry. 2: Elsevier; 1946. p. 37-77.
45. Horton D, Philips KD. The nitrous acid deamination of glycosides and acetates of 2-amino-2-deoxy-D-glucose. Carbohydrate Research. 1973;30(2):367-74.
46. Defaye J. 2, 5-Anhydrides of sugars and related compounds. Advances in Carbohydrate Chemistry and Biochemistry. 25: Elsevier; 1970. p. 181-228.
47. Tømmeraas K, Vårum KM, Christensen BE, Smidsrød O. Preparation and characterisation of oligosaccharides produced by nitrous acid depolymerisation of chitosans. Carbohydrate Research. 2001;333(2):137-44.
48. Sahoo D, Sahoo S, Mohanty P, Sasmal S, Nayak P. Chitosan: a new versatile bio-polymer for various applications. Designed monomers and polymers. 2009;12(5):377-404.
49. Sashiwa H, Saimoto H, Shigemasa Y, Tokura S. N-Acetyl group distribution in partially deacetylated chitins prepared under homogeneous conditions. Carbohydrate research. 1993;242:167-72.
50. Allan GG, Peyron M. Molecular weight manipulation of chitosan II: prediction and control of extent of depolymerization by nitrous acid. Carbohydrate research. 1995;277(2):273-82.
51. Hodge JE. Dehydrated foods, chemistry of browning reactions in model systems. Journal of agricultural and food chemistry. 1953;1(15):928-43.
52. Borch RF, Bernstein MD, Durst HD. Cyanohydridoborate anion as a selective reducing agent. Journal of the American Chemical Society. 1971;93(12):2897-904.
53. Domard A, Gey C, Taravel F. Glucosamine oligomers: 2. Nmr studies on a DP3. International journal of biological macromolecules. 1991;13(2):105-9.
54. Ames JM. The maillard reaction. Biochemistry of food proteins: Springer; 1992. p. 99-153.
55. Sarwat F, Qader SAU, Aman A, Ahmed N. Production & characterization of a unique dextran from an indigenous Leuconostoc mesenteroides CMG713. International Journal of Biological Sciences. 2008;4(6):379.
56. Breitenbach BB, Schmid I, Wich PR. Amphiphilic polysaccharide block copolymers for pH-responsive micellar nanoparticles. Biomacromolecules. 2017;18(9):2839-48.
57. Lewis SL, Bucher L, Heitkemper MM, Harding MM, Kwong J, Roberts D. Medical-Surgical Nursing-E-Book: Assessment and Management of Clinical Problems, Single Volume: Elsevier Health Sciences; 2016.
58. Ljungström K. The antithrombotic efficacy of dextran. Acta chirurgica Scandinavica Supplementum. 1988;543:26-30.
59. Dormandy JA. Influence of blood viscosity on blood flow and the effect of low molecular weight dextran. Br Med J. 1971;4(5789):716-9.
60. Sun Z, Wei Z, Wei K. A Model for Predicting the Optimal Conditions for Labeling the Carbohydrates with the Amine Derivatives by Reductive Amination (Supplementry Material). Letters in Organic Chemistry. 2009;6(7):549-51.

61. Bystrický S, Machová E, Malovíková A, Kogan G. Determination of the cross-linking effect of adipic acid dihydrazide on glycoconjugate preparation. Glycoconjugate journal. 1999;16(11):691-5.
62. Fina NJ, Edwards JO. The alpha effect. A review. International Journal of Chemical Kinetics. 1973;5(1):1-26.
63. Mo IV, Feng Y, Dalheim MØ, Solberg A, Aachmann FL, Schatz C, et al. Activation of enzymatically produced chitooligosaccharides by dioxyamines and dihydrazides. Carbohydrate Polymers. 2020;232:115748.
64. Chaur MN, Collado D, Lehn JM. Configurational and constitutional information storage: multiple dynamics in systems based on pyridyl and acyl hydrazones. Chemistry–A European Journal. 2011;17(1):248-58.
65. Kwase YA, Cochran M, Nitz M. Protecting-Group-Free Glycoconjugate Synthesis: Hydrazide and Oxyamine Derivatives in N-Glycoside Formation. Modern Synthetic Methods in Carbohydrate Chemistry. 2014.
66. Cosenza VA, Navarro DA, Stortz CA. Usage of α-picoline borane for the reductive amination of carbohydrates. ARKIVOC: Online Journal of Organic Chemistry. 2011.
67. Ruhaak LR, Steenvoorden E, Koeleman CA, Deelder AM, Wuhrer M. 2-Picoline-borane: A non-toxic reducing agent for oligosaccharide labeling by reductive amination. Proteomics. 2010;10(12):2330-6.
68. Poole CF. The Essence of Chromatography. 1st ed. Eastbourne, Great Britain: Elsevier Science B. V.; 2003.
69. H. F, editor. Basic One- and Two-Dimensional NMR Spectroscopy. 5th ed. Weinheim, Germany: Wiley-VHC Verlag GmbH; 2011.
70. Silverstein RM, Webster FX, Kiemle DJ, Bryce DL. Spectrometric Identification of Organic Compunds. 8th ed: Wiley; 2014.
71. Krężel A, Bal W. A formula for correlating pKa values determined in D2O and H2O. Journal of inorganic biochemistry. 2004;98(1):161-6.
72. Wang X, Sun T, Wang C, Wang C, Zhang W, Wei Y. 1H NMR determination of the doping level of doped polyaniline. Macromolecular Chemistry and Physics. 2010;211(16):1814-9.
73. Coudurier M, Faivre J, Crépet A, Ladavière C, Delair T, Schatz C, et al. Reducing-End Functionalization of 2, 5-Anhydro-d-mannofuranose-Linked Chitooligosaccharides by Dioxyamine: Synthesis and Characterization. Molecules. 2020;25(5):1143.
74. Martins SI, Jongen WM, Van Boekel MA. A review of Maillard reaction in food and implications to kinetic modelling. Trends in food science & technology. 2000;11(9-10):364-73.
75. Eichner K, Karel M. Influence of water content and water activity on the sugar-amino browning reaction in model systems under various conditions. Journal of Agricultural and Food Chemistry. 1972;20(2):218-23.
76. Martosuyono P, Pratitis A, Prasetya A, Prabawati EK. DESALINATION OF CHITOOLOGOSACCAHARIDES USING GEL FILTRATION AND ULTRAFILTRATION. Squalen Bulletin of Marine and Fisheries Postharvest and Biotechnology. 2014;9(3):127-36.

Appendix A: Molecular weights

Table A.1. Molecular formulas and molecular weights of selected compounds.

Name	Molecular formula	Molecular weight (Da)
2,5-Anhydro-D-mannose	$C_6H_{10}O_5$	162.1
D-Glucosamine	$C_6H_{13}NO_5$	179.2
Adipic acid dihydrazide	$C_6H_{14}N_4O_2$	174.2
O,*O*'-1,3-Propanediylbishydroxylamine dihydrochloride	$C_3H_{12}Cl_2N_2O_2$	179.0
α-Picoline borane	C_6H_7BN	103.9

Source: Kim S, Chen J, Cheng T, Gindulyte A, He J, He S, Li Q, Shoemaker BA, Thiessen PA, Yu B, Zaslavsky L, Zhang J, Bolton EE. PubChem 2019 update: improved access to chemical data. Nucleic Acids Res. 2019 Jan 8; 47(D1):D1102-1109. doi:10.1093/nar/gky1033.

Appendix B: Characterisation of fraction *m*

Fraction *m* (Section 4.1.1) is here characterised based on an acquired ^{1}H-NMR spectrum (Figure B.1). Peak assignment was performed based on data published by Tømmeraas et al.[1]

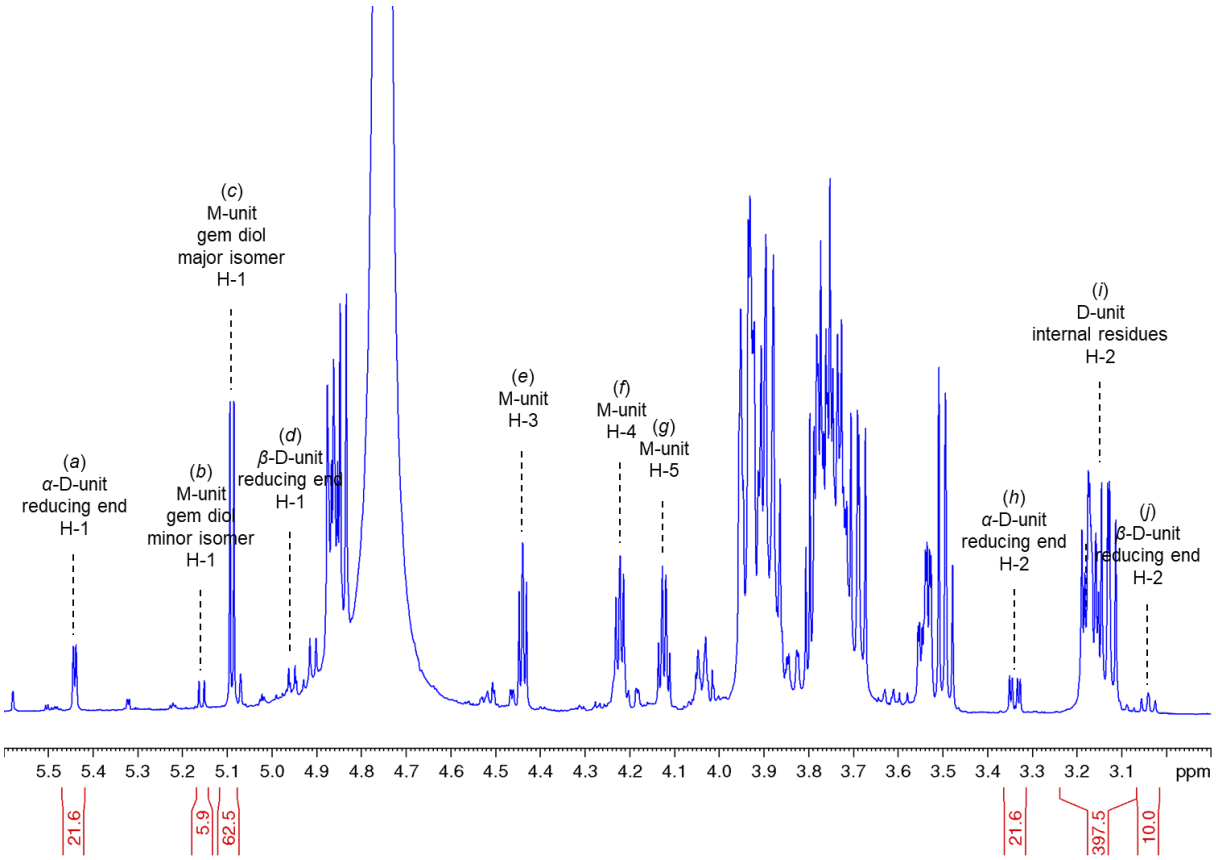

Figure B.1. ^{1}H-NMR spectrum of a nitrous acid depolymerised, fully de-*N*-acetylated chitosan (F_A = 0.01). Recorded at 600.18 MHz while running a standard Bruker zg30 pulse sequence. T = 25 °C. Solvent: D_2O. pH^* = 4.0. Number of scans, ns = 32. Dummy scans, ds = 2. Interscan delay, d1 = 1 s. Transmitter frequency offset, O1P = 6.175 ppm. Spectral width, sw = 20.03 ppm.

Estimation of number average degree of polymerisation (DP_n):

$$\mathrm{DP_n} = \frac{I_i}{I_a + I_b + I_c + I_j} + 1 = \frac{397.5}{100} + 1 = 4.975 \approx 5.0 \qquad \text{(B.1)}$$

Percentage breakdown of the four types of reducing ends:

M-unit, major isomer: 63 %

α-D-unit: 22 %

[1] Tømmeraas, K., Vårum, K. M., Christensen, B. E., & Smidsrød, O. (2001). Preparation and characterisation of oligosaccharides produced by nitrous acid depolymerisation of chitosans. *Carbohydrate Research*, *333*(2), 137-144.

β-D-unit: 10 %

M-unit, minor isomer: 6 %

Estimation of number average molecular weight (M_n):

M_n for internal D-unit residues:

$$\begin{aligned} M_{n,\,int.res.} &= M_{D\text{-}unit}(DP_n - 1) - M_{H_2O}(DP_n - 1) \\ &= 179.2\ \text{Da}(4.975 - 1) - 18.02\ \text{Da}(4.975 - 1) \\ &= 640.7\ \text{Da} \end{aligned} \tag{B.2}$$

M_n for reducing ends:

$$\begin{aligned} M_{n,\,red.end} &= M_{M\text{-}unit}\frac{I_b + I_c}{I_a + I_b + I_c + I_j} + M_{D\text{-}unit}\frac{I_a + I_j}{I_a + I_b + I_c + I_j} \\ &= 162.1\ \text{Da}\frac{62.5 + 5.9}{100} + 179.2\ \text{Da}\frac{21.6 + 10.0}{100} \\ &= 167.5\ \text{Da} \end{aligned} \tag{B.3}$$

The sum of Eq. (B.2) and (B.3) gives the final estimate:

$$M_n = M_{n,\,int.res.} + M_{n,\,red.end} = 640.7\ \text{Da} + 167.5\ \text{Da} = 808.2\ \text{Da} \approx 810\ \text{Da} \tag{B.4}$$

Appendix C: Characterisation of nitrous acid depolymerisate used to prepare activated chitosan

A nitrous acid depolymerisate of a fully de-*N*-acetylated chitosan, prepared by Marianne Øksnes Dalheim, is here characterised based on a ^{1}H-NMR spectrum acquired by Ingrid Vikøren Mo (Figure C.1). Peak assignment was performed based on data published by Tømmeraas et al.[1]

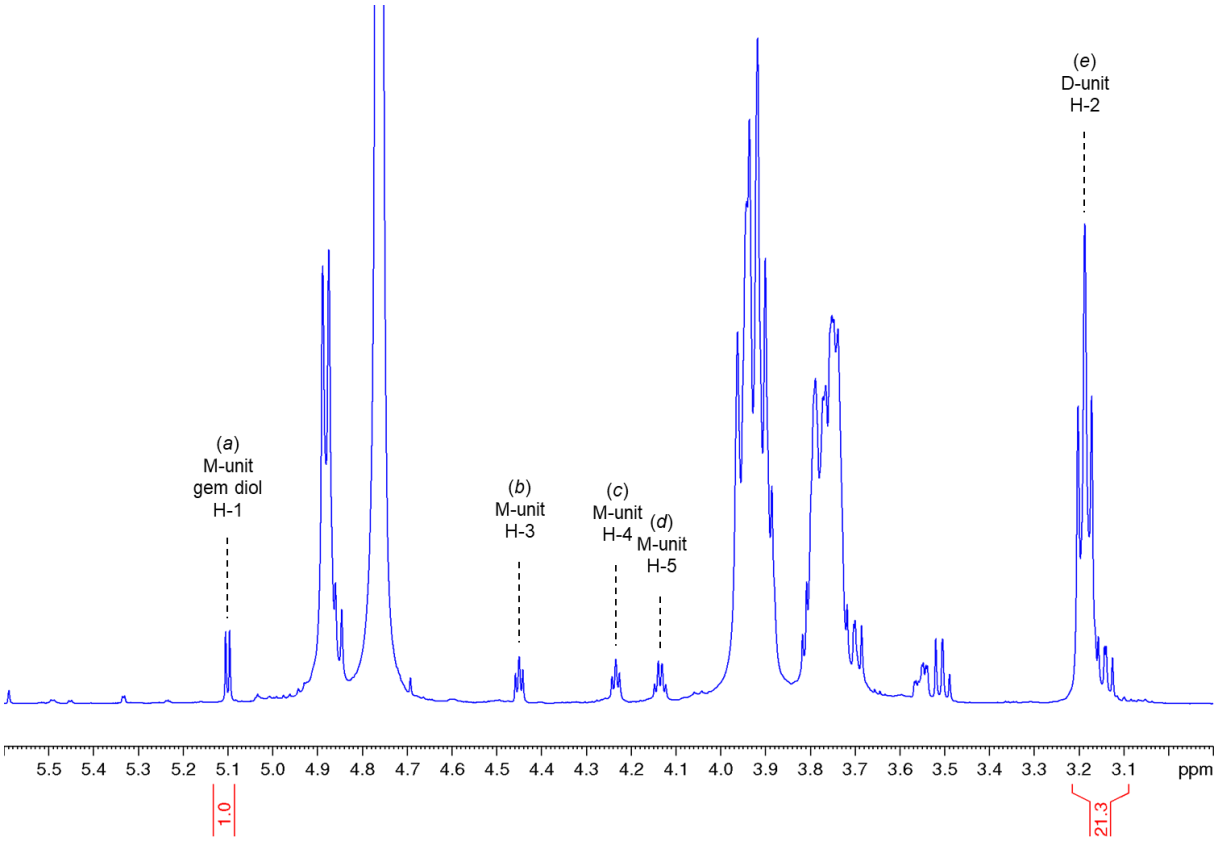

Figure C.1. ^{1}H-NMR spectrum of a nitrous acid depolymerised, fully de-*N*-acetylated chitosan. Recorded at 600.18 MHz while running a standard Bruker zg30 pulse sequence. T = 25 °C. Solvent: D_2O. Number of scans, ns = 32. Dummy scans, ds = 4. Interscan delay, d1 = 1 s. Transmitter frequency offset, O1P = 6.175 ppm. Spectral width, sw = 14.02 ppm. Acquired by Ingrid Vikøren Mo.

Estimation of number average degree of polymerisation (DP_n):

$$DP_n = \frac{I_e}{I_a} + 1 = \frac{21.3}{1.0} + 1 = 22.3 \approx 22 \qquad \text{(C.1)}$$

[1] Tømmeraas, K., Vårum, K. M., Christensen, B. E., & Smidsrød, O. (2001). Preparation and characterisation of oligosaccharides produced by nitrous acid depolymerisation of chitosans. *Carbohydrate Research*, *333*(2), 137-144.

Appendix D: Standard curves used to construct dialysis escape plots

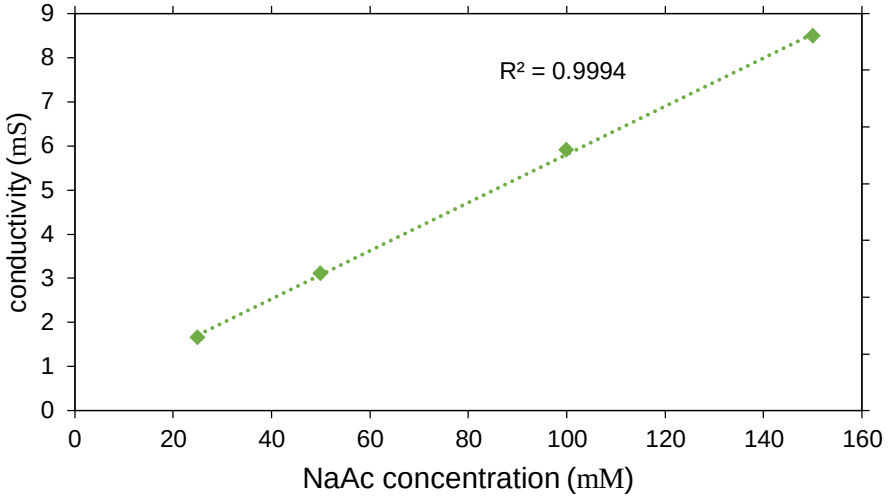

Figure D.1. Conductivity as a function of sodium acetate (NaAc) concentration.

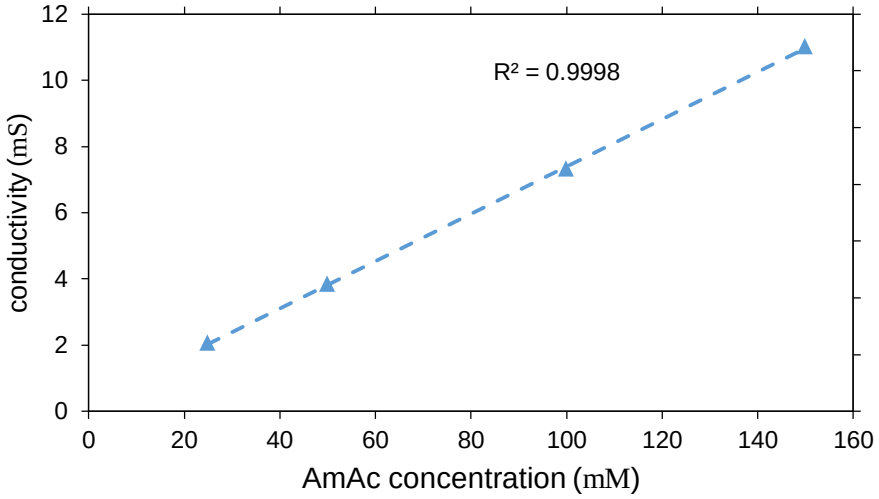

Figure D.2. Conductivity as a function of ammonium acetate (AmAc) concentration.

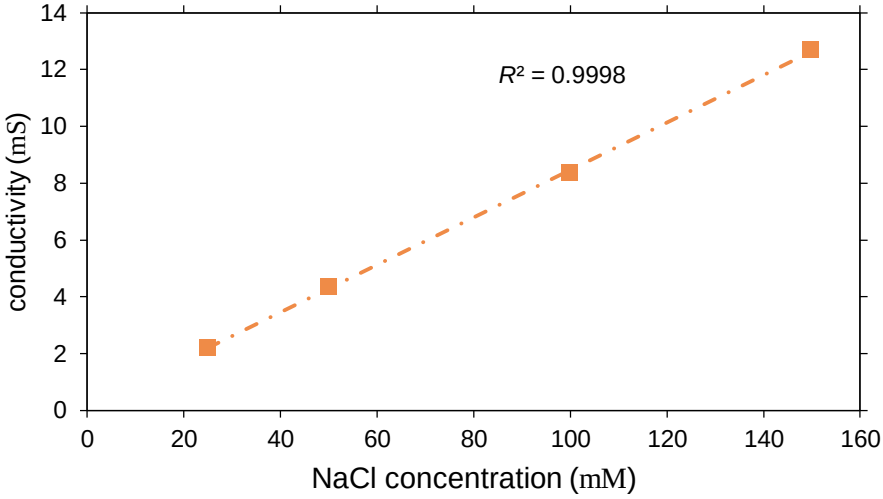

Figure D.3. Conductivity as a function of sodium chloride (NaAc) concentration.

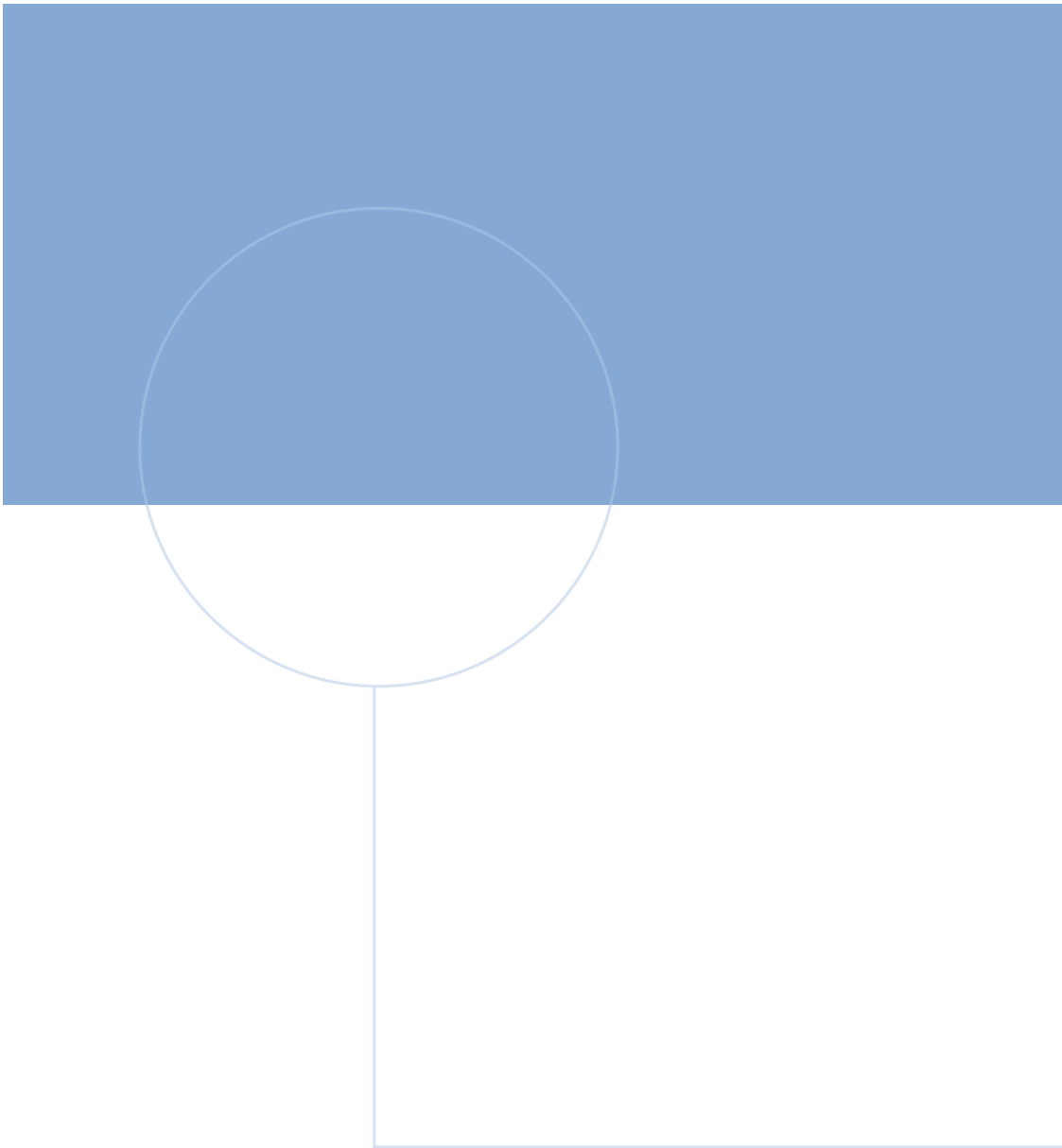

NTNU

Norwegian University of
Science and Technology